
1. INTRODUCTION AND OBJECTIVE OF THE RESEARCH

From the moment when the first biosensor for the determination of glucose was developed in 1962, the applications with biosensors have increased constantly, but not since the mid-90s there has been an increased recognition of the versatility and broad applicability of platforms based on piezoelectric acoustic biosensors (QCM- quartz crystal microbalance) for the analysis of molecular recognition and associated phenomena. Cooper, shows that during the period 2001-2005, there were a total of 1404 publications referenced as “quartz crystal microbalance” or QCM in the Web Science® database, of which 569 specifically involved molecular recognition studies (Cooper 2007). The number of publications per year grew steadily in this period, from 241 in 2001, to 369 in 2005. The areas of application, as defined by the class of analyte were evenly distributed between life sciences research and diagnostic assay development, although interactions involving small molecules, immunoassays, lipids, oligonucleotides and polymer coatings were predominant (Cooper 2007, Pavey 2002). Application to biological samples became possible when suitable oscillator circuits for operation in liquids were developed (Nomura 1982). At the beginning, the relationship between mass adsorbed to the surface and resonant frequency of the crystal were only applicable in air or a vacuum (Sauerbrey 1959). With appreciation in liquids, changes in density and viscosity, the sensor surface or within the bulk solution have influence the frequency of the quartz.

A new category of QCM based biosensor application, is online observation of cell-substrate contacts or interactions with living cells growing on the quartz (Heitmann 2007). Measurement of biochemical interactions or processes occurring in biological fluids is difficult in the traditional techniques. Accordingly, a lot of possible applications have been experimentally shown using QCM, amongst others, immunoassays (Gordon 2005, Halamek 2005, Michalzik 2005, Shen 2005), drugs screening (Johnson 2001, Long 2001, Tan 2001), detection of viruses (Amano 2005, Wu 2003), bacteriae (Pobanka 2005, Su 2005), and eukaryotic cells (Heitmann 2007).

The present work uses QCM technology to develop a groundbreaking technique for the real time analysis of the erythrocyte life cycle of *Plasmodium falciparum*, with special interest in the last six hours before the release of merozoites. Two main questions were asked: (I) Is it possible to measure changes in the frequency of the biosensor in association with merozoite release? (II) Once the merozoites have been released, will it be possible to

cause a reinfection of the healthy erythrocytes inside the biosensor system? Understanding these two processes allows several important statements about the mechanism of merozoite release and the invasion of new cells. Likewise, it also allows studying inhibitory effects on the release and reinfection of the erythrocytes of different inhibitory substances (protease inhibitors E64 and Leupeptin) as well as antimalarial drugs (Artesunate) and a lead compound of natural origin with possible biological activities on the cells (Chlorotonil).

In the year 2002, when the genome sequence of *P. falciparum* was completed, many of the barriers to perform state-of-the-art molecular biological research on malaria parasites were eliminated. Although new licensed therapies may not yet have resulted from genome-dependent experiments, they have produced a wealth of new observations about the basic biology of malaria parasites, and it is likely that these will eventually lead to new therapeutic approaches (Winzeler 2007). These observations of the basic biology of *P. falciparum* (invasion of merozoites, liberation of merozoites and traffic of proteins from the parasites to erythrocyte) have led to the use of new microscopic and molecular techniques. Another possibility is opening up with the use of QCM for the study of malaria.

The real-time study of the erythrocyte cycle using QCM is first presented with the characterisation and optimisation of the biological layer (used for immobilisation of a cell on gold electrode) and the observation of the biosensor signal for 48 hours (Chapter sections 4.1 and 4.2). The observation of infected and non-infected erythrocytes inside the biosensor system is described in chapter sections 4.3 and 4.4. The comparison obtained in the signal once the merozoites are released is presented validating the method with external analyses through flow cytometry and Transmission Electron Microscopy (TEM). The reinfection of the healthy erythrocytes inside the equipment on second quartz inside the system containing healthy erythrocytes is presented, while the efficiency of this technique is evaluated (chapter section 4.5). In addition, the viability of the merozoites is presented, comparing them to other isolation techniques. Finally, the study of the merozoite inhibition using inhibitor proteases (E64 and Leupeptin), an antimalarial drug (Artesunate) and a recently isolated substance of natural origin (Chlorotonil) is described (chapter section 4.6.).

2. THEORY

This chapter describes the theoretical aspects, as a basis for the study of the erythrocyte cycle with QCM. The first section of the chapter will deal with the biosensor theory: mechanisms of biosensor, piezoelectric effect, piezoelectric crystal, relationship between added mass and frequency shift and biosensors in cell biology and pharmacy. The second section will deal with epidemiology of the malaria disease, the biology of the parasite, describing the characteristic features of the invasion, release of merozoites of the *P. falciparum*, chemotherapy and drugs resistance. The third and final part will deal with the biological layer for the use with Quartz Crystal Microbalance.

2.1. BIOSENSOR

A biosensor is an analytical tool consisting of biologically active material used in close conjunction with a device that will convert a biochemical signal into a quantifiable electrical signal (*Kumar 2000*). Biosensors have many advantages, such as their simple and low-cost instrumentation, fast response times, minimum sample pre-treatment, and high sample throughput.

2.1.1 Mechanism of the biosensor

The receptor (biological part) is responsible for the selectivity of the sensor. The detector (physical transducer), translates the physical or chemical change by recognizing the analyte and relaying it through an electrical signal. The detector is not selective: the biological sensing element selectively recognizes a particular biological molecule through a physical or chemical process, specific adsorption, or a reaction, and the transducer converts the result of this recognition into a usable signal, which can be quantified (*Keusgen 2002, Kumar 2000*).

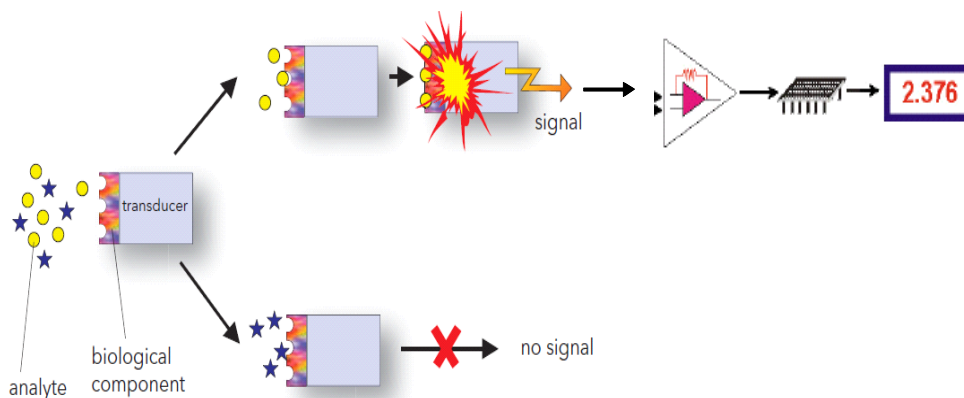


Figure 2-1. Principle of the function of a biosensor. One compound (circles) of a mixture of substances specifically interacts with the biological part of the sensor. The resulting biological signal is converted into a physical signal (e.g. electric, optical or electrochemical) by a transducer. The signal is amplified, processed and displayed. Substances incapable of interacting with the biological component will not produce any signal. Modified from (Bergeret 2004, Keusgen 2002)

As exemplified in Figure 2-1, a biosensor associates a bioactive sensing layer with any suitable transducer giving a usable output signal. Biomolecular recognition can be defined as the possibility of detecting analytes of biological interest, like metabolites, but also including drugs and toxins, using an affinity receptor which can be a natural system or an artificial one mimicking a natural one, able to recognize a target molecule in a complex medium among thousand of others (Blum 1991). To obtain a quantified output signal (correlated with the amount or concentration of the analyte present in the medium) multiple events must take place sequentially. Briefly, a first chemical or physical signal consecutive to the molecular recognition by the bioactive layer is converted by the transducer into a second signal, generally electrical, with a transduction mode that can be electrochemical, thermal, optical or based on mass variation (Blum 1991).

Table 2-1 summarizes a variety of biosystem-transducer combinations in terms of transducer, measurement mode and potential application.

Table 2-1 Biosensor Components (Kumar 2000)

<i>Transducer System</i>	<i>Measurement Mode</i>	<i>Typical Applications</i>
Ion-selective electrode	Potentiometric	Ions in biological media, enzyme electrodes
Gas-sensing electrodes	Potentiometric	Gases, enzymes, organelle, cell or tissue electrodes
Field-effect transistor	Potentiometric	Ions, gases, enzyme substrates, immunological analytes
Optoelectronic and Fiber Optic Devices	Optical	pH, enzymes, immunological analytes
Thermistors	Calorimetric	Enzymes, organelle, gases, pollutants, antibiotics, vitamins
Enzyme electrodes	Amperometric	Enzymes, immunological systems
Conductivity meter	Conductance	Enzyme substrates
Piezoelectric crystals	Acoustic (mass)	Volatile gases and vapors, antigen/antibody systems and other ligands/receptors

2.1.2. Analytical Applications of Piezoelectric Crystal Microbalance

2.1.2.1 Piezoelectric Effect

During their work on the discovery of radium, the Curies employed what they called a *quartz crystal balance*, with the first application of a piezoelectric device as a chemical sensor. Nowadays, the so-termed *quartz crystal microbalance* technique is well established in non-biological applications. The term piezoelectric describes the generation of electrical charges on opposing surfaces of a solid material upon deformation (torsion, pressure, bending, etc.) along an appropriate direction (Janshoff 2001).

Although a large number of crystals exhibit piezoelectricity, only quartz provides the unique combination for measuring mechanical, electrical, chemical, and thermal properties to make it usable (Janshoff 2001).

The core component of the device is a thin quartz disc, which is sandwiched between two evaporated metal electrodes used in this thesis, and is commonly referred to as *thickness shear mode resonator* (TSM resonator) or *bulk acoustic wave sensor* (BAW). As this quartz crystal is piezoelectric in nature, an oscillating difference in the potential between the surface electrodes leads to corresponding shear displacements of the quartz disc. The mechanical oscillation responds very sensitively to any changes that occur at the crystal surfaces (*Janshoff 2001*).

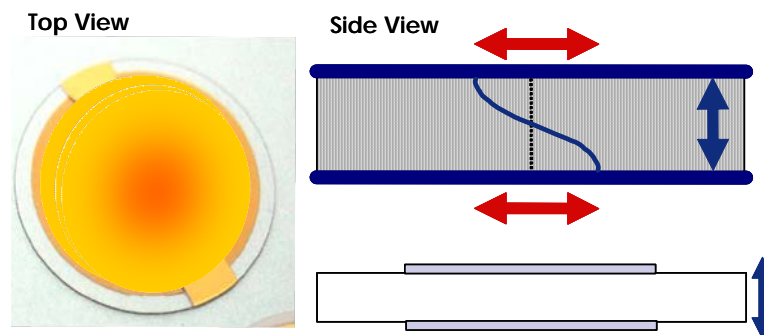


Figure 2-2. Mass-sensitive devices and acoustic wave propagation modes. Black arrows indicate particle displacement, white arrows wave propagation Modified from (Kaspar 2000)

Crystals have a natural vibration frequency, called resonant (or fundamental) frequency that depends upon their chemical nature, size, shape, and mass. Each vibration of a crystal involves its passing from a deformed configuration through its equilibrium configuration to an oppositely deformed configuration, and then back through the equilibrium configuration to the original configuration. This cycle occurs repeatedly as long as the crystal is vibrating (*Blum 1991*). The most well-known piezoelectric material is quartz (SiO_2). When the vibrating crystal is piezoelectric, this cycle of oscillating deformity produces an oscillating electrical field; the frequency of the electrical oscillation is identical to the vibration frequency of the crystal (*Blum 1991*).

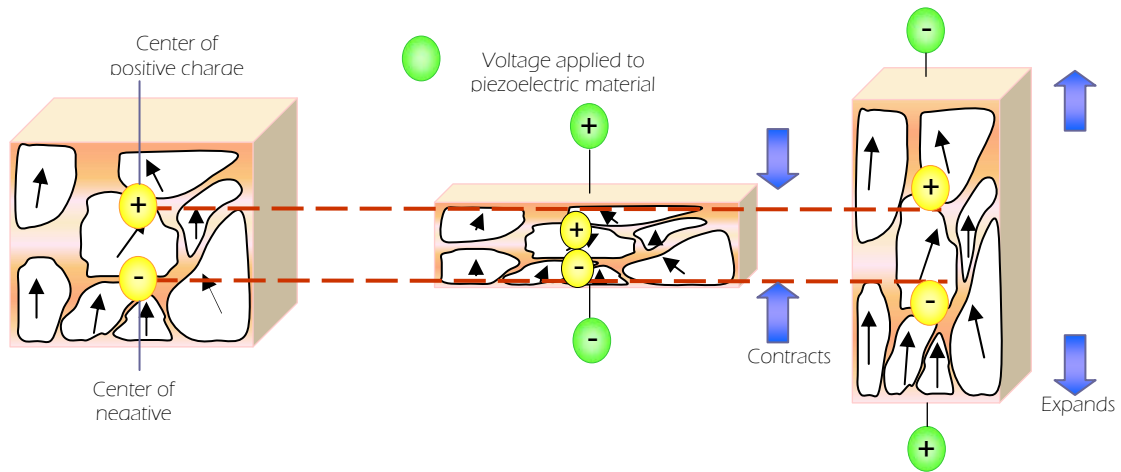


Figure 2-3. The piezoelectric effect. The Piezoelectric effect causes crystal materials like quartz to generate an electric charge when the crystal is compressed, twisted, or pulled. The reverse also is true, as the crystal material compresses or expands when an electric voltage is applied. Modified from (Johnston 2008).

For a crystal to exhibit the piezoelectric effect, this structure has to lack a centre of symmetry. Synthesized quartz (SiO_2) is therefore very suitable. The deformation forces its positive silicon and negative oxygen ions towards each other. The resultant shift in the centre of positive and negative charge generates an electric charge on the surface of the crystal. The orientation of the polar axes of the crystal with respect to the acting force determines the magnitude of the charge (Kistler). Three different effects can accordingly be discerned:

- Longitudinal Effect
- Shear Effect
- Transverse Effect

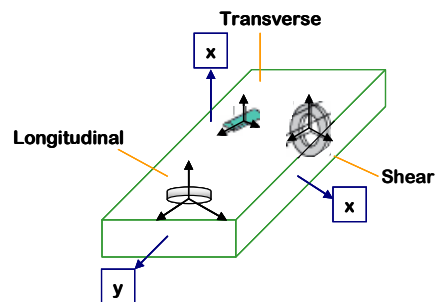


Figure 2-4. The orientation of the polar axes of the crystal. Longitudinal effect: occurs at the force contact surfaces and can be measured in this area. Transverse effect: a force F_y in the direction of one of the neutral axes y produces a charge on the surfaces of the corresponding polar axis x . Shear effect, similar to the longitudinal effect, the piezoelectric sensitivity occurring during the shear effect is independent of the size and shape of the piezoelectric element. The charge also occurs at the piezo element's surfaces under load. Shear-sensitive piezo elements are used for sensors measuring shear forces, torque and strain. Modified from (Kistler)

The piezoelectric effect can only happen in non-conducting materials. The characteristics of piezoelectric materials for sensor elements must exhibit very high mechanical strength

and rigidity above all else, as well as stable mechanical and electrical properties over a wide temperature range and a long service life. High sensitivity, good linearity, negligible hysteresis and high electrical insulation resistance are further advantageous characteristics (Kistler 2008).

2.1.2.2. The Piezoelectric Crystal

For use as a piezoelectric detector only AT- or BT-cut quartz plates are useful. AT and BT refer to the orientation of the plate with respect to the crystal structure ($35^{\circ}15'$ and $-49^{\circ}00'$, respectively)(Guilbault 1988). The AT-cut crystal is more stable than most other piezoelectric cuts and has a temperature coefficient of about $1 \text{ ppm} \cdot ^{\circ}\text{C}^{-1}$ over a temperature range of $10\text{--}50^{\circ}\text{C}$. These crystals operate in the TSM and are prepared by slicing a quartz wafer with the angle of $35^{\circ}15'$ to the optical z-axis (Figure 2-5). The AT-cut quartz shows a tremendous frequency stability of $\Delta f/f \approx 10^{-8}$ and a temperature coefficient which is close to zero between 0 and 50°C (Janshoff 2001).

The crystals most commonly used are 5, 9, or 10 MHz quartz of 10-16 mm disks, squares, or rectangles that are approximately 0.15 mm thick. The metal electrodes are 3,000–10,000 Å thick and 3–8 mm in diameter and can be made of gold, silver, aluminium, or nickel. For most applications the gold electrode is used because of its inert property (Blum 1991). For the research conducted here AT-cut ($35^{\circ}15'$) α -Quartz is used.

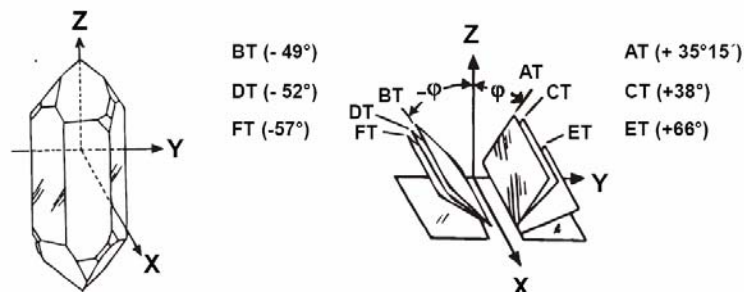


Figure 2-5. Cuts of α -quartz (Ikeda 1996)

The quartz wafer is sandwiched between two electrodes bonded to the wafer surface. These electrodes are used to induce an oscillating electrical field perpendicular to the surface of the wafer. The electrical field then produces a mechanical oscillation, a standing wave, in the bulk of the quartz wafer (Blum 1991).

Table 2-2 Physical parameters of the applied piezoelectric crystal (10MHz) (Gehring 2005)

Resonance frequency	F	10 MHz
Quartz-thick	ρ	2650 kg.m ⁻³
Quartz diameter		8,5 mm
Quartz diameter high/lower electrode		8 mm/ 5mm
Quartz thickness		0,166 mm
Acoustic impedance	Z_q	8,77.10 ⁶ kg.m-2s ⁻¹
Propagation speed	v_{tr}	3310 m.s ⁻¹
Penetration depth (H ₂ O)	δ	179 nm

2.1.2.3. Relationship between added mass and frequency shift

The basic equations describing the relationship between the resonant frequency of an oscillating piezoelectric crystal and the mass deposited on the crystal surface have been derived by Sauerbrey (Appendix 1).

The Sauerbrey equation relies on a linear sensitivity factor, Cf, which is a fundamental property of the QCM crystal. Thus, *in theory*, the QCM mass sensor does not require calibration. However, it must be kept in mind that the Sauerbrey equation is only strictly applicable to uniform, rigid, thin-film deposits (*Stanford Research System 2006*).

This Sauerbrey model is exclusively applicable to use of quartz oscillators in vacuum. It does not sufficiently define the behaviour of the quartz in the liquid phase.

When the QCM comes in contact with a solution, there is a decrease in frequency that is dependent upon the viscosity and the density of the solution. A quantitative understanding of the resonator behaviour is a prerequisite for proper interpretation of experimental results under total liquid immersion (*Stanford Research System 2006*). This aspect was first treated by Glassford (*Glassford 1978*), and later by Kanazawa and Gordon (*Kanazawa 1985*)

Kanazawa's treatment of the influence of the solution properties on the crystal permits the prediction of the change in resonance frequency which accompanies immersion of the crystal into a viscous medium (Appendix 1)

In a separate study (Martin 1991), a Butterworth-Van Dyke equivalent circuit model was applied to derive a linear relationship between the change in series resonance resistance, ΔR , of the quartz oscillator and $(Q_L \eta_L)^{1/2}$ under liquid (Appendix 1).

2.1.3. Biosensors in cell biology and pharmacy

Originally QCM was developed for molecular adsorption at the gas-solid interface after Sauerbrey 1959 (Sauerbrey 1959) identified the existence of a linear relationship between mass addition at the piezoelectric substrate surface and change in the recorded resonant frequency (Elsom 2008). Techniques in liquid phase and their biological applications such as characterisation of protein adsorption (Höök 1998), ligand-receptor interactions (Janshoff 1997), QCM based immunoassay (Aizawa 2001) and nucleic acid hybridisation (Furtado 1998) were developed.

The QCM is widely used in cellular biology to monitor cell-surface interaction in a dynamic and non-invasive way, without compromising cell architecture or the structure of proteins. Thence, the ability of this technique to monitor adhesion and proliferation of numerous cells *in situ* on the QCM surface has been proven.

Preliminary studies identified that integrin-mediated cell adhesion was detected by the surface of the detector. Progress in the topic stated has determined that this technique was sufficiently sensitive to discriminate amongst different substrata (as crystal surface modifications) and their impact on the adhesion processes of the cells, providing a level of QCM technology as a routine control tool in the field of biomaterials (Lord 2006) and in microbial biofilm research (Miečinskas 2007, Reipa 2006).

Taking into account the aforementioned, the advantages of quartz crystal microgravimetry (QCM) or quartz crystal nanogravimetry include high sensitivity (ng cm^{-2}), continuous data *in situ*, possibility to monitor the processes non-destructively, as well as to combine the measurements with other techniques (voltammetry, EIS, optical spectroscopy,

citometry, etc.), thus providing a wide range of possibilities for the study of infectious diseases, like the case of the present research.

Studies of Gehring (*Gebring 2005*), Claußen (*Claußen 2006*) have successfully demonstrated applications of QCM for blood type determinations using a newly developed device. Scheufele (*Scheufele 2009*) demonstrated a novel method for detection of antibodies in blood using the same device. These studies have opened the possibility to test new applications of this technique for the study of infectious diseases. In our case, studies of the erythrocyte life cycle of *P. falciparum*, particularly during the last six hours preceding the merozoite release and studies related to reinfection of free merozoites are the focus of our investigation.

Many biosensors have been successfully applied in the pharmaceutical industry not only for process monitoring or control, but also for the discovery and activities of new targets of drugs. The advantage of being able to directly detect small molecules or effects of the interaction to molecular recognition elements on the crystal surface make the technique well suited for a variety of biosensor applications in the area of drug discovery (*Kenneth 2007*). A number of recent reviews describe such applications (*Cooper 2005, Ghafouri 2001, Kenneth 2003, Pavey 2002*). These drug discovery approaches involve the specific detection of individual small analyte molecules of pharmaceutical interest. The drug characterization and the drug target-based assays involve important cell surface protein receptors to monitor drug effects using immobilized living cells (a cell biosensor) (*Kenneth 2007*).

2.2. MALARIA

2.2.1. Epidemiology

Malaria is probably one of the oldest diseases known to mankind recorded in history. The prehistoric man was infected and we are still at risk, despite all the efforts to eradicate the disease in the last 100 years (*Wahlgren 1999*). Malaria is more frequent today than ever and the death toll is increasing though certain areas of the world are less exposed. Although enormous and diverse efforts to control this disease have been made, malaria is among the top three most deadly communicable diseases and the deadliest tropical parasitic disease today (*Sachs 2002*). The management strategies to control malaria include chemotherapeutic agents, insecticides, vector control, education, development of vaccines and bed nets treated with insecticides. The combination therapy has shown an increase in efficacy by combining drugs (*Touré 2004*). The Global Malaria Eradication Program (GMEP) originally considered elimination feasible in countries with malaria of low or intermediate stability. World Health Organisation (WHO) downgraded the GMEP to Malaria control because many countries had experienced difficulties in initiating or sustaining national programs, often because of inadequate national commitment. Nevertheless, several countries successfully eliminated malaria, demonstrating that this goal remains a feasible option for other malaria-endemic countries (*Wernsdorfer 2009*). However, the malaria situation has deteriorated and mortality from malaria is probably increasing in sub-Saharan Africa due to factors such as drug resistance, insecticide resistance, war or civil disturbance, environmental changes, climatic changes, and increases in travel and population (*Aultman 2002, Greenwood 2002*). Malaria is responsible for 273 million clinical cases and 1.12 million deaths annually. More than 40% of the global population (>2.1 billion people) is estimated to be at risk (*Touré 2004*). Some statistics usually differ because, on some occasions, deaths caused by Malaria occur at home, lots of cases are misdiagnosed and microscopes are not available in all endemic areas. (*Greenwood 2002*).

Successful elimination of Malaria disease has been the result of different strategies, amongst which there are changes in construction and in agricultural practices, avoiding the formation of water deposits and the use of insecticides such as DDT (*Greenwood 2002*). Construction and industrialisation have also been instruments for the elimination of the disease in temperate countries (*Budiansky 2002*). Windows and walls have helped minimise

the contact of people with mosquitoes, thus being a contributing factor for eradication programmes as well. The importance of the mosquito in the life cycle of *P. falciparum* requires that the parasite be able to maintain an extended infection in order to ensure transmission ability during the following season (Kyes 2001). Changes between seasons result in low reproduction levels for the mosquito (Sachs 2002).

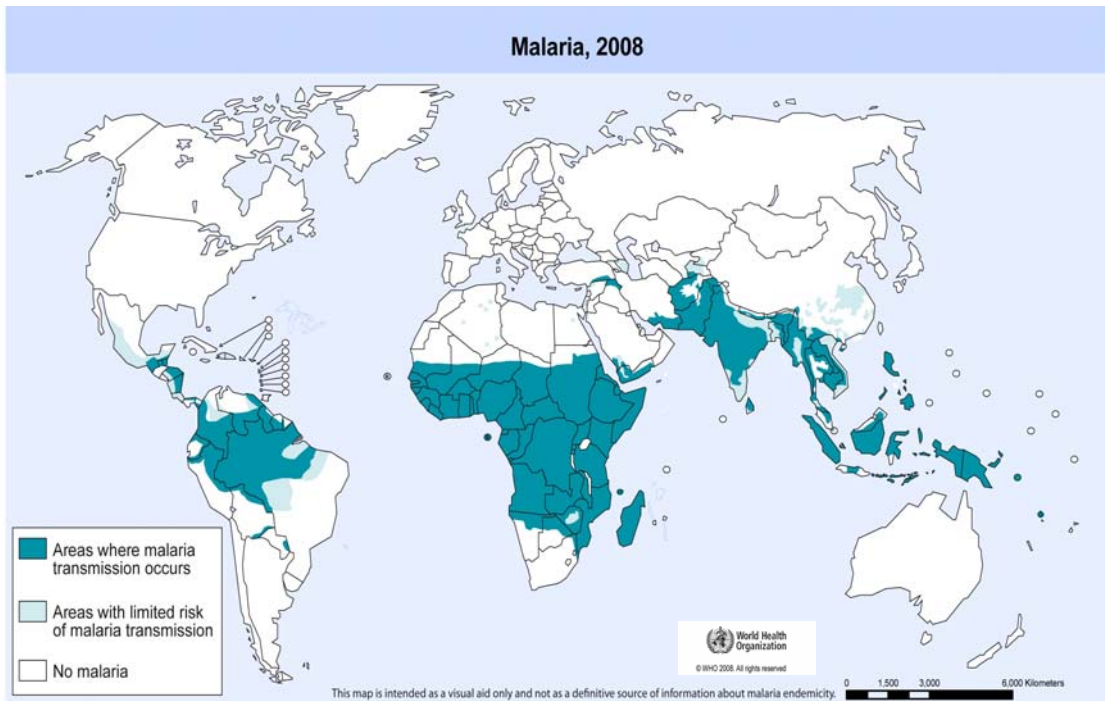


Figure 2-6. Geographical distribution of Malaria. 2008. The boundaries and names shown and the designations used on this map do not imply the expression of any opinion whatsoever on the part the World Health Organisation concerning the legal status of any country, territory, city or area of its authorities, or concerning the delimitation of its frontiers or boundaries. Dotted lines on maps represent approximate border lines of which there may not yet be full agreement. Taken from (WHO 2009).

2.2.2. Biology of the parasite

Malaria is caused by single-celled protozoan parasites of the genus *Plasmodium* (Touré 2004). Four species of *Plasmodium* that naturally infect humans, *P. vivax*, *P. malariae*, and *P. ovale* cause severe morbidity, whereas *P. falciparum* is responsible for nearly all malaria-specific mortality. Nowadays *P. knowlesi* is included. Two important characteristics of *P. falciparum* infection contribute to this virulence. First of all, it achieves much higher levels of parasitaemia than the other species, and second of all, it possesses the unique property of sequestration. Red blood cells infected with young forms of the parasite circulate freely, whereas erythrocytes infected with the more mature forms of the parasite

are bound to endothelial cells and thus are sequestered away from the peripheral circulation (Kyes 2001). Young forms have however also been found to show a type of adherence to endothelial cells (Lekana 2002).

Plasmodium is a protozoan parasite classified under the phylum Apicomplexa which also includes parasites like *Toxoplasma*, *Eimeria* and *Cryptosporidium*, all of which are endowed with a specialised apical complex for host cell invasion (Ramya 2002).

Malaria parasites undergo three distinct asexual replicative stages (exoerythrocytic schizogony, blood stage schizogony, and sporogony) (Figure 2-7), resulting in the production of invasive forms (merozoites and sporozoites) characterized by the apical organelles typical of apicomplexan species (Wiser 2008).

The interest of the study presented in this paper focuses on the release and invasion of merozoites, which are described in detail below.

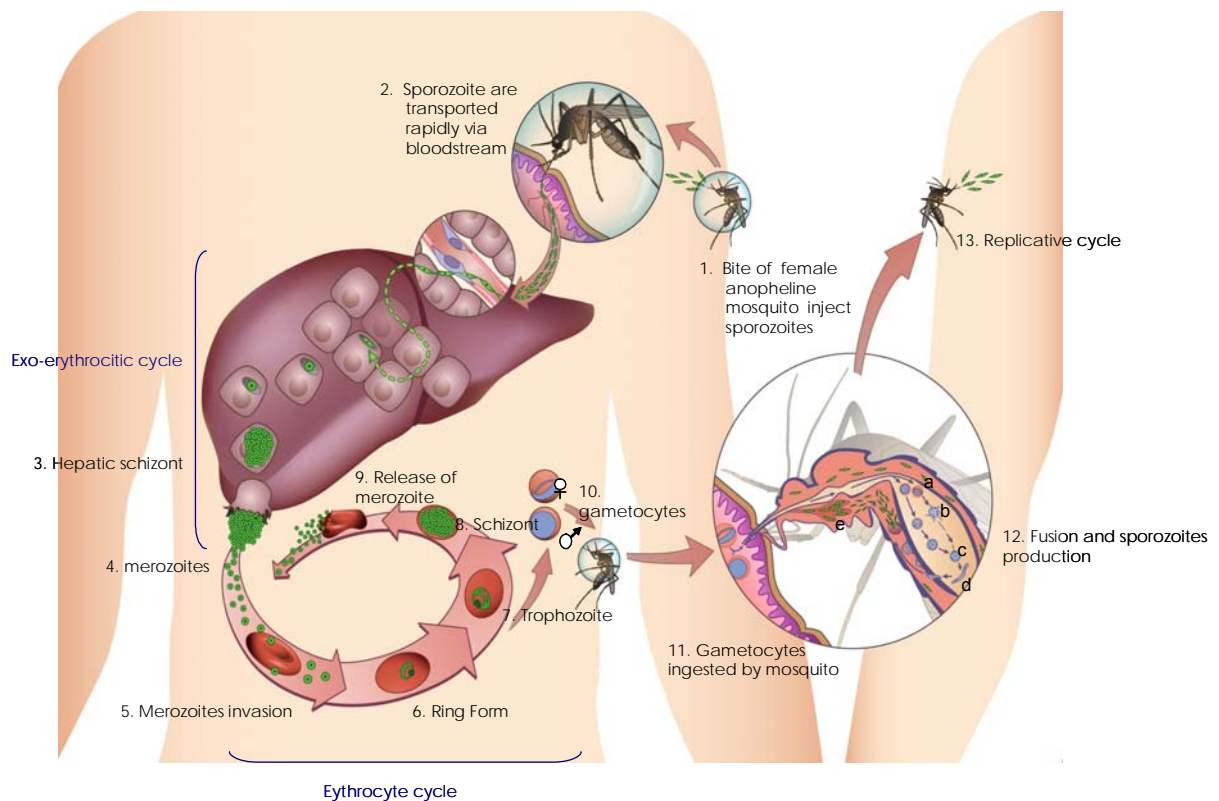


Figure 2-7. Life cycle of *Plasmodium falciparum*. The bite of an infected female anopheline mosquito injects sporozoites into the vertebrate host (1), where they are transported rapidly via the bloodstream to hepatocytes in the liver (2). Within hepatocyte, a parasite matures, differentiates (schizont), (3) and undergoes several rounds of asexual division, forming many thousands of infective haploid merozoites (4) that are released into the bloodstream. The time taken for this to occur is species-dependent (2–15 days) and does not give rise to any clinical symptoms, the so-called prepatent period. The released merozoites immediately (within seconds) invade host red blood cells (5) and again undergo a process of growth and asexual division (6-9) to produce 6–32 daughter merozoites over a period of 24–72 h depending on the species. When the daughter merozoites are fully mature (the schizont stage), the red cell bursts, releasing the merozoites to invade other erythrocytes (9). As an alternative to the asexual replicative cycle, the parasite can differentiate into sexual forms known as macro- or microgametocytes (10). Ingestion of gametocytes by the mosquito vector induces gametogenesis (i.e., the production of gametes) and escape from the host erythrocyte (11). Fusion and sporozoite production (12): Microgametes (a), formed by a process known as exflagellation (b), are flagellated forms which will fertilize the macrogamete leading to a zygote (c). The zygote develops into a motile ookinete (d) which penetrates the gut epithelial cells and develops into an oocyst (e). The oocyst undergoes multiple rounds of asexual replication resulting in the production of sporozoites. Rupture of the mature oocyst releases the sporozoites into the hemocoel (i.e., body cavity) of the mosquito. The sporozoites migrate to and invade the salivary glands, thus completing the life cycle. This cycle is replicative (13). (Kyes 2001, Matteelli A.)

2.2.2.1. Invasion of Merozoites

2.2.2.1.1. Structure of Merozoite

The merozoite is a life stage of a protozoan parasite belonging to the phylum Apicomplexa. Apicomplexan parasites are obligate intracellular protozoan organisms which, depending on the species, are able to invade a wide range of different host cells. A common feature of all members of this phylum is the unique collection of organelles found at the anterior end of their invasive forms (Preiser 2000).

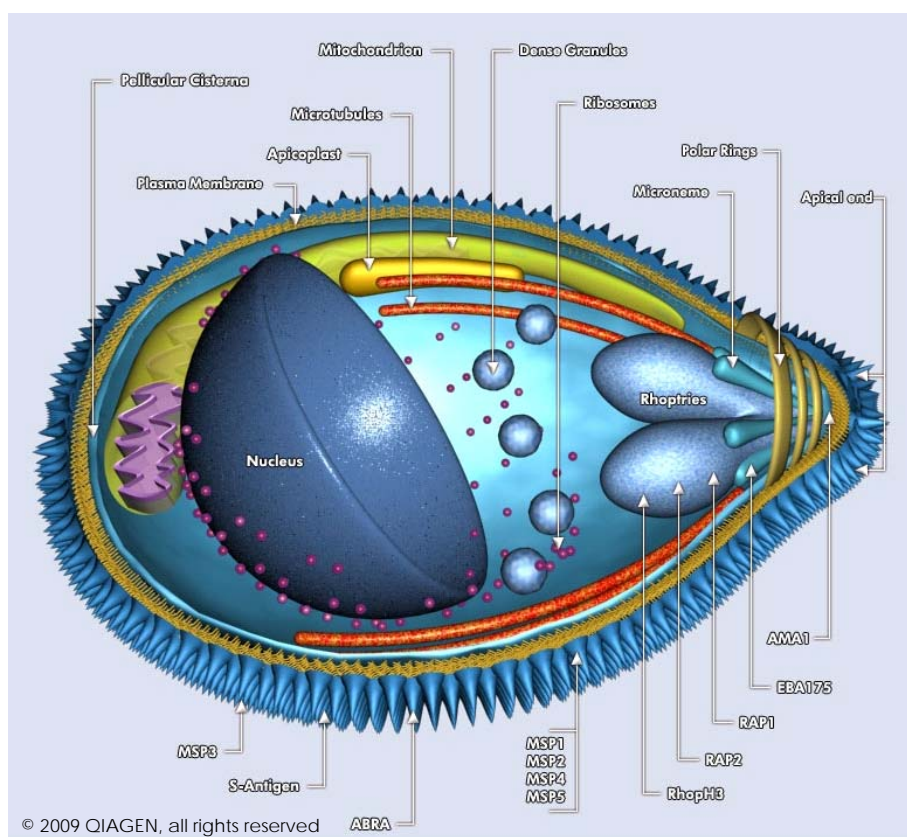


Figure 2.8 Structure of Merozoite (*Plasmodium falciparum*). Size $1.0 \mu\text{m}$. Taken from (Qiagen 2003b). Within the cytoplasm of the merozoite are found: the rhoptries, a pair of electron-dense, membrane-bound pear-shaped and ducted structures; micronemes, several small fusiform bodies that are attached to the rhoptry duct and dense granules, up to 20 (depending upon the parasite species) rounded structures present in all parts of the cytoplasm (Preiser 2000).

The structure of the merozoite (Figure 2-8) shows various organelles which are essential for the invasion process. Studies through electron microscopy (Bannister 1990, Bannister 1986b, Torii 1998) have stated the structure and function of each one of them during the invasion moment. The rhoptries organelles are pear-shaped membrane-bound vesicles occupying

the apical end of the merozoite. In mature stage, the rhoptry consists of two parts: an electron-dense rounded basal bulb and a somewhat less dense tapering rhoptry duct that ends blindly just beneath the plasma membrane covering the apical prominence. It is approximately 550 nm long and has a diameter of about 250 nm. The Micronemes, much smaller than rhoptries, vary in precise shape and numbers between species. In *P. falciparum* they are fusiform sacs about 120 nm long attached at one end to the rhoptry duct and fanning out into the apical cytoplasm of the merozoite. They are bounded by a typical cytoplasmic membrane, and have a fine granular interior. The Dense Granules (DGs), are spheroidal membranous vesicles, and they vary in size, according to the species of *plasmodium* (~80 nm in diameter) (Preiser 2000). Table in Appendix 2, presents the different proteins included in the organelles of the merozoite. Other membrane proteins also present are involved in the invasion process as merozoite surface protein (MSP)-1 (greater proportion), -2,-3 and -4 (Marshall 1997). Once the proteins of the organelles are secreted, the latter change their characteristics and thus the rhoptries discharge the tips of the ducts fuse with each other as well as with the merozoite plasma membrane, and the rhoptries become irregular in shape as they collapse. Micronemes disappear and dense granules move to the surface of merozoite (Preiser 2000).

Secretion times for the proteins contained in such structures vary according to the moment of invasion, so when the parasite gets in contact with the host cell surface, micronemes trigger calcium ion release and the discharge of the content of the micronemes, which then mediates parasite attachment. Release of rhoptry contents takes place immediately after adhesion of the parasite to the host cell surface in approximately 60 seconds and the molecules are internalized to form part of the PVM. In contrast to secretion of rhoptries and micronemes, which takes place at the apex of the invasive form, DGs release their contents at a subapical location of the parasite by fusion of the DGs membrane with the parasite plasma membrane (Kats 2008).

The secretion of these proteins occurs because of different aspects: (a) promoting exit from the schizont, a process which can be blocked by protease inhibitors (Hadley 1983), implying a protease component in either the micronemes or rhoptry duct; (b) selective adhesion to an appropriate red cell surface involving erythrocyte binding ligands and, where relevant, the Duffy binding protein from the micronemes; (c) localised uncoupling of the red cell cytoskeleton from the red cell membrane (perhaps again a protease-

dependent process likely to be related to micronemes or rhoptry duct proteins); (d) insertion of rhoptry components such as Rhop-1 (*Sam-Yellowe 1988*), and/or other rhoptry proteins and lipids into the red cell membrane, causing its expansion and invagination to form the parasitophorous vacuole; (e) finally, insertion of dense granule proteins into the parasitophorous vacuole membrane to cause its further expansion, and the movement of the ring infected erythrocyte surface antigen into the red cell cytosol to modify the red cell cytoskeleton (*Preiser 2000*).

2.2.2.1.2. Process of invasion

The merozoite form of the asexual life cycle in the blood stage attaches to the surface of the red blood cell (RBC) thus initiating the invasion process of this host cell. Inside the RBC the parasite replicates and matures into a schizont form which eventually ruptures to release new merozoites and complete the blood stage cycle (*Cowman 2000*). The invasion process presented in Figure 2.9 shows the various sequences of invasion which last ~60 s (*Cowman 2006*).

Morphological studies at the light and electron microscopy levels have revealed that invasion is a sequential, multistep process (*Bannister 1990, Dvorak 1975, Miller 1979*). Once the erythrocyte enters in contact with the merozoite, the merozoite attaches and orients its anterior end towards the erythrocyte. A region of tight apposition, or ‘junction’, develops between the membranes of the two cells. Membrane-bound organelles at the anterior end of the merozoite, the rhoptries, discharge their contents onto the erythrocyte surface, which begins to indent at the point of contact. The junction transforms from a localized patch to an orifice, through which the merozoite penetrates into a progressively deepening, membrane-bound vacuole. The membrane surrounding the fully internalized parasite is known as the parasitophorous vacuole membrane (PVM) (*Ward G. 1993*).

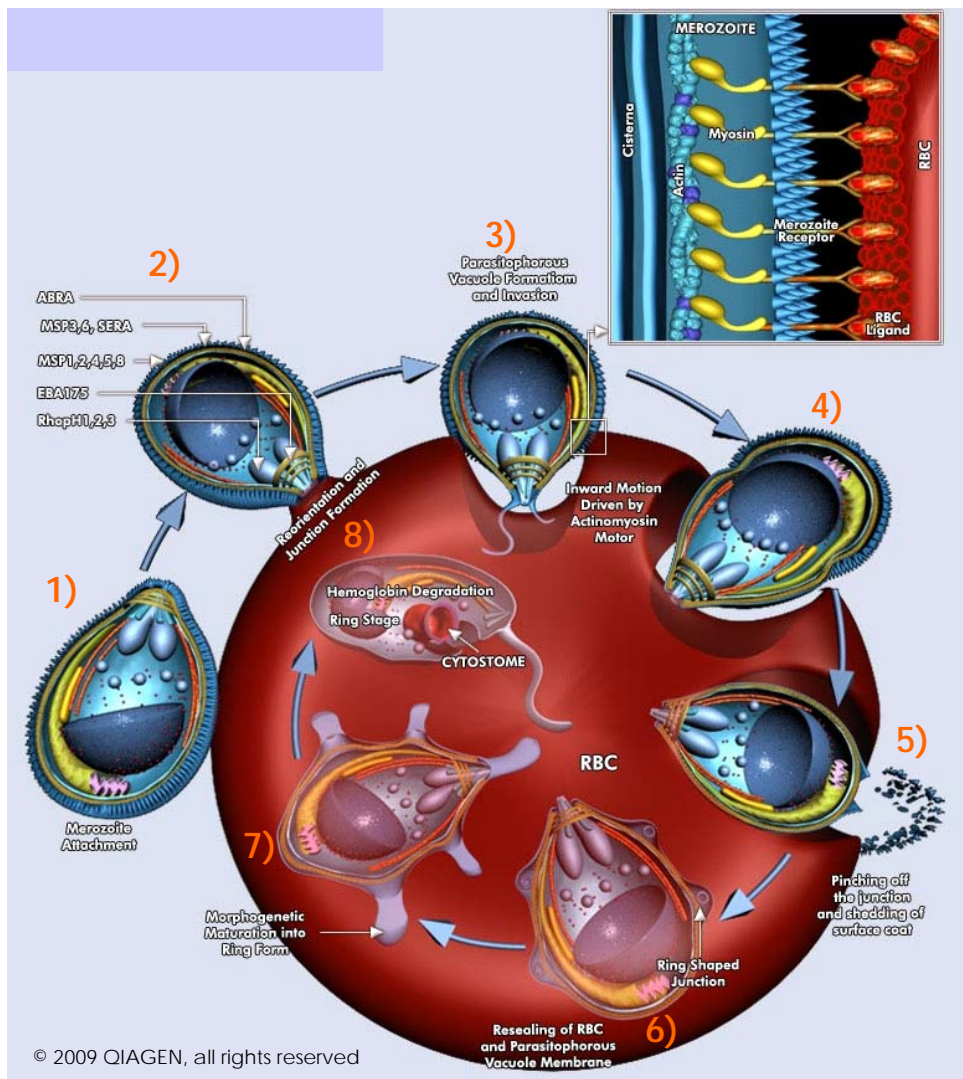


Figure 2-9. Merozoite invasion. (1) attachment of the merozoite to the RBC by any part of the parasite's surface (recognition of surface receptors); (2) re-orientation and tight junction formation involving high-affinity ligand, of the apical end of the merozoite towards the RBC membrane; (3, 4) This tight junction then moves from the apical to posterior pole powered by the parasite's actin-myosin motor. The surface coat is shed at the moving junction by a serine protease, or "sheddase". Upon reaching the posterior pole, the adhesive proteins at the junction are also proteolytically removed; (5) this time by a resident protease, most likely a rhomboid, in a process that facilitates penetration of the membrane. By this process, the parasite does not actually penetrate the membrane but invades in a manner that creates a parasitophorous vacuole; (6, 7, 8) development erythrocyte cycle of plasmodium. (Cowman 2006, Pasvol G. 2003, Qiagen 2003a). Graph taken from Quiagen.

PVM formation mechanism is unknown, though several studies propose many: One model is that PVM is formed during invasion by invagination of the erythrocyte membrane itself, rather than created *de novo* from material stored in the parasite. Alternatively, PVM may be formed by derivation from the parasite. In this model, the rhoptries contain a large store of lipid that is secreted in a controlled fashion and inserted into the erythrocyte plasma membrane during invasion (Bannister 1989, Bannister 1986b, Ward G. 1993).

The invasion of merozoite into the erythrocyte is another topic for study, but the movement of the parasite inside the vacuole has been found, apparently enveloping itself in a portion of host cell membrane (Bannister 1986a). At the same time, an electron-dense annular junction moves backwards over the parasite surface until internalisation is completed (Aikawa 1978). The origin of the driving force that impels the attached merozoite into the cell is unclear, but the action of the actin capping and depolymerising agent, cytochalasin B, argues for the participation of actin and thus for the existence of an actomyosin motor (Pinder J.C. 1998). Actin filaments inside the parasite were observed by Field (Field 1993). In fact, several cell processes are actin-dependent.

2.2.2.2. Release of Merozoites

Once the erythrocyte has been invaded, the development of the parasite begins. This includes the various stages of asexual replication shown in Table 2.4, with its morphological descriptions.



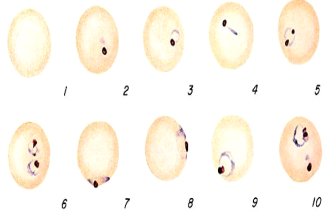
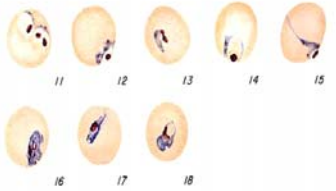
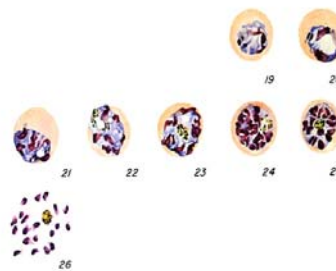

Figure 2-10. The asexual, blood stage of *Plasmodium falciparum*. Characterized by ring, trophozoite, and schizont forms of the parasite. Taken from (MedPedia. 2007)

The duration of the erythrocyte cycle varies amongst species and, for the case of *P. falciparum*, this one lasts ~48 hours. After invasion, the parasite flattens into the thin discoidal, flat or cup-shaped **ring** form of the trophozoite stage. The organelles of the erythrocyte are observed: Endoplasmic reticulum (ER), Golgi apparatus, nucleus, mitochondria and others. Due to the perimeter of cell swelling and the position of the nucleus, observations through Giemsa show this structure as a ring, thereby deriving its name.

Haemoglobin catabolism yields a haem derivate (ferriprotoporphylin IX) which is converted into inert brown haemozoin crystals that accumulate within the pigment vacuole throughout the erythrocytic phase of the life cycle. This phase can last ~26 hours, continuing with the erythrocytic development of the parasite, the **trophozoite**. The distinction between this stage and that of the ring depends on the cell, size and shape rather than any fundamental internal difference, and indeed the ring is more properly called the ring form of the trophozoite stage. Changes in the modifications of the internal structures of the erythrocyte caused by the export of parasite proteins (Golgi body, exocytic vesicles) starts to be observed. The surface area of the trophozoite is extended with the formation of a surface of irregular bulges and deep tubular invaginations. The export mechanism of protein remains unclear; though it is known that these proteins are incorporated into the growing area of the PVM, others traverse this barrier to pass as dense aggregates, often associated with Maurer's clefts, through the RBC cytosol to its surface, where they bind to the RBC cytoskeleton and membrane. Some of these proteins produce small angular elevations (knobs) on the RBC surface, which increase the adhesion of the parasited RBC membrane in deep visceral blood vessels, and the pathogenic obstruction of placental and cerebral vasculature (*Bannister 2004*). This development lasts ~12 hours. After the trophozoite, develops in the **schizont** stage.

A schizont is an intraerythrocytic parasite that is undergoing or has undergone repetitive nuclear division (*Bannister 2000*). In this stage, the ingestion of haemoglobin is almost total, adding more haemozoin crystals to the vacuole, which can be observed as a compact and dense pigment (Table 2-4). The surface of the erythrocyte becomes fairly irregular, distorting the cytoskeleton and membrane of the cell, with an increase in the number of knobs at its surface. The surface of the RBC often becomes quite angular in profile, as the exported parasite proteins distort the cytoskeleton and membrane of the cell, in addition to increasing the numbers of knobs at its surface. The nuclear division is accompanied by numerous cytoplasmic changes through the parasite, multiplication of mitochondria and plastids, and accumulation of one or more large lipid vacuoles. Numerous merozoite formation centres are created, assembling apical organelles in an established order and sequence. The merozoites appear in small sacs in a number of 16-32. (*Bannister 2004, Miller 2002, Wiser 2008*).

Table 2-4 Comparison of stages found in blood (*Plasmodium falciparum*).
Modified from (Abdalla 2004)

Stages found in blood	Images	Appearance of Erythrocyte (RBC)	Appearance of Parasite
Ring		normal; multiple infection of RBC more common than in other species; Maurer's clefts (under certain staining conditions)	Are often thin and delicate, measuring on average 1/5 the diameter of the red blood cell. Rings may possess one or two chromatin dots. They may be found on the periphery of the RBC (accolé, appliqué) and multiply-infected RBCs are not uncommon. Ring forms may become compact or pleomorphic depending on the quality of the blood or if there is a delay in making smears.
Trophozoite		normal; rarely, Maurer's clefts (under certain staining conditions)	seldom seen in peripheral blood; compact cytoplasm; dark pigment. Developing trophozoites of <i>P. falciparum</i> tend to remain in ring form, but may become thicker and more compact. The amount of pigment and chromatin may also increase. Compact or amoeboid forms may be seen in smears where there was a delay in processing the blood.
Schizont		normal; rarely, Maurer's clefts (under certain staining conditions)	Are rarely seen in peripheral blood of <i>Plasmodium falciparum</i> infections, except in severe cases. When seen, schizonts contain anywhere from 8-24 merozoites. A mature schizont usually fills about 2/3 of the infected RBC.
Gametocyte		distorted by parasite	Are crescent- or sausage-shaped, and are usually about 1.5 times the diameter of an RBC in length. The cytoplasm of the macrogametocytes (female) are usually a darker, deeper blue; the cytoplasm of the microgametocytes (male) is usually more pale. The red chromatin and pigment is more coarse and concentrated in the macrogametocytes than the microgametocytes. Sometimes in thin blood smears, the remnants of the host RBC can be seen; this is often referred to as a "Laveran's bib".

There are three ways proposed for merozoite release: (1) fusion of erythrocyte and parasitophorous vacuolar membranes (PVM) creating an opening for the merozoites to escape (*Clavijo 1998, Sherman 2004, Winograd E. 1999*); (2) liberation of parasites enclosed within the vacuole from the erythrocyte followed by PVM disintegration (*Salmon 2001*); (3) PVM first resulting in release of merozoites into what remains of the erythrocyte cytoplasm, followed by EPM breakdown resulting in release of merozoites into what remains of the erythrocyte cytoplasm, followed by EPM breakdown (*Wickham 2003*). The two latter were evaluated with the use of protease inhibitors. Glushakova reinterprets and reevaluates these three models, and proposes that the egress is preceded by breakdown of the erythrocyte cytoskeleton (and perhaps also weakening and fragmentation of the PVM), which, along with an increase in schizont volume during development, converts the infected cell into the distinctive ‘flower’ shape. Finally, the PVM and EPM quite literally blow apart, scattering the merozoites and forcing them into contact with new erythrocytes (*Glushakova 2005*).

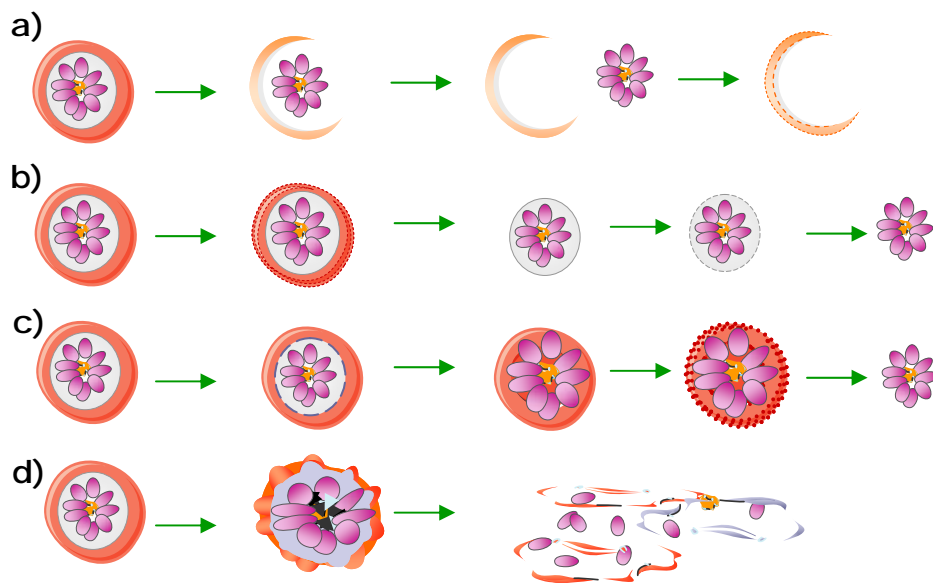


*Figure 2-11. Models for the release of Plasmodium merozoites from their host erythrocytes. (a) Membrane fusion. The erythrocyte plasma membrane (EPM, red) and parasitophorous vacuole membrane (PVM, gray) fuse, creating an opening through which clustered merozoites (blue) pass. The erythrocyte ghost then degrades over time (*Winograd E. 1999*). (b) Membrane breakdown: EPM first. Exported Plasmodium proteases break down the EPM and cytoskeleton first, releasing the entire PVM with the merozoites still contained inside. PVM breakdown then occurs in a second step, releasing invasive merozoites (*Salmon 2001*). (c) Membrane breakdown: PVM first. Exported Plasmodium proteases break down the PVM first, releasing the merozoites and any protein contents of the parasitophorous vacuole into the erythrocyte cytoplasm. The EPM and erythrocyte cytoskeleton then break down in a second step, releasing invasive merozoites (*Wickham 2003*). (d) Exploding flowers. An increase in merozoite size and concurrent breakdown of the erythrocyte cytoskeleton by exported Plasmodium proteases force the EPM and PVM into a distinctive ‘flower’ structure. Within minutes, the physical pressure blows the infected cell apart, scattering both the invasive merozoites and the remnants of the EPM and PVM, which remain largely segregated (*Glushakova 2005*). Modified from (*Rayner 2006*).*

It is interesting to point out that the merozoites of the *P. falciparum* raise interest as research study objects since, unlike other apicomplexan zoites stages, the *P. falciparum* will not glide on inert substrates, and may be motile only when a host cell is encountered. Microscopic studies explain this phenomenon; there is little need for merozoites to be motile when they exist in a circulating system with uninfected erythrocytes continually brushing past them and when the process of erythrocyte exit itself appears to literally throw the merozoites into contact with those erythrocytes (Mitchell 1988). Erythrocyte exit by *Plasmodium* merozoites therefore clearly bears some relation to host cell exit by other apicomplexan zoites, but in several crucial aspects might represent a unique case (Rayner 2006).

Amongst the studies of proteases during the erythrocyte exit, one class is found that can be inhibited with the cysteine-protease-specific inhibitor E64, which acts to break down the PVM; and second class that can be inhibited with the more general protease inhibitors leupeptin and antipain, which break down the EPM and/or components of the erythrocyte cytoskeleton (Salmon 2001, Wickham 2003). Numerous candidate proteases have been identified that could function in either of these roles (Rosenthal 2004), but the definitive association of any given protease with a specific erythrocyte exit function awaits further studies.

2.2.3. Chemotherapy and drug resistance

Several antimalarial drugs are available. Many factors are involved in the decision of the major treatment for malaria like the species of the parasite, the severity of the disease (e.g. complicated type), the age of the patient, the immune status, susceptibility to different drugs, the cost and the availability of the drugs. Likewise, different drugs act differentially to the various life cycle stages (Wiser 2008).

In the continuing absence of clinically proven vaccines, preventing or treating malaria parasite infections in the human host has always depended heavily upon chemoprophylaxis and chemotherapy (Hyde 2007). According to a WHO report issued in 2001, there are only a limited number of drugs which can be used to treat or prevent malaria (Bloland 2001). The most widely used are: quinine and its derivatives (chloroquine, amodiaquine, mefloquine); antifolate combination drugs (combinations of dihydrofolate-

reductase inhibitors: proguanil, chlorproguanil, pyrimethamine, and trimethoprim and sulfa drugs dapson, sulfalene, sulfamethoxazole, sulfadoxine, and others); atovaquone (in combination with proguanil); artemisins and its derivatives (artesunate, artemether, arteether). It has also been observed that the use of two antimalarials simultaneously, especially when the antimalarials have different mechanisms of action, has the potential for inhibiting the development of resistance to either of the components (*Bloland 2001, Kremsner 2004*).

Fast-acting blood schizontocides, which act upon the blood stage of the parasite, are used to treat acute infections and to quickly relieve the clinical symptoms. Chloroquine is recommended for the treatment of patients with *P. vivax*, *P. ovale*, *P. malariae*, and uncomplicated chloroquine-sensitive *P. falciparum* infections. Primaquine (a tissue schizontocide) is effective against the liver stage of the parasite, including hypnozoites, and will prevent future relapses. The combination of chloroquine and primaquine is often called 'radical cure'. Severe, or complicated malaria requires urgent treatment. Treatment typically requires parenteral drug administration (i.e. injections) since the patients are often comatose or vomiting, and thus cannot take the drugs orally (*Wiser 2008*).

Antimalarial drug resistance is defined as the “ability of a parasite strain to survive and/or multiply despite the administration and absorption of a drug given in doses equal to or higher than those usually recommended but within tolerance of the subject” though the “gain access to the parasite or the infected red blood cell for the duration of the time necessary for its normal action” (*Bloland 2001, Bruce-Chwatt 1986*) has also been included. Resistance of malaria parasites arises from several factors, including overuse of antimalarial drugs for prophylaxis, inadequate or incomplete therapeutic treatments of active infections, a high level of parasite adaptability at the genetic and metabolic levels, and a massive proliferation rate that permits selected populations to emerge relatively rapidly (*Hyde 2007*). This resistance to antimalarial drugs is a vitally important public health concern (*Wongsrichanalai 2002*).

There are two issues particularly relevant to the future scenario of drug-resistant malaria: new antimalarial regimens and the use of molecular information for the control of parasite drug resistance. Within the new administration regimen of drugs, there is the combination of antimalarial drugs: (chloroquine plus sulfadoxinepyrimethamine, artesunate plus sulfadoxine-pyrimethamine, artesunate plus mefloquine, chlorproguanil plus dapson)

[LAPDAP]), and those involving new agents (artemether plus lumefantrine [Coartem, Riamet]). However, the efficacy of combinations involving old drugs may be short-lived, since resistance-conferring mutations already exist (*Wongsrichanalai 2002*). In the second aspect of the use of molecular information, taking advantage of the discovery of the genome sequence of *P. falciparum*, it is likely that more alleles that lead to drug resistance can be identified. This information will lead to the knowledge of new drug targets, allow the construction of an effective vaccine, or the designing of a tool for rapid diagnosis of antimalarial resistance.

2.2.4. IMMOBILISATION ERYTHROCYTES FOR THE ANALYSIS WITH QCM

When immobilised biological components are used to detect any targets of the QCM, the recognition sites of both, immobilization receptor layer and target must have specific properties to enable detection by the biosensor system.

The development of a piezoelectric sensor should be directed towards three aspects: (1) Functionalisation of the piezoelectric signal, (2) Specificity and reproducibility of the experiments and (3) Possible regeneration of the sensor surface (*Claußen 2006*).

In other words, the biological component or the biological analyte have certain properties that can be specifically detected by recognition elements of a biosensor system. Using QCM, it is possible, among other things, to (1) form and study biomimetic systems (*Hook 2001, Hook 1998, Tan 2001*); (2) investigate a range of fundamental biological/biochemical processes; (3) create biosensors by immobilizing biological/biochemical components (nucleic acid, protein) or whole cells onto the QCM surface or within a polymeric film on the surface; (4) investigate drug-target interactions for drug discovery applications (*Kenneth 2003*).

The adsorption of proteins onto solid surfaces is an extremely important process with applications especially in medicine, biotechnology, diagnostics, and food technology. Consequently, TSM sensor devices have been widely employed to monitor biomolecule adsorption onto quartz, gold, self-assembled monolayers (SAMs), graphite, polymer films, hydroxyapatite, lipid films and many other surfaces (*Cooper 2007*).

According to Bickerstaff, the “immobilisation of protein of intact red blood cells (RBCs) can be valuable for different reasons. In vivo, RBC carrying specific ligands can be targeted to cells exposing specific antigens, eventually for the delivery of drugs encapsulated in the same RBC. Alternatively, RBC carrying antigens or enzymes on the extracellular surface of their membrane can performs as antigen delivery systems or as bioreactor for the degradation of toxic metabolites. In vitro RBC carrying proteins can be used as diagnostic reagents in agglutination or haemolytic assays. Several methods are available for coupling proteins to intact erythrocytes: disulfide bond formation, electroinsertion and the coupling through biotin-avidin-biotin” (*Bickerstaff 1997*).

The selectivity of biosensors is usually obtained by utilising natural or artificial biomolecular function units such as antibodies, enzymes, transmembrane proteins, *etc.* This requires the preparation of arrays of biomolecules on planar surfaces, in sufficient density and with their functional groups exposed. Figure 2-12 shows examples for the immobilisation of biological recognition units on transducer surfaces: entrapment in polymeric matrices, physisorption, direct covalent attachment, ionic attachment, embedding in lipid membranes, coupling to ordered Langmuir-Blodgett or self-assembled monolayers with covalent or affinity-like linkers, *etc.* Another example is the formation of nanocomposite films, polyelectrolytes or biological molecules (Göpel 1995).

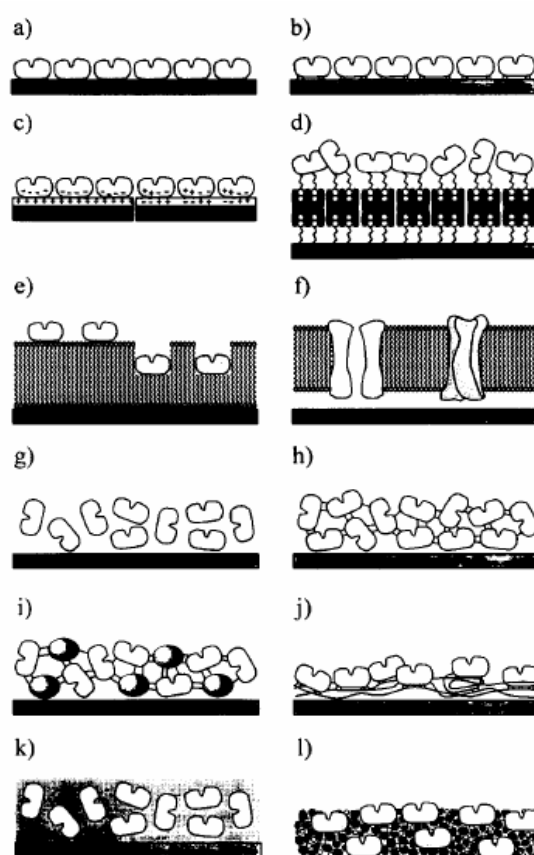


Figure 2-12. Typical interfaces in biosensing. Examples for the immobilisation of biological recognition units on transducer surfaces. (a) direct adsorption (physisorption), (b) covalent linking to the substrate, (c) adsorption by electrostatic forces, (d) coupling via biotin-avidin linkage, (e) adsorption at mono- or bilayers, (f) embedding in lipid bilayers, (g) entrapment behind a membrane, (h) cross-linking of biological molecules, (i) cross-linking by other large molecules (e.g. BSA), (j) covalent linking to polymer chains, (k) entrapment within a gel of a polymer (non-conducting medium), (l) entrapment by mixing with carbon paste, conducting polymers or organic salts (conducting medium). Taken from (Göpel 1995).

A number of methods have been developed to immobilise red blood cells for subsequent optical microscopy or scanning electron microscopy. Some of these methods have in turn been either adopted or adapted for atomic force microscopy of red blood cells.

For the specific case of the present research project, the immobilisation of the erythrocyte membrane is done through a polycationic agent (Poly-L-Lysine).

A number of different techniques for immobilising RBC onto solid surfaces have been demonstrated. Studies on adhesion of red blood cells to solid surfaces often take advantage of polycationic agents through the interaction between their cationic charges and anionic charges on the surface of the cell (*Mazja D. 1975*). Ribaut et al. show RBC immobilisation using antigen/antibody crosslinking based on the bonding of anti-D with the corresponding antigen of the RBC membrane that is shared by all erythrocytes from the positive rhesus group (O⁺) (*Ribaut C. 2008*).

An important principle behind the method is that the polycationic polylysine molecules have some cationic sites that strongly adsorb to various solid surfaces, while enough free cationic sites to combine with the anionic sites on the cells surfaces. The carboxyle group of N-acetylneuraminic acid (sialic acid) is responsible for the majority of the negative charges. This acid is fixed at the peripheral end of a protein called glycophorin that penetrates the lipid layer (*Cook 1961, Eylar 1964, Seaman 1963*). Assuming a uniform distribution the charge density is about 1 charge site per 1000 square Angstrom (*Boxer 1974, Segrest 1973*). The negative charge of the sialic acids prevents erythrocyte aggregation (*Rogers 1992*) and facilitates a smooth blood flow in normal blood vessels (*Born 1985*). In the case of the erythrocytes infected with plasmodium in schizont stage, protusions or knobs are found (*Nagao 2000*) (chapter section 2.2.2.2.) which do not affect the direct adsorption of the cells on the gold surface.

Studies carried out by the Biosensor Research Group of the Institute for Clinical and Experimental Transfusion Medicine at the University of Tübingen successfully demonstrated determination of various blood types through the interaction of erythrocytes with immobilised antibodies on a QCM.

The mechanism of an oscillator biosensor (Figure 2-13) is described in the following steps: (I) A receptor molecule for the analyte target is immobilised to the metallic surface using adsorption or covalent coupling forming a monolayer or a sandwich construction. (II) The quartz is mounted in a flow cell and its resonance frequency monitored. (III) After the frequency becomes stable, the solution containing the target molecules (infected and non-infected erythrocytes) is injected. (IV) The resonance frequency decreases because the effective mass of the resonator is increased by the binding reaction between the receptor and target molecules. The frequency behaviour obeys the exponential function and the exponential coefficient gives the binding affinity. The extent of the frequency change gives the information on concentration of the target molecules. (V) When the molecules' desorption occurs spontaneously or when a solution for dissociation is injected, the target molecules are released from the oscillator surface and the resonance frequency returns to the initial value.

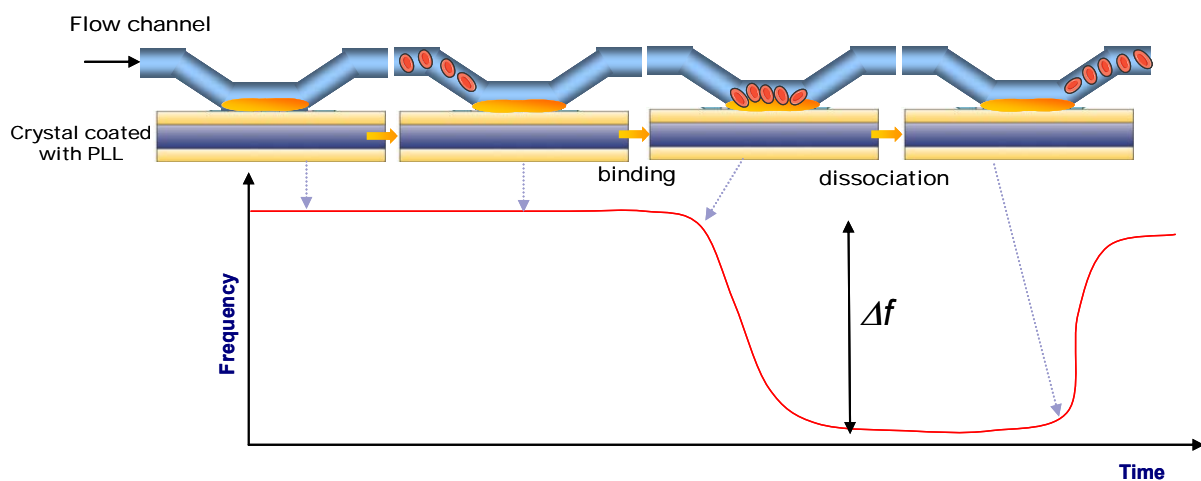


Figure 2-13. Mechanism of an oscillator biosensor. Modified from (Cooper 2007)

3. METHODS

3.1. PREPARATION OF GOLD SURFACE

3.1.1. Cleaning and adhesion of Quartz

Quartz crystals were cleaned by immersion in Acetone for 1 min, washed with distilled water and dried with N₂ (5.0). Afterward, the quartz was treated with "Piranha" solution for 1 min, washed with distilled water and dried with N₂ (5.0). This was shown to provide a suitably hydrophilic surface. Finally, the quartz crystals were adhered with a plastic film on a Teflon ring. Iron soldering was used to reinforce and fix the parts.

3.1.2. Coating with Poly-L-Lysine (PLL)

The freshly cleaned gold surface was exposed with 20 mL of PLL (0,5 mg/mL) for 25 min at 37°C previously dried the polication agent with N₂ (5.0) atmosphere. Then the gold surface was washed vigorously (+++) with distilled water several times to remove the excess PLL. Coating was done two hours before the experiment.

3.2. PREPARATION OF INFECTED ERYTHROCYTES

3.2.1. Malaria culture

The malaria cultures were conducted with *P. falciparum* strains 3D7 and D10. Parasites were obtained from MR4 (ATCC, USA) and maintained in continuous culture in human O+ erythrocytes in RPMI 1640 medium (Gibco Laboratories, Grand Island). Red blood cells were resuspended in parasite culture medium to a hematocrit of 5% and incubated for 24 hours in 37°C and gaseous atmosphere (CO₂ (4.5) 5%, O₂ (4.5) 5%, N₂ (5.0) 90%) and controlled the next day. All the materials infected were disposed of in autoclave bags and the contaminated remnants of reactive were put inside a bottle with Perform®.

3.2.2. Giemsa staining and parasitemia estimation

Approximately 20 µL of malaria culture were collected on the slide and then air-dried. Thin films were stained with 10% Giemsa solution in phospat buffer for 30 min, before fixation with Methanol 100% for 1 min and rinsed in water. The smears were examined using a Leica microscope, with the x100 oil-immersion objective. The Giemsa-stained thin bloods were screened by counting the number of 100 erythrocytes in the small fields. By extrapolating, the equivalent of 1000 erythrocytes was examined

(regarding parasites). Repeat the counting at least twice for a total examination of three different parts of the slide. Take the mean number of infected erythrocytes per 1000 erythrocytes and divide by 10 to get the percent infected erythrocytes (*Ljungström I. 2004*).

The Giemsa stain is used to differentiate nuclear and/or cytoplasmic morphology of platelets, RBCs, WBCs, and parasites (*García 2000*). The most dependable stain for blood parasites, particularly in thick films, is Giemsa stain containing azure B. Liquid stock is available commercially. The stain must be diluted for use with water buffered to pH 6.8 or 7.0 to 7.2, depending on the specific technique used. Either should be tested for proper staining reaction before use. The stock is stable for years, but it must be protected from moisture because the staining reaction is oxidative. Therefore, the oxygen in water will initiate the reaction and ruin the stock stain. The aqueous working dilution of stain is good for 1 day only. The solution of Giemsa must be filtered through a paper strainer to remove lumps of stain and thus obtain a homogeneous solution which does not affect the observation of the thin film.

3.2.3. Dilution of malaria culture

For a proper parasite growth, it is recommended not to have >2% parasitaemia.

Parasitaemia 1–2%: The parasite culture medium was measured and diluted 1:10 with culture medium RPMI 1640-complete and RBC to 5% hematocrit.

Parasitaemia <1%: The parasite culture medium was collected and measured (supernatant of the bottle of culture), and then fresh RPMI-complete at 37°C was added.

3.2.4. Synchronization of parasites

The parasite culture was centrifuged at 1800 rpm x 5 min before collection of supernatant. The pellet was incubated with 5% sorbitol solution in water x 10 min and then was washed two times with RPMI 1640 complete at 37°C. The cells were transferred into the bottle of culture and diluted to 5% hematocrit and fresh RPMI 1640 complete.

This method is designed to eliminate the trophozoite and schizont stages hence selecting for ring-stage parasites. The most important thing for synchronization is to be sure that you have enough ring-stage parasites. For tighter synchronization, this method should be done several times until the ring-stage predominates in the cultures (*Llinas 2008*). For the synchronisation of cultures, sterile (5%) sorbitol in water was used. The sorbitol lysed the erythrocytes containing mature parasites but not those with rings. Cultures initiated with parasites separated by these techniques maintain their synchronous growth for at least 2-3 generations, after which time asynchrony develops (*Lambros 1979, Trigg 1985*). The erythrocyte membrane is normally impermeant to sorbitol, but the channels induced by the malaria parasite in the infected cell membrane allow the passage of sorbitol and when mature parasitized erythrocytes are suspended in an isosmotic sorbitol solution, there is a net uptake of sorbitol and water into the erythrocyte, resulting in cell swelling and hemolysis (*Bouyer 2006, Go 2004*).

The young parasites increase in size slowly during the first twenty-four hours, after which they grow much more rapidly. Segmentation begins in about thirty-six hours from the smallest ring-form stage. The chromatin granule first divides into two parts, and in segmenting cultures parasites containing any number up to about twenty segments can be found. The largest number is seen in tertian plasmodia (*Bass 1912*). To keep the parasites synchronized, the sorbitol treatment must be performed once a week.

3.2.5. Separation of schizont stages

To obtain parasitemias higher than 90%, a technique with MACS (magnetic cell sorting) columns (Miltenyi Biotec, Bergisch Gladbach, Germany) after the sorbitol treatment, was used. MACS® Cell Separation Columns were developed for the gentle separation of a wide range of cells. When MACS Columns are placed in a MACS Separator – a strong permanent magnet – the MACS Column matrix provides a magnetic field strong enough to retain cells with minimal amounts of MACS MicroBeads (*Miltenyibiotec 2009*).

This technique profits of the property of all human *Plasmodium* species to degrade haemoglobin (an Fe(II) diamagnetic complex) into haemozoin (an Fe(III) paramagnetic complex). This technique was used, making possible the magnetic purification of parasitized red blood cells containing haemozoin. The high degree of purity that can be

obtained for the synchronization of in vitro cultures of *Plasmodium falciparum*, either on asexual or sexual erythrocyte stages, and the usefulness of magnetic separation for the enrichment and purification of *Plasmodium* parasitized red blood cells from infected malaria patients (Ribaut 2008, Ublemann 2000). The exploitation of the paramagnetic properties of haemozoin is a very powerful technique in routine culture and analysis of *P. falciparum* parasites. The method is both easy to perform, rapid, and non-toxic, allowing the enrichment or depletion of late-stage-infected RBC without the need for any labelling or processing of culture material (Ublemann 2000).

The magnetic method has been previously utilized to concentrate Plasmodium-infected erythrocytes without any significant influence on the viability of the parasite. Concentration and synchronisation by the magnetic method proved most effective when schizonts were dominant (Sun-Young 2008).

Parasite culture material in RPMI medium was applied to the column 25LD, which was subsequently washed at least two times with RPMI (LD: approx. 1 ml). When no more RBC from the parasite culture was apparent in the flow-through, the magnet was removed, and the cells retained in the column were eluted with RPMI 1640 complete. To determine the purification efficiency, aliquots of the original culture, flow-through and eluate were spread on microscope slides, fixed in methanol, stained with Giemsa, and analyzed under the microscope.

3.2.6. Sample preparation for use with the biosensor

The separation procedure of the parasites in schizont stage must be performed maximum 2 hours before the experiment since the infected erythrocytes are more sensitive to changes in temperature, shaking or manipulation at that moment.

Infected erythrocytes in schizont stage were centrifuged at 1800 rpm x 5 minutes. The pellet was measured and diluted (1:10) with RPMI-1640 complete without carbonat (the medium for use inside the biosensor) in a micro-tube test (~1 mL).

Note: Dilute the pellet carefully, avoiding excessive shaking. On average, the pellet of infected cells in schizont stage obtained is around 50 μ L.

3.3. EXPERIMENT WITH QCM

The organic layers suitable for development of a Quartz crystal sensor for blood analysis were controlled by F. Gehring (*Gehring 2005*).

The central element of the sensor unit is a temperature-sensor platform with two measure chambers that can be operated in series or parallel. The chamber can be observed through a window, both visually as well as with a CCD camera with threefold magnification. The filling can be monitored and documented: bubble production and cell immobilisation. The measuring device allows a simple mounting and dismounting of the quartz crystal microbalances.

The biosensor system allows stable programming of the temperature over a wide range for prolonged time. For our experiment, we used cells at $\sim 37^{\circ}\text{C}$ for periods of 48 hours and longer. This temperature could be kept steady and without significant variations which might affect viability.

The two measure chambers have a continuous flow injection system through a peristaltic pump. These pumps can be programmed according to the injection flow, in dimensions of μL and allow the use of different hose diameters (mm). One of the pumps offers the possibility to work together with a valve of eight ways connected through Teflon hoses to five different bottles working as reservoirs for different substances. Due to the complete tempering of the device, the signal noise was minimal.

The complete control of the sensor system and the recording of the data are done with user-friendly software, delivering of real-time data of frequency, temperature, time, pump injection volume, amongst others. The availability of real time data and observation makes this biosensor system quite suitable to evaluate biological, chemical, etc. systems, thus adding a new category as biosensor to this instrument.

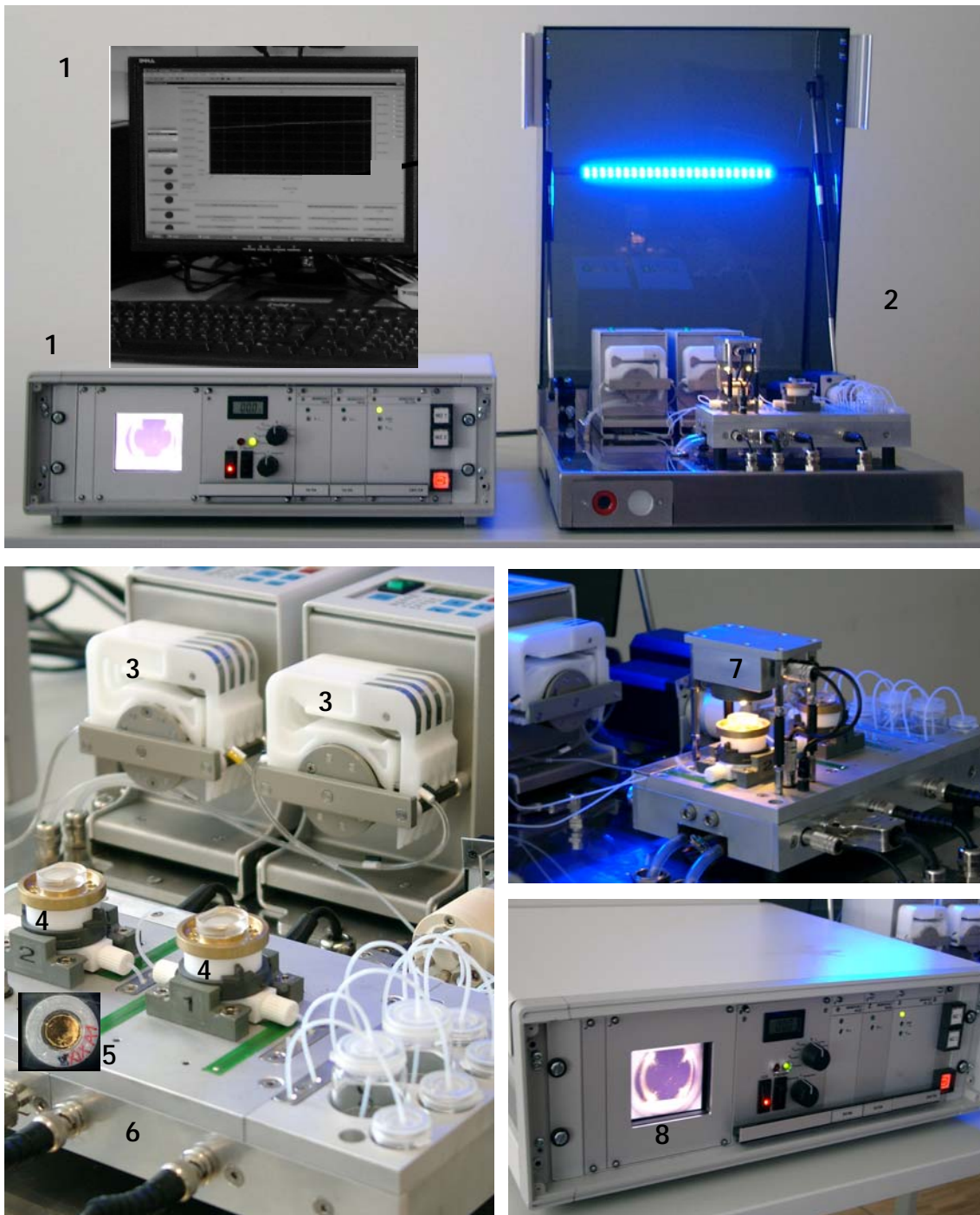


Figure 3-1. Sensor platform (Fidget-Type). (1) Control electrical system and (2) sensor unit. The sensor unit consists of: (3) micropump for the injection of fluids through hoses, (4) two measuring cells, (5) quartz, (6) thermostat sensor platform (7) CCD camera (charge coupled device) adapted on the measuring cells, (8) display to observe the measuring cell. The entire system can work thermostated on the sensor platform. The complete control of the sensor system, and the recording of the data is done with user-friendly software (Gebring 2005).

Figure 3-1 shows the construction of the sensor platform as used for our studies. Once the biosensor system has been disinfected and the sterility test of the materials has been performed (see chapter section 3.5.1. and 3.5.2), the following is carried out:

1. Equipment at 37°C, minimum one hour before the beginning of the experiment; checking the stability of the temperature signal
2. Coating of quartz with PLL (preparation maximum 2 hours before the experiment)
3. Preparation of materials and reagents (medium degasified and sterile)
4. Preparation of infected cells as stated in item 3.4.5 and putting them at 37°C
5. Assemblage of quartz covered inside the measuring cell and controlling the frequency (~10Hz)
6. Adaptation of the camera on the measuring cell
7. Pumping of medium (RPMI-complete medium without the carbonate) in constant flow of 100 $\mu\text{L}/\text{min}$ and controlling stable frequency signal (variability < 20 Hz for 10 minutes).
8. Injection of samples separately into measurement cells (infected erythrocyte and non-infected erythrocytes) in a parallel manner. The amount of sample is 20-50 μL
9. Pumping of medium in continuous flow (100 $\mu\text{L}/\text{min}$) into the chamber simultaneously and observation of the signal.
10. Performing parallel controls of the sample with Giemsa stain (section chapter 3.3.2.)

3.3.1. Disinfection of the biosensor system

The biosensor system was disinfected, both at the beginning and at the end of the experiment, using sodium hypochlorite 4% and an old quartz.

The quartz was assembled on the cells and 1 mL of disinfecting solution injected at a constant flow of 250 $\mu\text{L}/\text{min}$. The pump was stopped and the system was left for 10 minutes, then sterile water was pumped for two hours before the experiment with the same flow rate.

3.3.2. Sterility tests for materials and reagents

Since the biosensor system is not a closed system all materials used (bottles, micro-test tubes and the medium – amongst others) needed to be sterilised. Bottles and micro-test tubes were sterilised by autoclaving at 122°C and 1 atmosphere for 22 minutes. RPMI 1640 complete medium was degasified and filtered using a millipore 0,22 µm filter.

The equipment used to determine sterility is the BacT/Alert, in which the system uses a colorimetric sensor and a light reflected to monitor the presence and production of CO₂ dissolved in the culture medium. If there are microorganisms in the sample, CO₂ is generated as a product of the microorganisms metabolising the substrata of the culture medium. Due to this, the gas-permeable sensor installed at the bottom of every bottle of culture changes from green to yellow, indicating that it is positive. This positivity is perceived by the sensor in the instrument, which activates an alarm and turns on a light in the cell of the corresponding bottle. The BacT/ALERT Culture Bottles include BacT/ALERT Aerobic Culture Bottle (SA), BacT/ALERT Anaerobic Culture Bottle (SN), BacT/ALERT BPA Aerobic Culture Bottle (BPA) and BacT/ALERT BPN Anaerobic Culture Bottle (BPN) were developed to provide suitable nutritional and environmental conditions for organisms commonly encountered in blood infections, normally sterile body fluids and platelets. An inoculated bottle is placed into the BacT/ALERT Microbial Detection Instruments where it is incubated and continuously monitored for the presence of microorganisms that will grow in the BacT/ALERT Bottle (FDA 2002).

The samples incubated at 35°C inside the BacT/Alert equipment were: Medium RPMI 1640 complete without carbonate and sterility sample for bottles (standard micro test tube y vials mL x 20 and 10 mL). They were incubated in BPN, BPA, SNC, PNB media. Incubation time for the samples was 14 days, performing daily follow-up.

3.3.3. Microscopic control of the quartz

3.3.3.1. Light microscopy

The quartz crystals were carefully and softly rinsed with PBS at the end of experiment. Then the quartz was incubated in a 4% PFI solution for 4 hours and transferred into a 2,5% Glutaraldehyde solution in PBS for 4 hours. Finally the quartz was washed with PBS and dried. It was stained with Giemsa x 30 minutes, washed and dried.

Using immersion oil and reflected microscopy, observe the cells at the end of the experiment. The microscope offers the option of taking photos directly on the quartz.

3.3.3.2. Transmission Electron Microscopy (TEM)

Repeat the previous step to affix the cells but do not stain with Giemsa. Disassemble the quartz from the ring and plastic film.

3.4. CYTOMETRIC ANALYSIS

Parasited red blood cells collected during the experiment (see chapter section 4.5.1.) where analysed by flow cytometry. The samples were stained with Acridine Orange (1 μ L AO/mL PBS) and were analysed using a standard BD FACSCanto II flow cytometer (Becton-Dickinson, USA). Laser of 488 nm was used. Erythrocytes were gated on the basis of their Forward Scatter and Side Scatter signals using logarithmic scales. Parasites were gated on the basis of their positive staining with AO.

4. RESULTS AND DISCUSSIONS

The objective of the present work is to study, in real-time, the erythrocyte cycle of the *P. falciparum* with a biosensor piezoelectric system using quartz crystals. Application of a piezoelectric element for the study of *P. falciparum* is novel, and it may open the way for similar studies of other infectious diseases.

This chapter is organised as follows: First, the optimisation of Poly-L-Lysine layer on the surface of the gold electrode are described in chapter section 4.1. In chapter section 4.2, the optimisation of the signal for 48 hours in the QCM system is analyzed. Through chapters sections 4.3 and 4.4, the results of the parallel observation and the validation of infected erythrocytes and of non-infected erythrocytes inside the system of the biosensor are shown. Chapter section 4.5 shows the reinvasion of non-infected erythrocytes within the system. Finally, in chapters section 4.6, the effects on merozoites release and reinfection of erythrocytes are monitored in our system with the known antimalarial drug Artesunat and the effects of an experimental substance Chlorotonil is compared to effects of the protease inhibitors: E64 and Leupeptin.

4.1. OPTIMISATION OF THE POLY-L-LYSINE LAYER

RBC do not adhere to biological adhesion molecules like fibronectin, vitronectin, fibrinogen or collagen (*Ribant C. 2008*). Due to their strong negative surface charges, they do however readily interact with cationic molecules, which, at the same time, strongly and irreversibly (physiosorption) adsorb to the negative charges present on a gold surface. Therefore what we have done is to use poly-l-lysine as anchor molecule to strongly, homogeneously and stably adsorb erythrocytes native or infected with *P. falciparum* on to the electrode of our QCM.

Immobilisation with Poly-L-Lysine must comply with the following requirements, both for the infected erythrocytes as well as for the non-infected ones: (I) the layer of the polycationic agent must adhere firmly to the gold electrode, (II) the groups of infected and non-infected erythrocytes must not be denaturalised during immobilisation, (III) immobilisation must be stable for periods longer than 24 hours at 37°C (study of the erythrocyte cycle of the parasite).

On the basis of previous results by Gehring (*Gehring 2005*) with immobilisation of erythrocyte ghost, we used Poly-L-Lysine Hydrobromide with 70-150 KDa for our experiment.

The development of the optimisation of the immobilisation technique of the cells using the Poly-L-Lysine 0.5 mg/mL was developed in five steps: (I) determination of the way in which the polycation agent covers all the surface of the gold electrode. (II) Incubation time. (III) Washing the quartz to leave it with proper thickness. (IV) Preparation times and use of the quartz covered in Poly-L-Lysine. (V) Treatment and life time of the quartz covered.

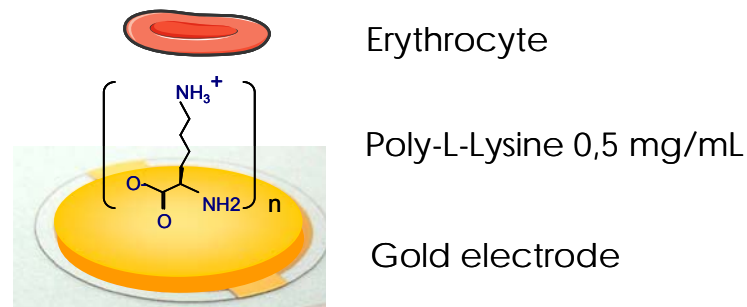


Figure 4-1 Schematic representation of the immobilisation of Poly-L-Lysine (PLL) over the gold electrode. A union of the erythrocytes both infected and non-infected over the surface of the electrode is performed through the electrostatic reaction of the group ammonium NH_3^+ with the carboxyl group of the proteins of the erythrocyte membrane. The thickness of the PLL films is approx. 1 nm.

Different immobilisation tests are done outside the equipment (Fidget-Type) using quartz covered with 20 μL Poly-L-Lysine in concentration of 0.5 mg/mL (70,000-150,000 Da), dried slowly with N_2 atmosphere, incubated 25 min at 37°C and washed vigorously with distilled water.

According to the microscopic observation of immobilised erythrocytes, the tests were then performed within the system, using RPMI Medium 1640 without NaHCO_3 (described in the Appendix 4 Reagents and Equipments) in a flow of 100 $\mu\text{L}/\text{min}$.. Figure 4-2 shows the drop of the frequency obtained when the erythrocytes were captured immediately on quartz surface coated with PLL. The frequency change was >1000 Hz.

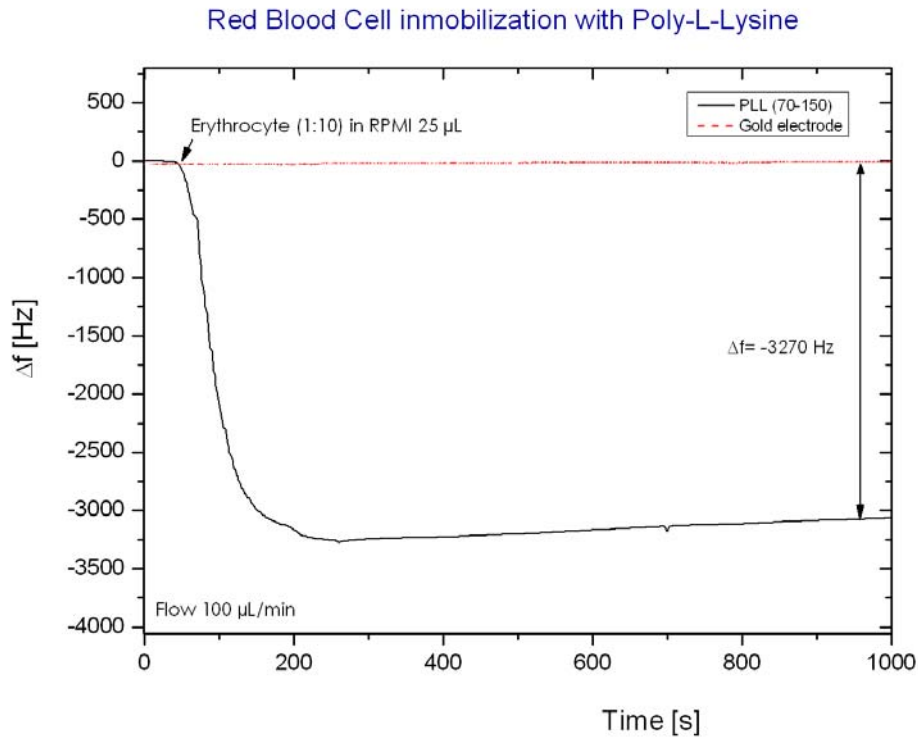


Figure 4-2 Change in resonance frequency of a PLL (70-150 KDa) covered quartz upon injection of 25 μL of an erythrocyte suspension (1.10^6 RBC/ μL) into the flow line of the Fidget-Type. Flow rate 100 $\mu\text{L}/\text{min}$. The resonance frequency of the quartz before addition of erythrocytes was 10 MHz. Frequency did not change when erythrocytes were injected over a control quartz without PLL cover.

Figure 4-3 shows photographs of erythrocytes immobilized onto the surface of the quartz using PLL 0, 5 mg/mL in water (70-150 KDa). The number of erythrocytes bound to the surface was counted microscopically and calculated as ~ 23.500 RBC/ mm^2 for an erythrocyte concentration of 1.10^6 RBC/ μL . The erythrocytes showed normal morphologic characteristics: stable, rigid, concave shape in the middle. There was no agglomerate build-up and every cell was individually attached to the quartz.

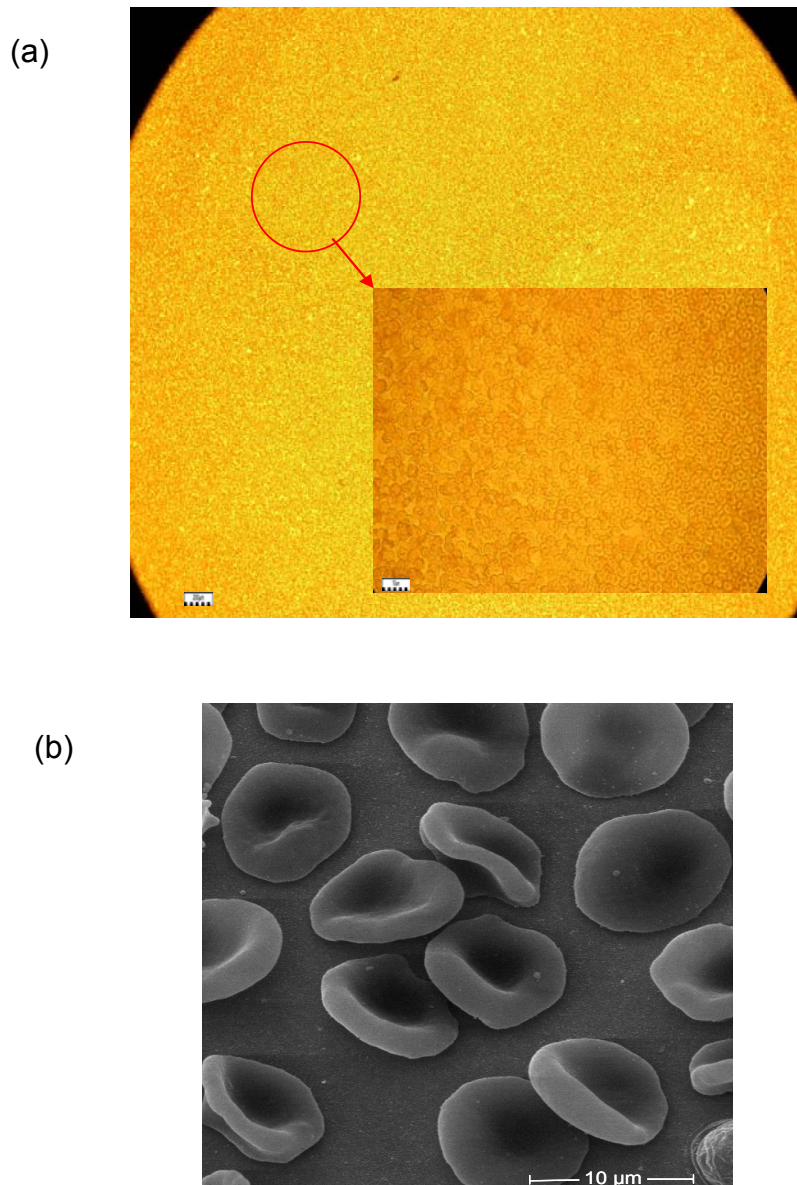


Figure 4-3 Immobilised erythrocytes on the PLL covered gold electrode of a quartz: (a) Photograph with the optic microscope shows the uniform immobilisation over the entire surface of the quartz. The morphology erythrocyte membrane is well preserved. (b) Photograph using the TEM ($\times 300000$) shows the membrane of the erythrocyte in detail. Both photographs were taken at the end of the experiment (a) the cells were photographed leaving the quartz wet with the medium RPMI (b) cells fixed with P-formaldehyde 4% in PBS (4 hours) and Glutaraldehyde 2.5% in PBS (4 hours). The number of cells estimated for the quartz (a) around 1.10^6 RBC/ μL ca. 23500 RBC/ mm^2 .

Preliminary experiments had shown that under certain conditions binding of erythrocytes in absence of a frequency change signal can occur. Therefore the influence of incubation time, incubation temperature, washing, storage of the quartz before use, regeneration, MW of PLL was investigated. Table 4-1 shows a series of different experiments using different parameters as temperature and time of incubation of the quartz, washing of the quartz with PLL, storage of the quartz before use and molecular weight of PLL.

Table 4-1 Optimisation of the PLL layer and treatment of the quartz

Exp	PLL (KDa)	quartz	Incubation temperature	washing	preparation time
1	70-150	new	RT x 5 min	+++	2 hours before the experiment
2	70-150	new	RT x 10 min	+++	2 hours before the experiment
3	70-150	new	RT x 25 min	+++	2 hours before the experiment
4	70-150	new	37°C x 5 min	+++	2 hours before the experiment
5	70-150	new	37°C x 10 min	+++	2 hours before the experiment
6	70-150	new	37°C x 25 min	+++	2 hours before the experiment
7	70-150	new	37°C x 25 min	+	2 hours before the experiment
8	70-150	new	37°C x 25 min	+++	24 hours before the experiment
9	70-150	new	37°C x 25 min	+	24 hours before the experiment
10	70-150	regenerated	37°C x 25 min	+++	2 hours before the experiment
11	70-150	regenerated	37°C x 25 min	+++	24 hours before the experiment
12	30-50	new	37°C x 25 min	+++	2 hours before the experiment

Table 4-1. Different parameters used by the treatment of the immobilised quartz. Different quartz covered with PLL are taken using the protocol described in chapter 3 (Methods). The new quartz covered with PLL undergoes different incubation times, washing forms and preparation times to assess their stability in time. Regenerated quartz only undergoes different incubation times. The quartz covered with different PLL and incubation temperatures are prepared one day before. +++= vigorous washing, += no vigorous washing

I) Effects of incubation time and temperature

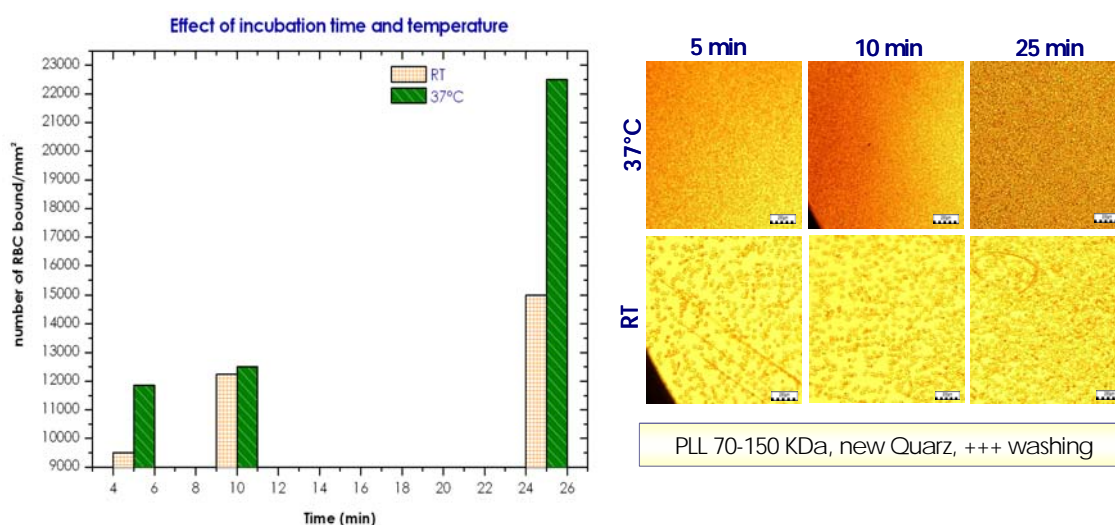


Figure 4-4. Effect of incubation time and temperature.

Results show that 25 minutes and 37°C are necessary for an optimal bound of RBC on the quartz covered with PLL 70-150 KDa and washed vigorously (+++). The number of RBC bound to quartz determined microscopically corresponds to 22430 RBC/mm².

Regarding the relationship between incubation time and temperature, 37°C cause the polycation agent to be adhered in a stronger way and higher stability to the surface of the quartz. The results obtained show that quartz under the same conditions of wash, preparation and use, MW PLL, new quartz shows good sensitivity responses but much more significant for quartz incubated for 25 minutes at 37°C. See graphs 4-8 c) -2865 Hz and f) -89 Hz.

In the literature, cell adhesion with PLL onto solid surfaces is reported for different applications at different T and incubation conditions: adhesion over gold electrodes for electrochemical characterisation (Chirea 2005), covalent attachment and derivatization of Poly (L-lysine) monolayers on gold surfaces as characterized by polarization-modulation FT-IR spectroscopy (Frey 1996), and Thermostable Peroxidase-Polylysine Films for Biocatalysis at 90°C (Guto 2007). Amongst these and many other references, polylysine films are used at different incubation times and temperature, showing great stability for this polycation agent at ambient and body temperatures (~37°C).

The bioability of the PLL to adsorb cells is also limited by the time of preparation of the quartz. Reports available state that the PLL solution was stable for long periods of time at temperatures below zero, but no reports were found of quartz covered with this polycationic agent. In the experience the results suggest to use the quartz always prepared two hours before the experiment.

II) Effect of washing and storage of the quartz before use

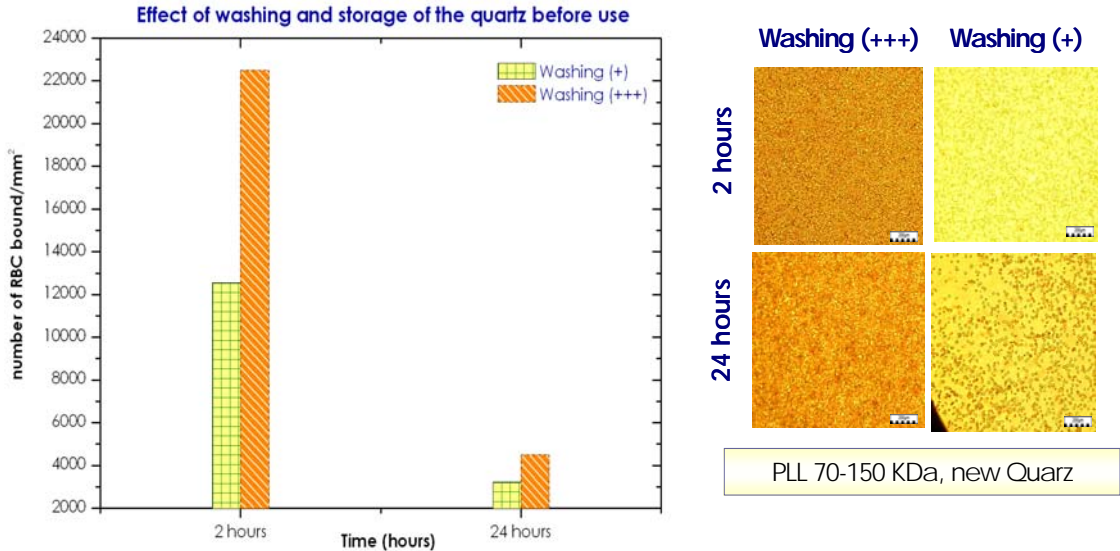


Figure 4-5. Effect of washing and storage of the quartz before use

Figure 4-5 shows that a vigorous washing (+++) and storage of the quartz 2 hours before use has the effect to bind RBC on the quartz. The number of RBC bound on the quartz using vigorous washing (+++) and no vigorous washing (+) were 22500/mm² and 12550/mm² respectively for 2 hours and 4500/mm² (+++ washing) and 3220/mm² (+ washing) for 24 hours.

Taking into account that the thickness of the PLL layer must not be too high, washing is an essential step to obtain a good response in terms of sensitivity of the quartz uniformity. Describing quartz wash could turn subjective, but the aspect which can be described objectively is that a vigorous wash with abundant distilled water and a lot of strength decreases the thickness of the layer of the polycation agent. Approximately 250 mL of water were used along with strong and direct discharges from the washing bottle. (+++)= vigorous washing, (+)= no vigorous washing. See graphs 4-8 c) -2865 Hz and d) -833 Hz.

III) Effect of regeneration

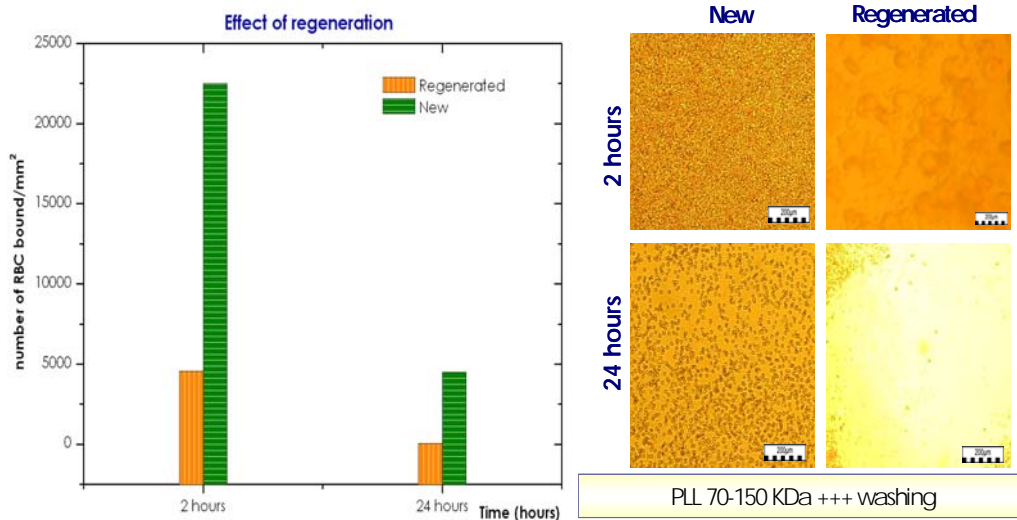


Figure 4-6. Effect of regeneration

Figure 4-6 shows that the regeneration of the quartz with NaOH 0.1 M (30 seconds) in comparison with a quartz freshly cleaned with Piranha solution (1:3) has an effect on the bind of RBC on quartz. The relationship to time of storage of the quartz before use is observed. The number of RBC bound on the quartz with quartz regenerated was 4544/mm² while the number was 22500/mm² with storage of the quartz two hours before of use. Observation with a microscope showed immobilisation of RBC and was not symmetrically uniform over the surface of the quartz and patch formation.

This asymmetric adsorption of polylysine caused an intrinsic transmembrane potential (Diederich A. 1998) and consequently a signal with very low sensitivity. These quartz only showed results of -307 Hz (incubation time 25 min at 37°C) and -89 Hz (incubation time 25 min at RT) (Figure 4-8).

IV) Effect of molecular weight of PLL

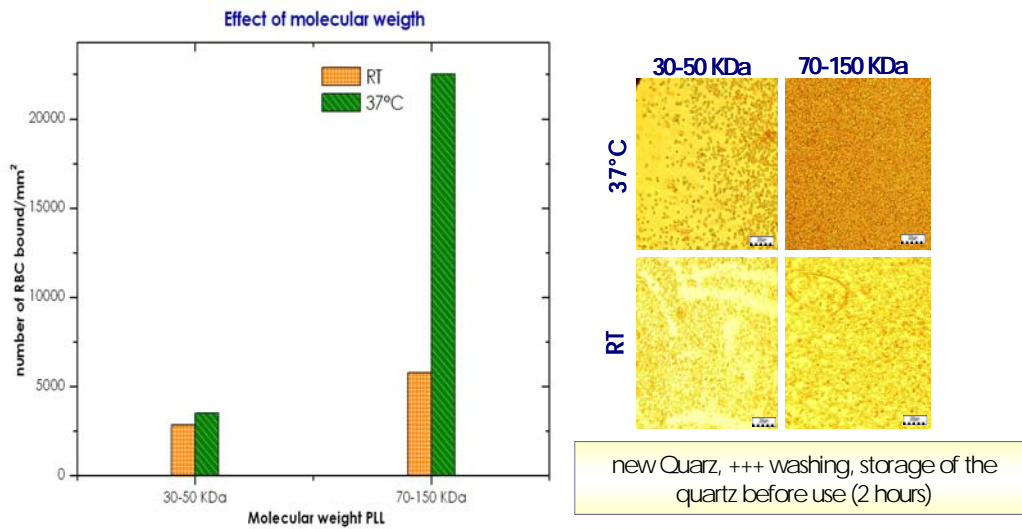


Figure 4-7. Effect of molecular weight of PLL

Although previous experiments had suggested to use PLL 70-150 KDa as standard for our experiments, we also tested the effect of MW for comparison. Microscopic observation showed insufficient immobilisation of erythrocyte on quartz.

$\Delta F[\text{Hz}]$ for PLL of a lower weight does not show higher cell adsorption (-275 Hz) if compared to the ones of MW higher than -497 Hz (Figure 4-8). The dependence of the transmembrane potential on the MW of the surface-attached PL can be understood by the formation of polymer train-tail-loop structures on the membrane surface.

A possible reason could be the persistence of PLL of longer length at lower ionic strength, and this longer length is conserved after PLL adsorption to the charged membrane surface. In the case of a black lipid membrane, they may connect large regions of the bilayer, thus hindering the thinning process. If the asymmetric adsorption of PL causes a drastic curvature of the membrane, the film area should consequently increase significantly

In graph 4-8 the comparison of the drop of frequency of PLL films on gold electrode is presented.

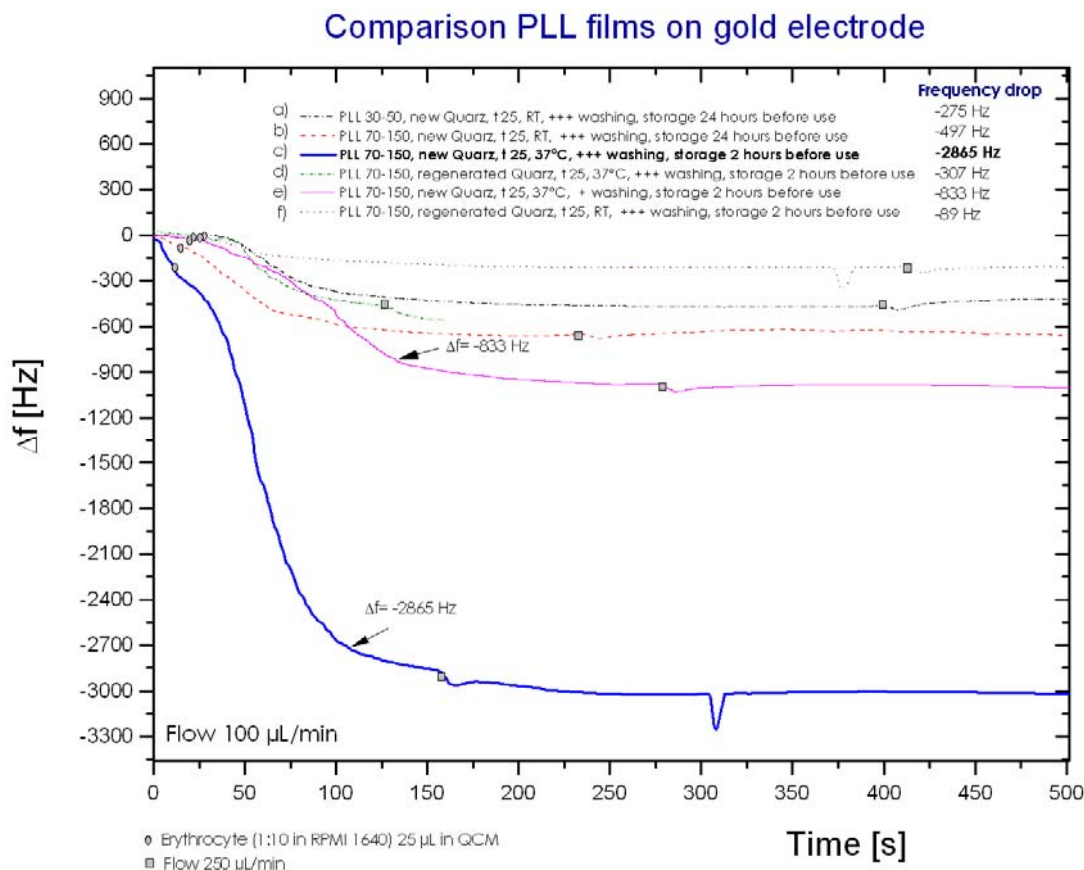


Figure 4-8. Comparison of the different films of PLL on gold electrode. d) and f) For quartz regenerated with NaOH 0.1 M per 30 seg using PLL 70-150 using +++ washing (vigorous), storage of the quartz two hours before use but with different incubation temperature d) T 37°C and f) RT, drops of -307 Hz and -89 Hz respectively. For new quartz cleaned with Piranha solution (1:3) covered with PLL 70-150 but with incubation at RT and vigorous washing (b) shows a drop in the frequency differential of -497 Hz. Quartz (c) and (e) with the same incubation temperature but with different washing (+) and (+++) respectively showed drops in the frequency differential of -833 Hz and -2865 Hz. For quartz (a) using PLL 30-70 KDa, incubation temperature at 37°C, +++ washing and storage 24 hours before the experiment show a value of -275 Hz.

A relationship is observed between the microscopic observation and the results obtained in the measurement of the frequency differential shown in the previous graph. Quartz with incubation times of 25 minutes, PLL 70-150 KDa, washed vigorously and with storage times not higher than two hours before the experiments showed higher sensitivity and uniformity of cell immobilisation over the polycationic agent. In this way, the experiments were reproduced for the study of the erythrocyte cycle of *P. falciparum* for this paper

4.2. OBSERVATION OF THE BIOSENSOR SIGNAL FOR 48 HOURS

Once the PLL layer on the gold electrode was optimised, we needed to show that a constant biosensor signal could be obtained in the device for ≥ 48 hours at 37°C using RMPI 1640 complete without NaHCO_3 . In previous investigations carried out by the biosensor team, the measurements and experiments had been carried out at ambient temperature ($\sim 22^{\circ}\text{C}$) only, an no longer than two hours and with aqueous solutions different from RMPI 1640. Since the study of the erythrocyte cycle of the parasite needs optimal conditions inside the equipment, the behaviour of the cells needs to be assessed continuously during the experiment. A 48-hour test was performed since this is the time the erythrocyte cycle lasts in human beings.

Considering this background information, three main questions were asked for the development of the observation method of the biosensor signal for 48 hours: first, can erythrocytes be kept sterile under the circumstances given and the RBC left intact in the equipment during this period of time? Second, is the PLL layer stable to bind erythrocytes? Third, does the signal remain stable for 48 hours?

In the literature, no tests have been described with parasites inside the QCM measuring chamber.

The basic experimental setup in shown in Figure 4-9.

4.2.1. Sterility

Sterility was measured in the effluent chamber after 48 hours of culture using BactAlert system. There was no growing of bacteria during 14 days under aerobic or anaerobic conditions.

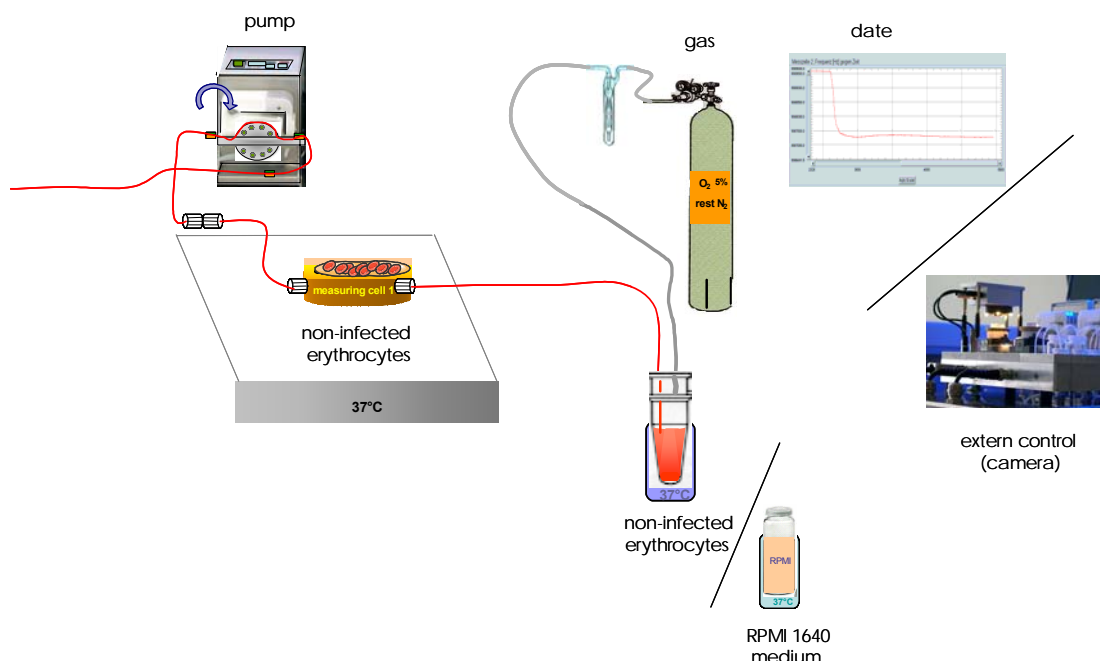


Figure 4-9. Graphic representation of the biosensor system used for the observation of erythrocytes. The erythrocytes (1:10 RPMI 1640) are injected through the hoses as a result of the pumping process of the micropumps. When erythrocytes are immobilised by the PLL 70-150 KDa film (0,5mg/mL) a drop in the signal is caused due to the change in mass adsorbed by the quartz. After the immobilisation of the erythrocyte and a stable signal after the drop in the frequency, the hose is changed to the vial bottle with continuous flow (9 $\mu\text{L}/\text{min}$) for 48 hours of the RPMI 1640 medium which had been degasified and was equilibrated with a sterile gaseous atmosphere of O₂ 5%, rest N₂. The erythrocyte was injected at a flow rate of 100 $\mu\text{L}/\text{min}$ followed by pumping of RPMI with the same flow rate per three hours to stable signal. Then the flow rate was reduced to 9 $\mu\text{L}/\text{min}$ for the following 48 hours. All the system is at a constant temperature of 37°C. The external control is performed through a camera adapted above the cell, by observing the filling of the microchamber and the presence of bubbles. The diameter of the hoses used was 0.38 mm.

4.2.2. Stability of the PLL-erythrocyte layer over 48 hours

Graph 4-10 presents the external observation of the cells through a microcamera located above the cell. Though this observation did not show the state of the cells microscopically, it serves to show the optimisation of the filling of the equipment as well as the medium, of the immobilisation and the presence of bubbles. This observation indicated that using a degasified medium, the protocol established for these experiments was successful to allow 48 hours of continuous bubble free culture at low flow rate. In graph 4-11, the microscopic observation of the quartz 48 hours later is showed. To such an end, the quartz was kept humid and photographed quickly to avoid erythrocyte dehydration. The typical morphology of the erythrocytes was observed as well as the uniformity of their immobilisation. No significant loss of cells and stability of the PLL on the surface of the electrode was observed.

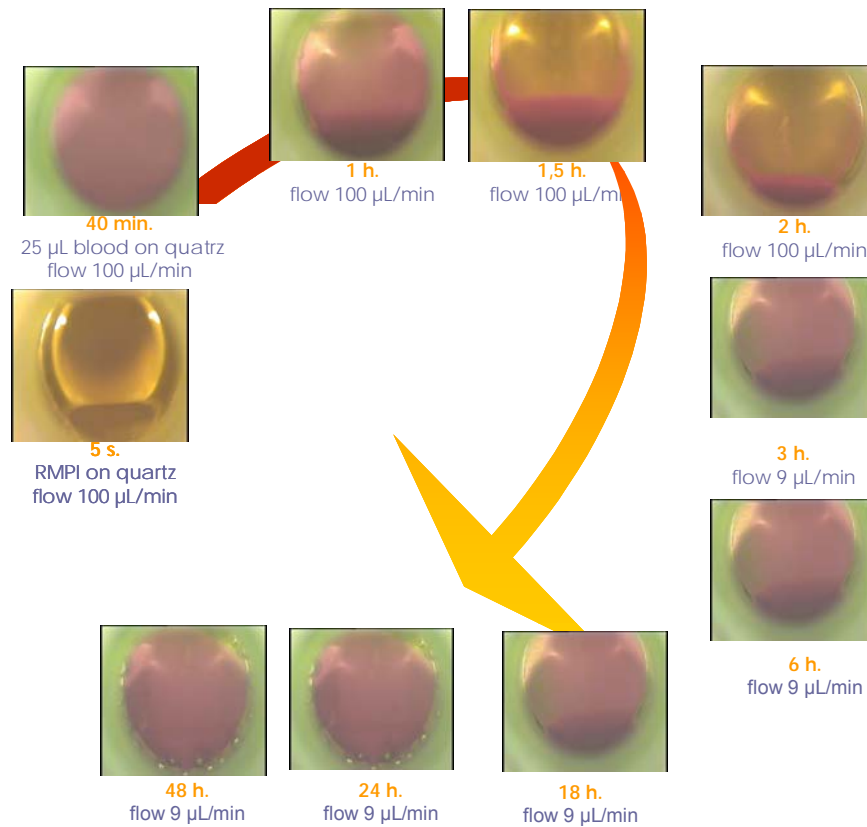


Figure 4-10. External observation of the erythrocytes on the quartz for 48 hours. These photographs taken with the microcamera installed above the quartz show a perfect filling of the medium and the immobilisation of the erythrocytes with time. No presence of bubbles inside the cell is observed. The small bubbles around the quartz do not pose any danger for the cells, or a variation in the signal.

This shows that erythrocytes can be bound firmly by the PLL layer for 48 hours at 37°C under constant flow rate of RPMI 1640 without NaHCO₃ and sterile conditions with minimal losses and keeping their normal shape.

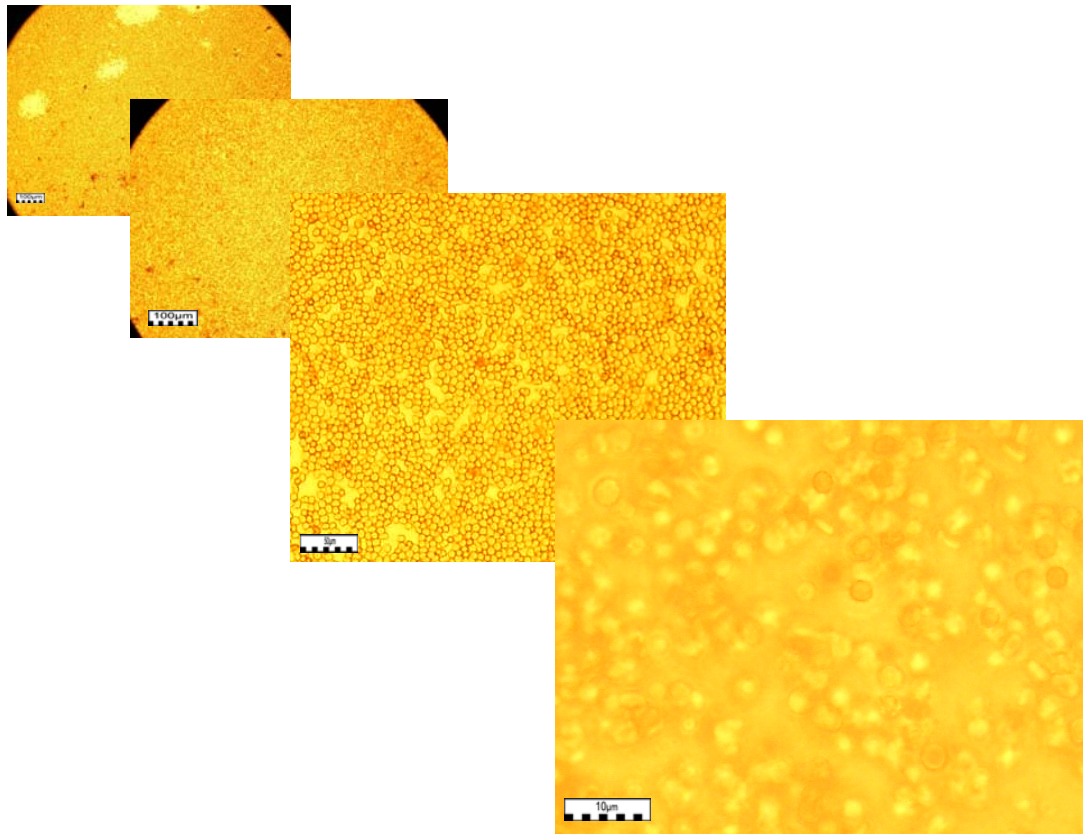


Figure 4-11 Microscopic optical pictures. 48 hours after immobilising the cells and having optimal conditions to survive, different photographs of different sizes are taken to the quartz humidified with the medium RPMI 1640 to observe their morphological characteristics. Uniformity in the immobilisation of the cells is observed, with some losses in a few parts of the quartz. An estimated number was 20000 RBC/mm², slightly smaller than the initial immobilisation obtained in part 4.1. of this chapter.

According to the method used, which is described in Graph 4-9, the results of measuring the frequency and the cells' stability after being immobilised for a 48-hour-long period were obtained from external observation of the signal.

The results presented in graph 4-12 show that the signal obtained remained stable for a period of over 40 hours after the change of continuous flow of the RPMI 1640 medium at 9 $\mu\text{L}/\text{min}$. 24 hours afterwards, the vial containing the medium was changed to a new fresh medium (previously heated at 37°C) to keep the sterility of the medium. A variation of 220 Hz was reported in a 30-hour-long period, which might be due to the loss of cells through time, but which did not turn out to be significantly valuable, considering that at the end of the 48 hours, microscopic observation showed cells being immobilised in an even manner over the entire surface of the quartz and keeping their morphological characteristics, i.e. healthy and vital.

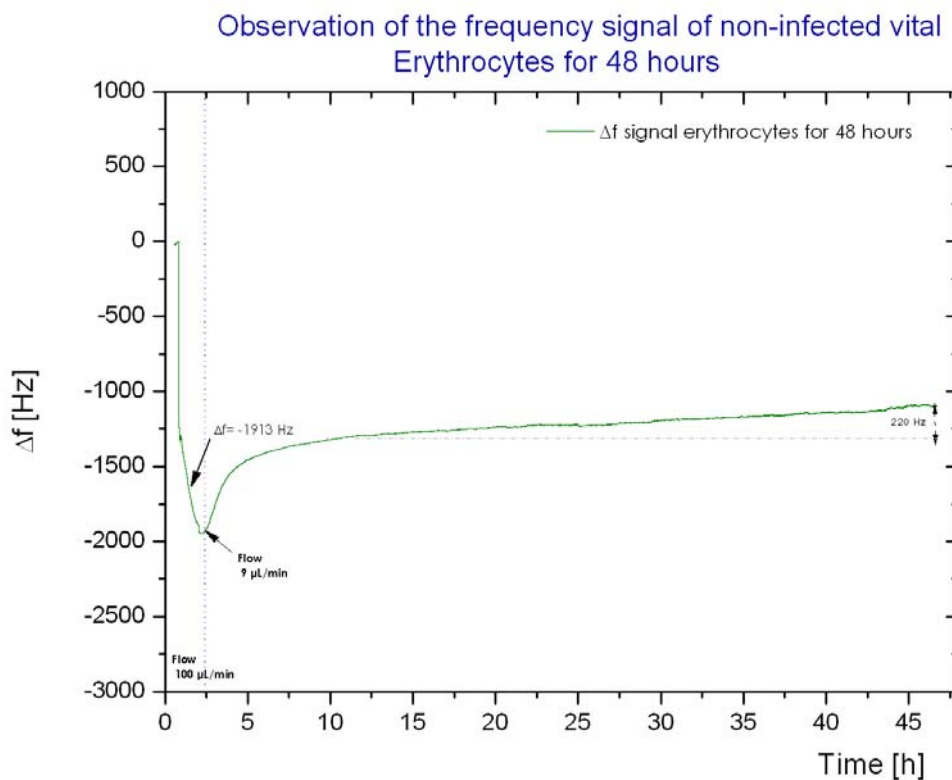


Figure 4-12. Observation of the frequency signal of non-infected vital erythrocytes for 48 hours. The signal is stable through time. At the moment of changing the flow to 9 $\mu\text{L}/\text{min}$ to leave the experiment with continuous flow day and night, there is an increase in the frequency, becoming stable after four hours. There is a 220 Hz variation in a 30-hour-long period. The amount of sample injected is 25 $\mu\text{L}/\text{min}$ in concentration 1:10 in RPMI 1640 complete without NaHCO_3 . Greater amounts of sample cause it to be deposited over the quartz, thus making its output difficult. At the end of the experiment, the microscopic observation of the quartz is performed, thus establishing the vitality of the erythrocytes.

4.3. OBSERVATION OF INFECTED AND NON-INFECTED ERYTHROCYTES INSIDE THE BIOSENSOR SYSTEM

After having established the biological conditions inside the biosensor device, the experiments were carried out using the infected erythrocytes obtained from the Institute of Tropical Medicine of the University of Tübingen.

This being the first time this kind of experiments was done in the QCM system, there was no reported data in the literature.

For the design of the experiment, the following guidelines were taken into account:

- 1) Concentration of the infected cells
- 2) Handling infected erythrocytes
- 3) Experimental controls

4.3.1. CONCENTRATION OF THE INFECTED CELLS

Which should be the optimal concentration of the infected erythrocytes used to obtain optimal sensitivity of the equipment?

The biosensor system used works with a transducer system consisting in a piezoelectric crystal, which shows a relationship between its resonant frequency and the mass deposited on the crystal surface. During the merozoite release, the change in mass associated with the breakage of the erythrocyte membrane is the crucial moment in which the equipment must detect such a process.

In theory, the process of merozoite release is translated into desorption of the infected cells due to the breakage of the membrane. In these experiments, this assumption had to be proven and allow the observation of two essential aspects: normal development of the release process and sensitivity of the equipment to detect it. To do so, the design of the experiment was carried out in three stages, as shown in graph 4-13, where the first one is the filling of the measuring chambers with the medium RPMI 1640 without NaHCO_3 ; the second, the injection of the infected and the non-infected erythrocytes separately in each one of the measuring chambers and the third one, continuous flow of the medium for the observation of the signal and the merozoite release.

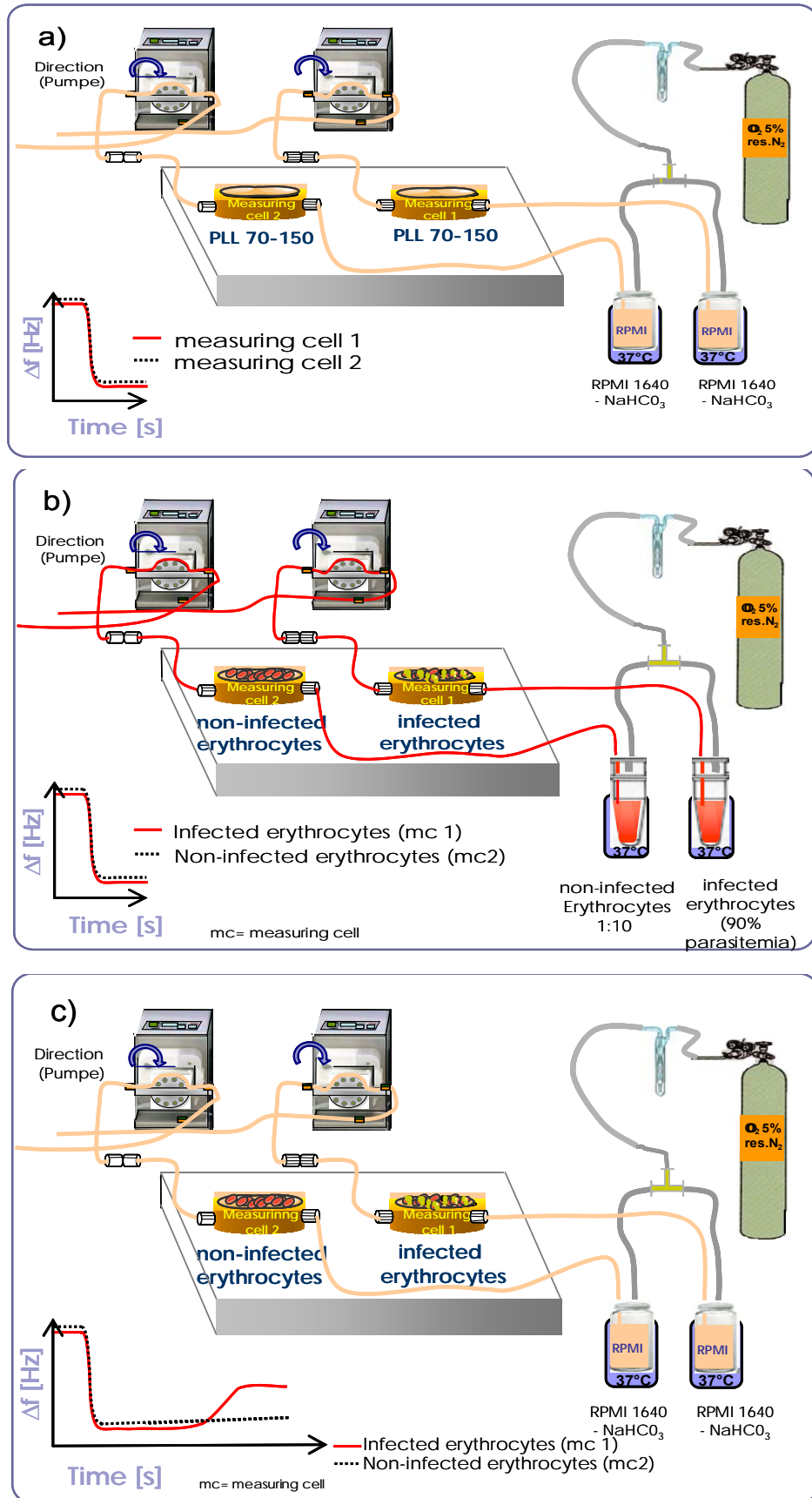
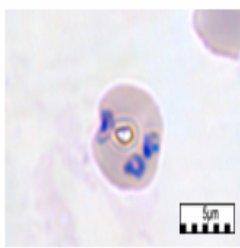
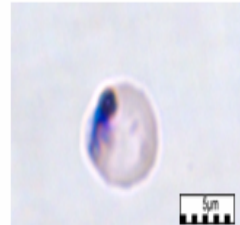
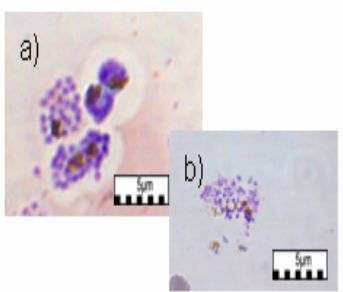


Figure 4-13 Experiment design for the observation of infected and non-infected erythrocytes. A) Injection of the medium until stable signal on the quartz covered with PLL b) injection of infected and non-infected erythrocytes separately on each gold electrode c) continuous flows after immobilisation.

To determine the concentration of the parasites to be used in the experiments, three essential steps had to be taken: 1) maintenance of the culture of synchronised parasites, 2) estimation of parasitemia and 3) separation or purification of the parasites in schizont stage. All methods are described in Chapter 3.

Table 4-2 shows the observations of the morphological characteristics of the *Plasmodium falciparum* (Pf), specific to each erythrocyte stage of the parasite: ring, trophozoite and schizont. Every stage was carefully observed with Objective x100 and immersion oil.

Table 4-2 Microscopic observations of the different stages of the *P. falciparum*: ring, trophozoite and schizont.

Stages found in blood	Figure	Appearance of Erythrocyte (RBC)	Appearance of Parasite
Ring		Normal	Forms with two chromatin. measuring on average 1/5 the diameter of the red blood cell (0.15-0.5 diameter of RBC), cytoplasm very fine
Trophozoite		Normal, unaltered in size	Pigment dense brown or black mass, compact cytoplasm
Schizont		Normal, unaltered in size	a)Parasites about 0.6 of RBC, b)nuclei or merozoites 16, Pigment clumped, black

The diagnosis of the disease caused by the *P. falciparum* varies by the parasitemia percentage present in the blood. In the table Clinical correlation of parasitemia (Appendix 3), the different parasitemia/ μ L percentages are observed. If low parasitemia levels (0.002%) are taken, is any sensitivity found in the detection inside the biosensor system? To optimise, which concentration must be used for the experiments? Cultures of infected erythrocytes were incubated with different percentages of parasitemia.

The optimal development of a parasite culture in accordance to the protocols established suggests a parasitemia level not higher than 2%, since abundant parasites in the medium do not yield appropriate conditions, presenting waste products which result in variations of the pH, the composition of the medium and their death (Trager 2005). Although many laboratory-adapted parasite lines tolerate 5% parasitemia or more, this is not the case for most patient isolates (Ljungström I. 2004).

4.3.2. HANDLING THE ERYTHROCYTES INFECTED WITH *P. falciparum*

In accordance to the protocols established for the handling of the parasites described in the chapter of methods, two questions were asked. First, what should be the handling of the infected cells once they are purified? Second: how much time should elapse from the moment in which they were obtained until the beginning of the experiment?

The strains used for the research were 3D7 and D10 obtained by the Institute of Tropical Medicine. 3D7 and D10 are from ATCC/MR4. D10 originally comes from Southeast Asia and 3D7 (a clone of NF54) from Netherlands (presumably originally from Africa).

The parasite strains must preserve their optimal conditions at all times to keep their vitality. The following conditions must be met permanently: temperature at 37°C, proper amount of nutrients needed, proper gaseous atmosphere and the parasites must be kept in sterile manner.

For the experiments using parasitemias of 0.2% and 2% 50 μ L of culture injected directly inside the equipment were used, while parasitemias obtained through the MACS method were concentrated in the following manner:

-
- Centrifuge the infected erythrocytes obtained from the purification by the MACS system (approx 2mL) at 1800 rpm x 5min
 - Remove the supernatant
 - Take and measure the pellet of infected erythrocytes
 - Dilute at a concentration of 1:10 in RPMI 1640 without NaHCO₃

Once this concentration was obtained, >90% of parasitemia of the erythrocytes infected, the sample (50-100 µL) was injected inside the measurement chamber. The same was done with the non-infected erythrocytes in concentration 1:10.

Since the infected cells are in schizont stage, the release of the merozoites will occur at any moment within the next six hours. As nuclear division produces two or more nuclei the parasite enters the stage of a schizont (*Matteelli A.*). In the schizont stage, the cell prepares for reinvasion of new RBCs by replicating and dividing to form up to 32 new merozoites (*Bozdech 2003*).

The erythrocyte membrane changes its permeability as its erythrocyte cycle evolves (*Ginsburg 2004, Kutnera 1982*). Due to the high sensitivity and permeability of the membrane at this stage, the proper medium for cell survival must be supplied. Stirs as well as changes in temperature affect the normal development of the cycle. Consequently, once cells have been separated in the schizont stage, they must be used immediately, even more when the effect of the release of merozoites is to be seen.

4.3.3. EXPERIMENTAL CONTROLS

By performing the observation of the infected erythrocytes, the negative control (non-infected erythrocytes) was considered, observing the two signals in the equipment in a parallel and simultaneous manner:

Two external controls were used:

- a) Thin blood films before and after the experiment

The control films were fixed with Methanol x 1 minute and coloured with Giemsa stain at 12%. The morphological characteristics both of the non-infected erythrocytes and those of the infected erythrocytes were observed (schizont stage).

b) Quartz: at the end of the experiment

Another microscopic observation was performed to the quartz, after the fixation of the infected and non-infected erythrocytes. The technique described in the chapter 3 (*Methods*) was performed with Paraformaldehyde 4% in PBS (PFI 4%) x 4 hours, followed by Glutaraldehyde 2.5% in PBS and finally a stain with Giemsa 10% for 30 minutes and washing with distilled water for the pieces of quartz observed with the optical microscope. In the case of the observation of TEM, the same procedure was performed but without the Giemsa stain.

The fixation of the infected erythrocytes on the gold quartz had not been reported in the literature. The preservation of the ultra-structure is essential to perform the observation of the release of the merozoites, the structure of the erythrocyte membrane and the morphological cell characteristics in detail. Different techniques for the fixation of the cells are reported like the ones used for the slides (*Ljungström I. 2004*). In the experiments, the optimisation of the biological layer was done without previous fixation of the erythrocyte cells, only maintaining the humidity of the quartz. In this case, since the aim is to see the infected cells, it is necessary to perform the stain with Giemsa, requiring the fixation of the cells to maintain their structure.

The methanol used in the slides shows good cell fixation since these are distributed evenly when performing the sweeping of the film, but in the case of the quartz, these are immobilised directly over the PLL. The distribution over the quartz pieces is different due to the aspects mentioned above, including the presence of lumps and evidence of cells not clearly defined in fixations with methanol.

An endless stream of techniques for cell attachment is reported in the literature (*Rengifo A. 2007*). The subject of fixation and preservation is a major scientific topic in the methodology of microscopy and it deals with many aspects of the living state and the nature of the organisms to be fixed. The fixation of living cells and tissues simply means an immediate stop of the life processes taking place within and around them (*Halit 2000*). Time becomes frozen for living things after fixation.

Any fixation must also be a tool for preservation for a long time, otherwise it may cause disintegration of the structures, which is obviously not our aim. In general, fixation strengths and times are considerably shorter for cells than on the thicker, structurally complex tissue sections. Cross-linking reagents (such as paraformaldehyde) form intermolecular bridges, normally through free amino groups, thus creating a network of linked antigens. Cross-linkers preserve cell structure better than organic solvents, but may reduce the antigenicity of some cell components, and require the addition of a permeabilisation step, to allow access of the antibody to the specimen. Different fixation methods are described. (ICH 2007).

The fixation of infected and non-infected erythrocytes to TEM was established with PF 4% and GA 2.5 in PBS. This protocol was performed in association with the Max Planck Institute of the University of Tübingen and with the assistance of Jürgen Berger, specialist in this kind of microscopy, there were excellent results.

In accordance to the objective of the research set for the study of the erythrocyte cycle of the *P. falciparum*, the focus was especially on the last six hours of the cycle: before the release of the merozoites, it was observed that the change in mass associated with the merozoite release process yielded a change in the measurement of the frequency.

As it was explained above, the processes of adsorption and desorption of the immobilised cells create frequency changes associated to changes in mass which are detected by the biosensor system. Taking into account that every schizont has an average of 16-24 merozoites (up 36 merozoites) (Wiser 2009) and every merozoite has an average diameter of 1.0 a 1.2 μm (Kumaratilake 2000) and a length of 1.5 μm (Bannister 2000, Torii 1998), the mass associated to the breakage of every erythrocyte is significantly representative and even more when the erythrocytes can have two or three nuclei.

In the results obtained with different parasitemia concentrations, it is observed that in concentrations higher than 90% (separated with the MACS system), there is a change in the signal compared to parasitemia concentrations, schizont stage, of 0.2%, 2% and 50%.

Figure 4-14 shows the comparison of parasitemias at different concentration levels, obtaining change in the signal in percentages of infected cells higher than 90%. Due to the

fact that the ring and throphozoite stages do not affect the appearance of the erythrocyte, i.e. its membrane remains well-defined, as well as its size, the infected erythrocytes remain stable on the PLL.

Comparison of signal changes with different concentrations of parasitemia

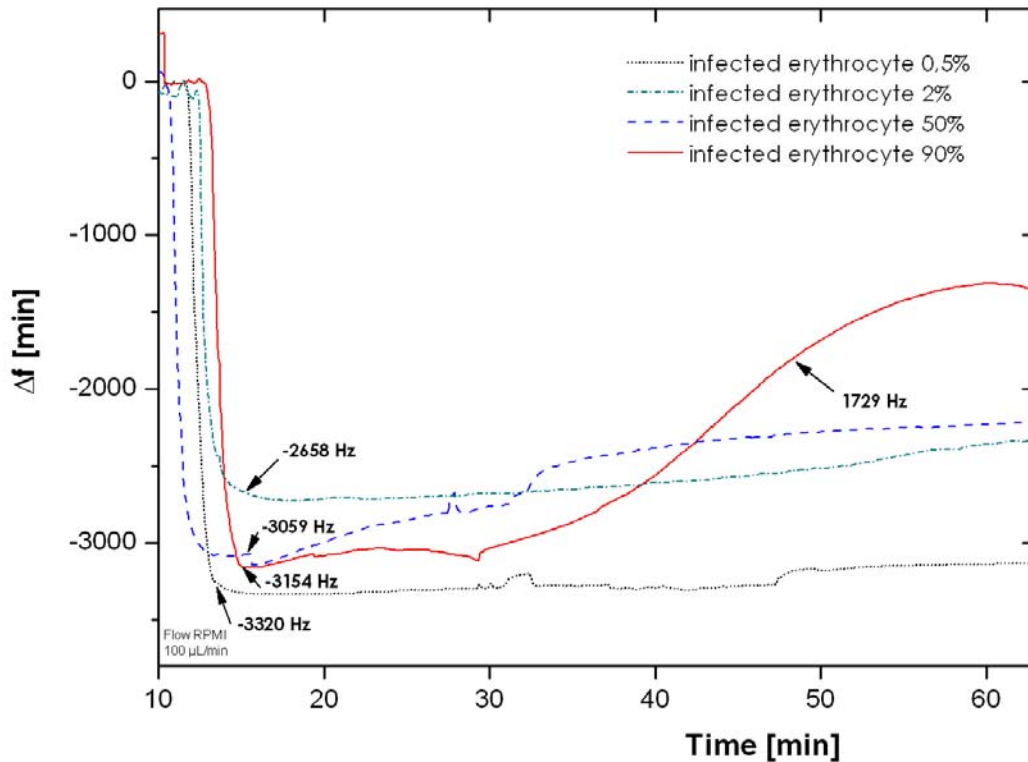


Figure 4-14. Comparison of signal changes with different concentration of parasitemia. The infected erythrocytes with 90% parasitemia produce an increase of the signal (1729 Hz). Other concentrations of parasites do not produce changes of the signal.

Figure 4-15: The results obtained indicate that the binding of infected and non-infected erythrocytes results in a frequency drop of ~ 3000 Hz. The infected erythrocytes (90% parasitemia) produce an increase of 1700 Hz after 135 min, while the non-infected ones lead to a stable frequency. Another sample of infected erythrocytes was monitored in parallel outside of the sensor device (positive control) under identical conditions of temperature and medium. Both the status of the infection as well as the condition of the parasites was rechecked through the thick film method and observation under the microscope.

Experiments with infected erythrocytes and non-infected erythrocytes

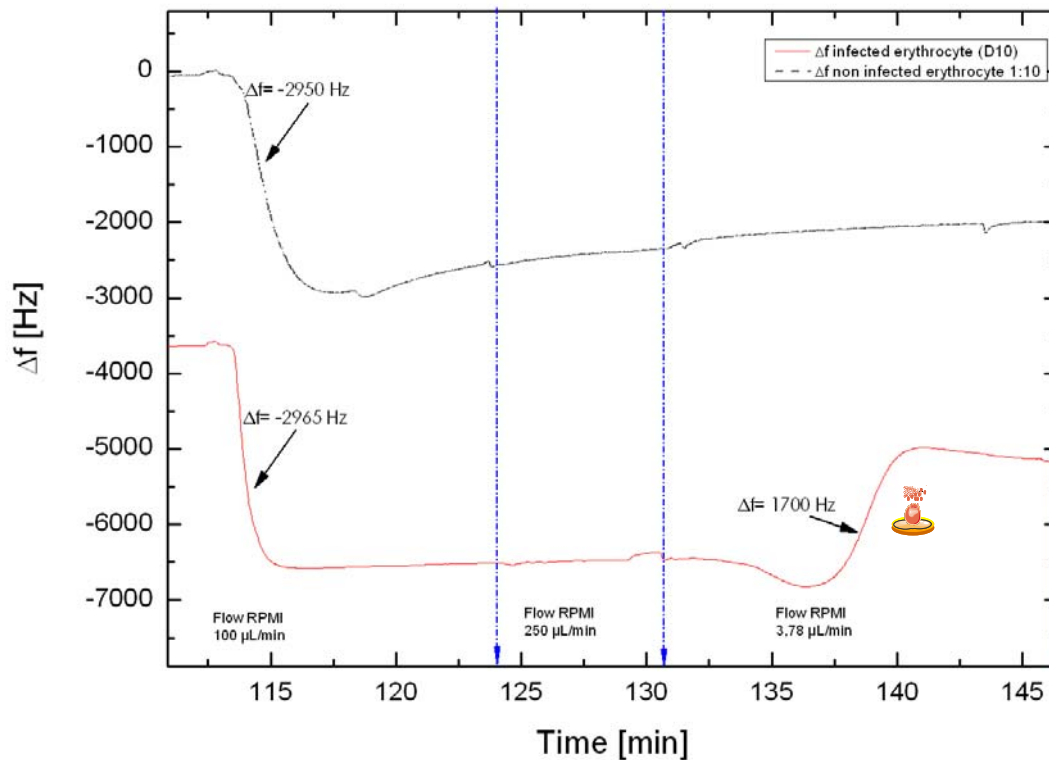


Figure 4-15 Comparison of the measurement of the frequency differential for infected and non-infected erythrocytes. The parasites used in schizont stage show a change in the signal after 135 minutes while the signal of the non-infected erythrocytes keeps constant.

These responses of increase in the signal in the measurement cell which contains the infected erythrocytes was reproducible using the parasites synchronised in the schizont stage and purified by the MACS system. The increase times varied between 15 minutes and 30 minutes maximum. This implies that within the schizont stages, there are different maturity degrees: early schizont and mature schizont, which results in variations in the increase times of the measurement of the frequency.

Another important factor which is related to the release time of the merozoites is the stress stages of the parasite. According to what has been stated above, in this stage, the membrane of the infected erythrocyte has higher permeability, an aspect which affects its rigidity and causes conditions such as stirring, changes in temperature or availability of the parasites to be able to change both the merozoite release time and the death of the infected erythrocytes. Consequently, the controls before the experiment play a key role to

determine the stage of the infected erythrocytes and to make an analysis of the behaviour of the experiment.

Graphs 4-14 and 4-15 show different increase times of the signal in 140 minutes and 65 minutes, respectively. Taking into account the microscopic observations before the experiments, both for experiment 1 and experiment 2, the parasites were in an early schizont stage and in mature schizont stage.

The increase time in the signal can last from 1 minute to 30 minutes, even in synchronised stages of the parasite. This indicates a sensitivity of the equipment to detect significant changes in mass associated to the breakage of the membrane of the infected erythrocyte.

The important aspect of the result obtained is that they show that, when there is lysis of the erythrocytes caused by the release of merozoites, they can be detected by the biosensor system.

The external controls through thin film slides both at the beginning of the experiment as well as at the end of it show that the increase in the signal obtained is related to the release of the merozoites. Microscopic observations of the quartz at the end of the experiment show the release of merozoites.

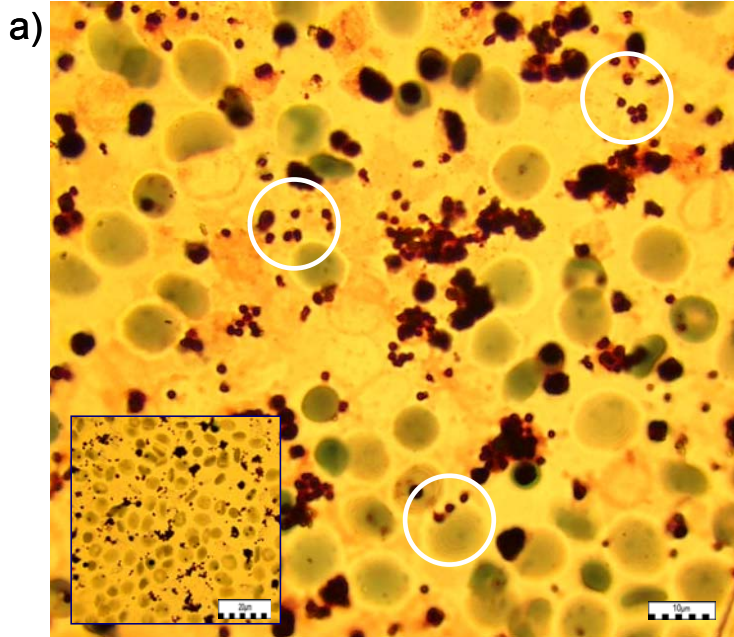
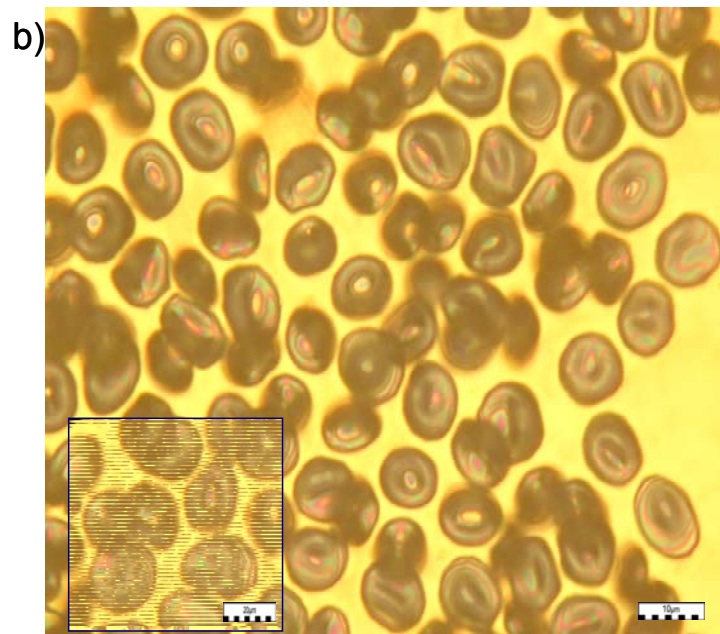


Figure 4-16. Photographs of the quartz at the end of the experiment.

a) Quartz of the measurement cell 1, where the infected cells in schizont stage were injected shows merozoite release (circles). These turn pink in colour on the glass films, but they take a darker colour on the quartz. The staining was done with Giemsa $\times 30$ mn. Also, fragments of the erythrocyte membrane adhered on the PLL are observed. In the same way, non-infected erythrocytes, which are not stained by Giemsa, are observed. An estimated release of 90% merozoites regards the immobilised parasites.

b) Quartz of the measurement cell 2 shows the non-infected erythrocytes. The erythrocyte cells show their morphological characteristics: concave disc, approx. size aprox 7.0 – 8.0 nm, smooth membrane. No intense stain with Giemsa is shown. The immobilised cells are uniform and there is no denaturalisation or lysis related to them.



To validate the presence of this response with parasites in mature stage (merozoites almost released), an equivalent experiment was done. The control performed before the experiment shows that more than 80% of the parasites had already released the merozoites, which implies that there were only erythrocyte membranes, haemozoin and parasite products. Even like this, the infected, not lysed erythrocytes were immobilised in the PLL.

The results shown in graph 4-17 show that there is no increase in the signal after 30 minutes after liberation of merozoite. The microscopic observations, both of the quartz and of the slides, at the end of the experiment show that more than 90% of the cells infected have undergone haemolysis caused by the exit of the merozoites.

In stages different to the schizont, no change in the signal was observed, which indicates that the sensitivity of the QCM was optimal and it could show in real-time what occurred inside the parasite.

Comparison of signal changes with >80% schizont hemolysed and non-infected erythrocyte

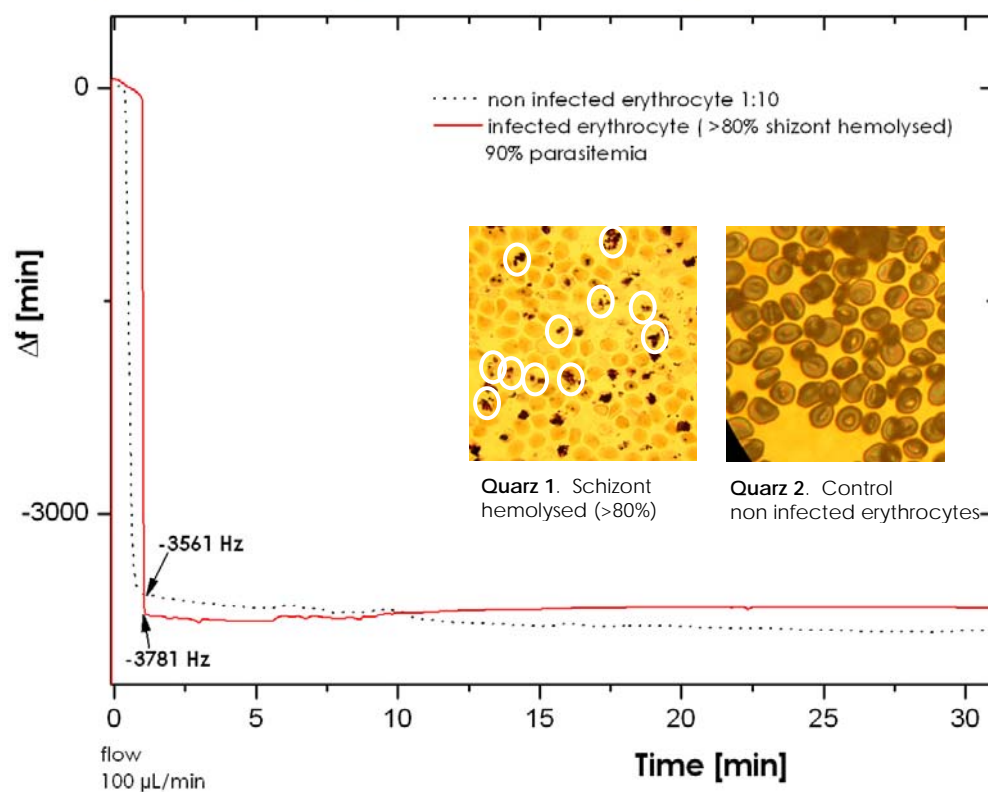


Figure 4-17. Comparison of signal changes with >80% schizont hemolysed and non-infected erythrocyte

4.4. VALIDATION OF THE FREQUENCY MEASUREMENT FOR THE INFECTED ERYTHROCYTES AND THE NON-INFECTED ERYTHROCYTES INSIDE THE BIOSENSOR SYSTEM.

According to the observation of the infected and the non-infected erythrocytes in number 4.3 above, a detailed validation was intended of the changes suffered in the infected cells before, while, and after the release of the merozoites and their relationship with the signal obtained.

The results of the increase in frequency were reproducible and they worked as basis for the study of other processes of the erythrocyte cycle as “in vitro” reinvasion, merozoite vitality, tests with drugs, amongst others, which will be analysed below.

Graph 4-18 shows the methodology to correlate the frequency for the group of (infected and non-infected) erythrocytes. This time, external control was intended, not only at the beginning of the experiment, but with special emphasis on the moment in which the signal increases and which thus determines two issues: First: can the signal be translated into a real release of the merozoites? Second: is the method for the experiments optimal to reproduce these results?

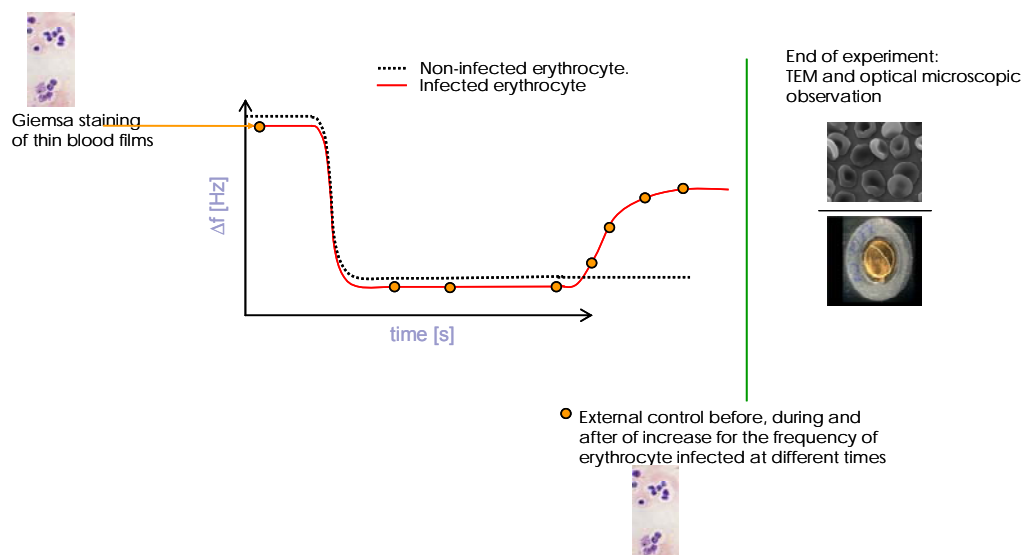


Figure 4-18. Controls performed to establish the validation between the frequency measurement for the infected erythrocytes and the non-infected erythrocytes. On this occasion, microscopic observations are made at all times during the experiment. At the end, new microscopic evidence is included using TEM.

Release of malaria parasites from infected RBC at the end of the asexual erythrocyte cycle occurs approximately every two days, asynchronously in parasite culture and synchronously *in vivo*. It remains one of the most elusive processes of the parasite life cycle. According with Glushakova, there are several reasons for why the release of malaria parasite is so poorly studied: First, release is a very short-lasting event. Second, it is difficult to observe release *in vitro* directly under the microscope because schizonts are very sensitive to the culture conditions. Third, schizonts have low physical stability and high sensitivity towards different temperature, pH, osmotic pressure, and lighting conditions (Glushakova 2007).

Traditional microscopic observation (by using thin films which allows the control of cycle of plasmodium) indicates the end of the previous cycle and the beginning of the new one. The quantification of parasite release without any contribution of parasite invasion is the prerequisite for studying parasite release from host cells, a largely unexplored aspect of parasite biology (Glushakova 2007).

The release of merozoites is described by Trager (Trager 2002) and documented by Dvorak (Dvorak 1975). The conditions of the experiment play a key role for the development of such processes and the reproducibility of the results. Firstly, the conditions of temperature, medium, atmosphere and duration of observation influence the pattern of merozoite release. Secondly, in fresh samples, during the last few minutes preceding rupture there is a dramatic morphological change; the infected cell becomes bright, highly refractile with a central pigment clump. Thirdly, the merozoites are released abruptly with a scattering movement. Fourthly, with time on a warm stage, merozoite release changes to a 'drop-out' clustered pattern, without scatter. Finally, the merozoite release process appeared to be quite similar in different *Plasmodia* species (Lew 2005).

How can these changes be made visible or at least approach us to the observation of the merozoites and the response in the signal?

In first place, the signal obtained was reproduced showing changes in the increase of the frequency in the cell of the infected erythrocytes, just as in number 4.3. With this, it is proven that the conditions of the experiment are optimal for the reproducibility of the result in the graph. Again, graph 4-19 presents another experiment with this characteristic

in the curve of infected erythrocytes compared to the stability of the signal of the non-infected erythrocytes.

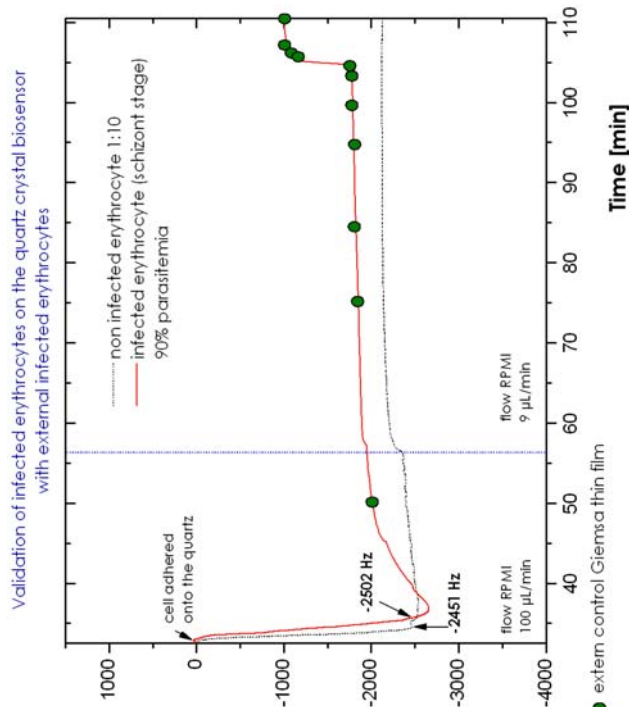
Secondly, the microscopic observations on the slides show the development of the schizont, i.e. the change from schizont stage until the release of the merozoites with certain specificities like the presence of hemozoin (dark yellow pigment), fragments of the membrane, merozoite release (pink-purple in colour), but it is limited in seeing the parasitophorous vacuole membrane (PVM) or the digestive vacuole in detail. Consequently, another microscopic technique was used to be able to observe 3-D structures of the schizont and of the merozoites and test if these cells kept their continuous development on the gold quartz.

The photographs presented in graph 4-20 show a continuous development of the schizont. At the beginning of the experiment (1 hour after the purification and of the optimal conditions of T°, gaseous atmosphere, medium of nutrients, sterility, etc.) the infected erythrocytes in schizont stage observed are more than 90%.

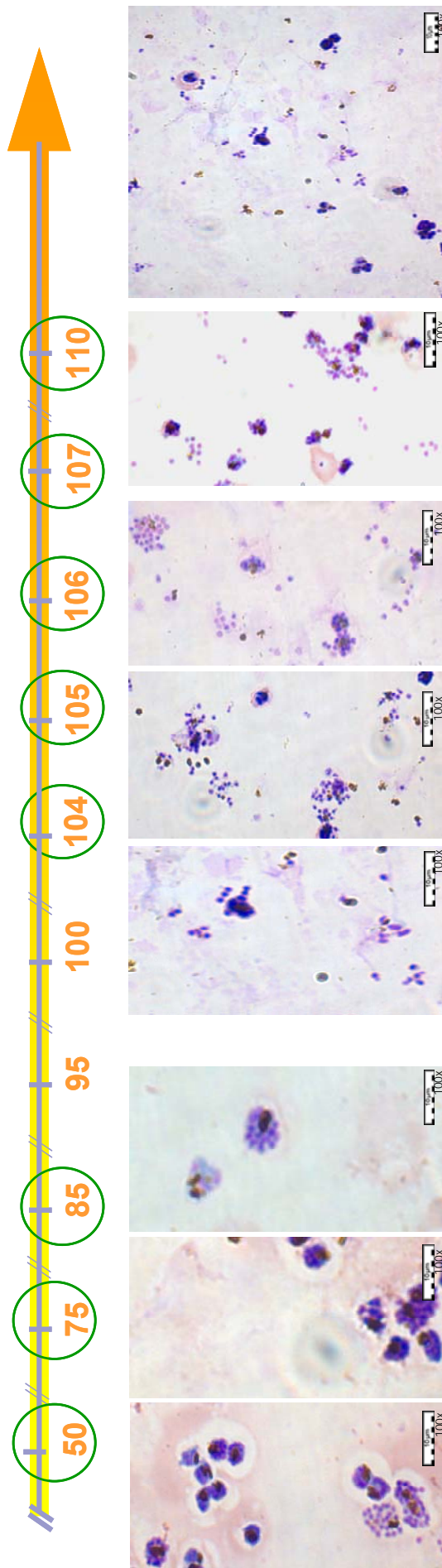
Graph 4-19 The photographs presented, taken through optical microscopy, show a continuous development of the schizont related to the time of the experiment.

Time 32 min: The non-infected and the infected cells are immobilised on the PLL, showing a drop in the frequency of -2.250 Hz and -2.500 Hz respectively.

Time 50, 75, 85 min: A stable frequency signal is observed in both measurement cells. The photographs of the slides show perfectly defined schizonts. There is no merozoite release yet. Erythrocytes remain intact. Many erythrocytes have two schizonts. The digestive vacuole is observed, hemozoin, typical of this stage. **Time 104, 105, 106, 107 and 100 min:** These controls, taken during the entire signal increase, show erythrocyte lysis caused by the merozoite release. The percentage of merozoite release at time 100 is higher than 90%. As from time 100, the frequency signal is constant.



Time (min.)



The issues mentioned above show two essential aspects: I) Relationship of the merozoite release with the response obtained in the biosensor system. II) Stability in the signal once there are no significant changes in the mass.

The fixation was determined for the observation of the infected erythrocytes on the quartz by TEM at the end of the experiment. Though the TEM handles standard protocols, tests were carried out with different chemical fixations like Methanol, PFI 4%, PFI 4% and Glutaraldehyde 2.5%. According to the previous explanation, the selected fixation was the mixture of these two (PFI and Glutaraldehyde) with excellent results.

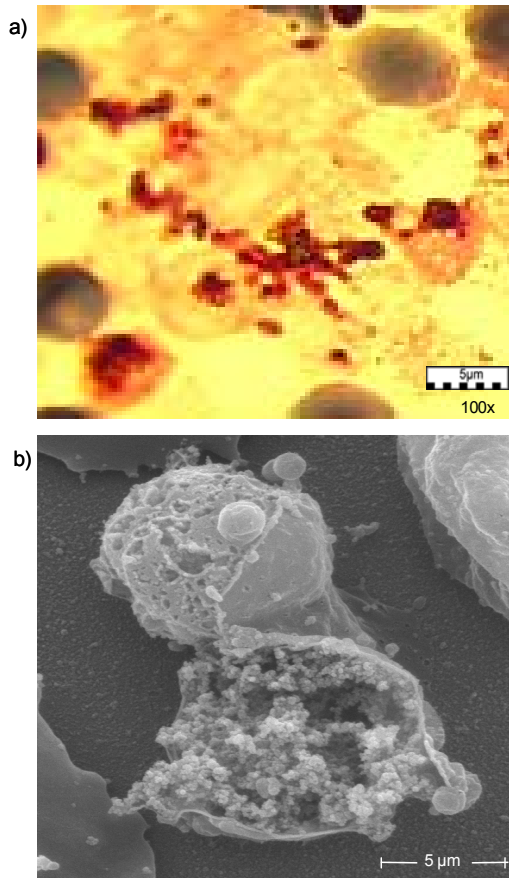
In the literature, there are no reports of fixations of cells infected with *P. falciparum* on gold quartz. The photographs presented in 4-21 allow the observation of very interesting aspects about the morphology and the characteristics of both the infected and the non-infected erythrocytes.

The merozoite release is confirmed with these microscopic observations by TEM. Membrane fragments, merozoites with the typical shape of a sphere. The size relationship between the merozoites (1.0 μm in diameter) and the erythrocytes ($\sim 7.0 \mu\text{m}$) allows the confirmation that optimal conditions were present all through the experiment to keep the cells in perfect condition. In reports, there are studies of the *P. falciparum* (Guenberg 1983) describing characteristics like the presence of knobs in the trophozoite stage and the schizont compared to the non-infected erythrocytes.

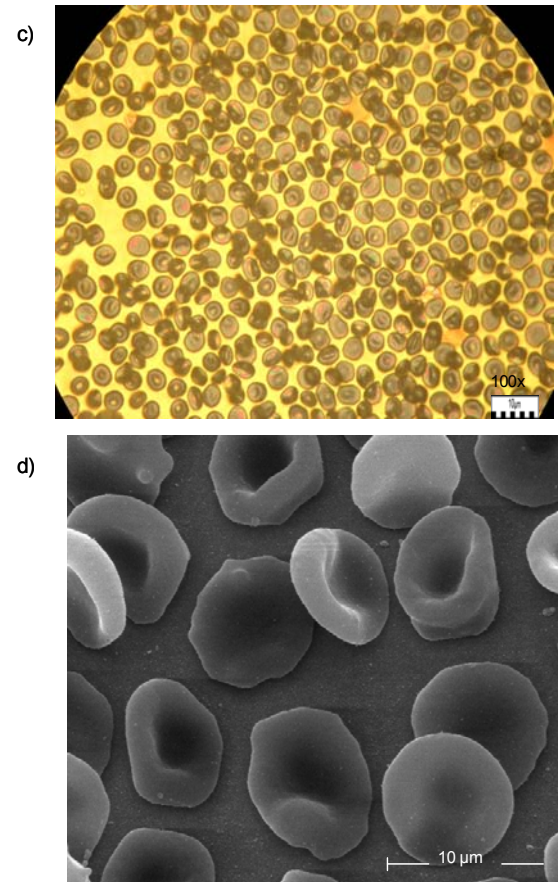
Other evidence of these photos is the normal development of the erythrocyte cycle which is not affected by the immobilisation on the PLL. Though a part of the membrane is immobile on the polycation agent, the parasites keep their development. This suggests that the outer membrane is not affected and that the maturity of the parasites inside the inner membrane of the erythrocytes keeps its cycle.

The issues mentioned above open a way for the study of other parasites and their translation into a quantifiable signal of the changes undergone, whether chemical, biochemical, or biological, amongst others.

Quartz infected erythrocyte



Quartz non infected erythrocyte



Graph 4-20. Photographs of Quartz 1 and 2 after 24 hours. Quartz 1: Infected Erythrocyte a) Optical Microscope shows the merozoite release, fragments of the erythrocyte membrane, dark-colour hemozoin. b) TEM shows hemolysed erythrocytes with fragments of the membrane and free merozoites. Quartz 2: non-infected erythrocytes c) and d) show morphological characteristics of the erythrocytes without alteration of the erythrocyte membrane. The quartz was fixed with PFI 4% and Glutaraldehyde 2.5%.

4.5. REINFECTION OF THE HEALTHY ERYTHROCYTES INSIDE THE EQUIPMENT

In the last 40 years, there have been attempts to study the complex process of erythrocytes being invaded by merozoites in malaria. The formation of the parasitic vacuole (*Bannister 1990, Bannister 1986, Murphy 2007, Ward G. 1993*), selection of the host cell and merozoite capture (*Butcher 1973, Miller 1975*), proteases involved in the invasion (*Donse T.J. 2008, Hadley 1983*), merozoite motility (*Baum 2006, Miller 1979*) and a vaccine with proteins present in the merozoites (*Deans J. A. 1988, Matuschewski 2007, Thera 2008*) are some of the issues which have made this an interesting process to be studied.

The merozoite of *Plasmodium* is a transitory stage of the malaria parasite that emerges from schizont-infected erythrocytes and proceeds to attach to and invade new erythrocytes. The associated processes are collectively termed reinvasion (*Lyon J. 1986*). The invasion process of the merozoites is complex and highly sensitive. Numerous reports are found on the study of the release (*Winograd E. 1999*) and invasion of the merozoites (*Ward G. 1993*) and many mechanisms remain unclear.

The erythrocytes are invaded by the merozoite form of the parasite, and the process of invasion depends on the capability of merozoites to recognize ligands on the erythrocyte membrane. Identification of parasite receptors and their ligands is important for understanding the invasion process and for developing immunologic and chemotherapeutic weapons against the parasite (*Camus 1985*). Invasion depends on distinct molecular interactions between ligands on the merozoite, the invasive form of the parasite, and host receptors on the erythrocyte membrane (*Ghislaine 2009, Preiser 2000*).

The merozoite release occurs in a very short time (not more than 1 second) (*Gilson 2009*). Once merozoites have been released, a structurally stable infected erythrocyte “ghost” can be detected. This membranous structure does not vesiculate or disintegrate even after a prolonged period of observation (>60 min, not shown) (*Winograd E. 1999*). Videomaging (*Dvorak 1975*) also demonstrated the rapidity of invasion, completed in about 1 min, and the strange convulsions undergone by the RBC surface during the process, which are still not understood (*Bannister 2009, Gilson 2009*).

Due to the complexity of this process and the short time of the invasion of the merozoites, the conditions to perform the “in vitro” reinvasion on non-infected erythrocytes adhered on the PLL in a second quartz inside the system causes all the conditions of the experiment to be extremely controlled. The study of this reinvasion process inside the QCM system is performed for the first time.

Graph 4-21 shows the experimental design, this time performing the union of the two measurement cells. The study of the reinvasion on a second quartz piece on the non-infected cells comprises the next steps:

- I) Immobilisation of the infected and the non-infected cells separately inside the system
- II) Observation of the merozoite release (cell of infected erythrocytes)
- III) Transfer of the released merozoites to the cell of the non-infected merozoites for the infection of the healthy erythrocytes inside the system
- IV) Observation of the signal both of the release (Quartz 1) and of the reinvasion (Quartz 2)
- V) External controls for the validation of the process

For parts (I) and (II), the same procedure mentioned in number 4.4 was followed, where a change in the signal is obtained (increase in the frequency) when the merozoites are released compared to the healthy erythrocytes, where the signal remains stable. The essential step for the reinvasion inside the QCM focused on (III) where the transfer of the merozoites from one cell (quartz 1: infected erythrocytes) to the other cell (quartz 2: healthy erythrocytes) is carried out and the invasion of the merozoites is allowed.

The protocol established for the reinvasion process was:

- a. Preparation of the equipment at 37°C, disinfection and sterility of the materials and the medium. In the same way, preparation of the quartz with the PLL coating (as a minimum, two hours before the experiment)
- b. Filling the cells with RPMI 1640 complete until there is a stable signal, with a flow of 100µL/min (variation in the signal not higher than 20 Hz for 10 minutes)

-
- c. Concentration of the parasites previously purified through the MACS system (schizont stage) 1:10 in RPMI complete. Preparation of the healthy erythrocytes in concentration 1:10 in RPMI complete
 - d. Injection 50-100 μ L infected erythrocytes (Quartz 1) and the non-infected erythrocytes 20 μ L (Quartz 2) in a parallel manner and at the same time in a flow of 100 μ L/min
 - e. Observation of the signal: drop of the frequency (cell immobilisation on the PLL), stability of the frequency (cells are still on the PLL), increase in the signal for the infected erythrocytes (merozoite release) and for the reinfected erythrocytes (change in the signal)
 - f. When the system is stable, the flow of the medium is reduced from 100 μ L/min to 9 μ L/min to leave the experiment 24 hours to avoid bubble production inside the cell and to optimize the use of the medium.
 - g. External controls: collection of the released merozoites with injection of healthy erythrocytes at different times to then be incubated for 24 hours and analysed by FACS
 - h. Photographs by optical microscopy or TEM of the quartz pieces at the end of the experiment (24 hours afterwards)

The reinvasion process through this method was validated by using a short-distance hose \sim 2cm (diameter 0.38 mm) to link cell 1 and cell 2 and allow the immediate and safe transfer of the merozoites towards the healthy erythrocytes inside the system.

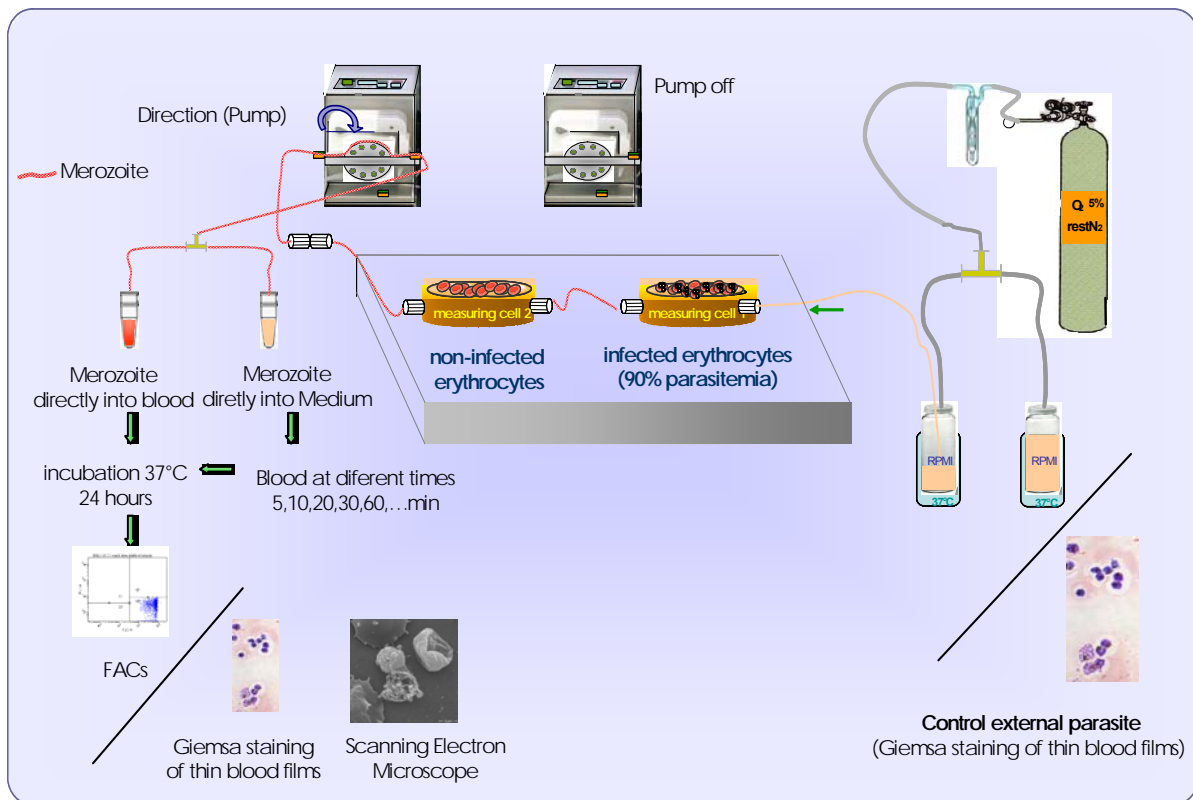


Figure 4-21. Illustration of reinfection on the quartz in the biosensor system and their external control. Once the merozoites are released from quartz 1 (measurement cell 1), they are transported through constant flow of medium RPMI 1640 complete by a short hose (diameter 0.38 mm) towards the other quartz 2 (measurement cell 2), where the non-infected erythrocytes are immobilised. The entire system is in optimal condition: temperature at 37°C (measurement cells, medium, hoses), gaseous atmosphere, medium of nutrients RPMI 1640 complete, sterility. Parallel controls are performed at the beginning of the experiment to check the stage of the parasites, during the experiment while the merozoites release signals are observed, and at the end of the experiment, collecting samples of merozoites and infecting healthy erythrocytes at different times. Analyses of the incubated samples are performed for 24 hours at 37°C and with medium RPMI 1640 complete through FACS and microscopy. The quartzes are photographed by TEM.

At every moment during the experiment, the flows of the medium RPMI 1640 complete must be continuous, at a constant temperature of 37°C and with supply of an appropriate gaseous atmosphere since the merozoites are very sensitive to external changes and they invade healthy erythrocytes in a very short time.

The biosensor equipment platform allows the parallel observation of two signals of the group of erythrocytes. The relationship of these two signals from the moment of release and the reinvasion is shown in graph 4-22. The infected erythrocytes (quartz 1) and the non-infected erythrocytes (quartz 2) show drops in the signals of frequency of -1250 Hz and -2030 Hz, respectively. After ~2 hours, there is an increase of 750 Hz in the frequency for quartz 1, which indicates the release of the merozoites in accordance to the

external control performed by the thin film. In this moment, the reinvasion to quartz 2 is performed through the union of the two cells through a hose. The signal of quartz 2 after hours does not show a significant change in frequency, but it does show a trend to increase in the frequency ~ 100 Hz for the next three hours and then becomes stable. Presumably, this change in frequency is related to the invasion of the merozoites to the healthy cells.

Reinfection of healthy erythrocytes on a second quartz within one QCM system

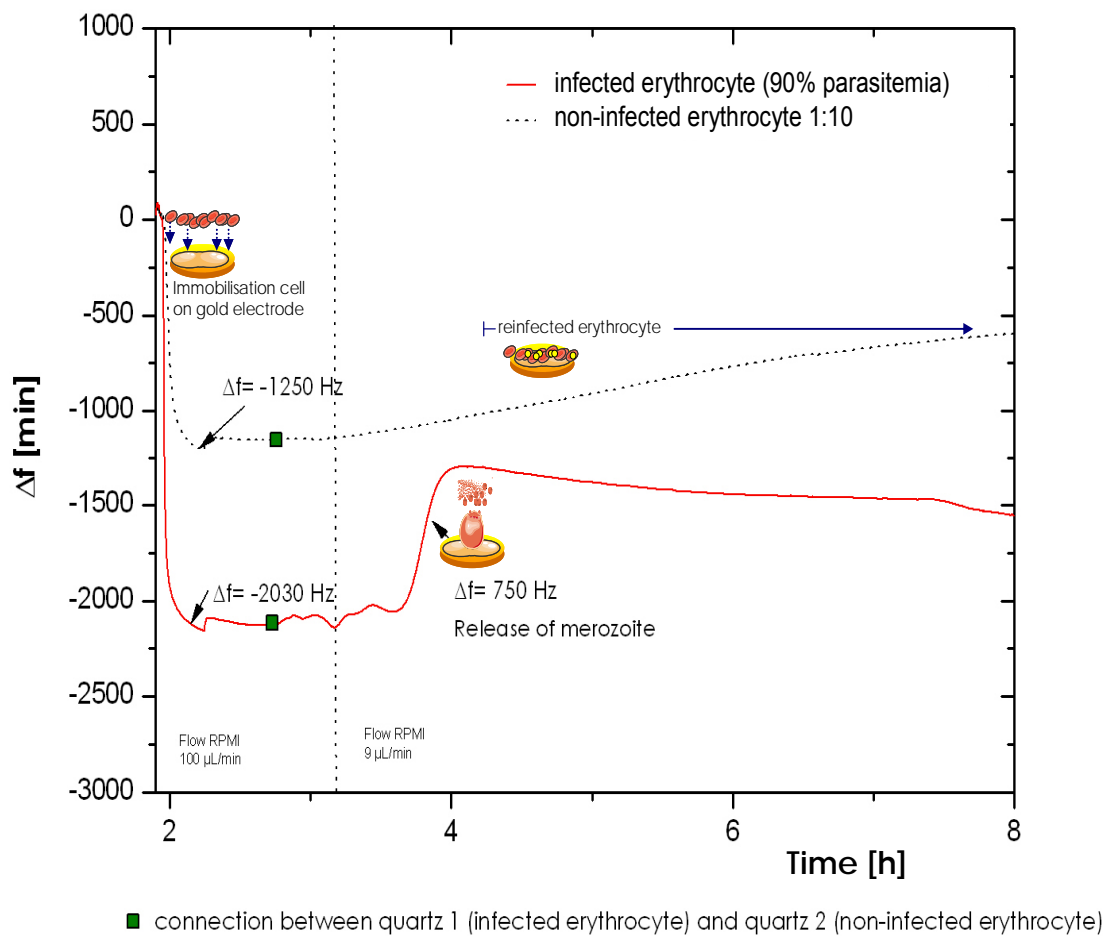


Figure 4-22. Reinfection of healthy erythrocytes on a second quartz within one QCM system. The results show the release for the infected erythrocytes in quartz 1 with an increase in the signal of 745 Hz while the signal of quartz 2 remains constant. After the release, the curve of reinfected erythrocytes on quartz 2 does not show a significant increase in the signal but it does show an increasing trend as time goes by.

To analyse this process in detail, see the different stages of the invasion of the merozoite and the relationship with a possible signal in the system:

(I) First contact (attachments and reorientation): The initial contact between the merozoite and erythrocyte is a crucial step, as the parasite must distinguish between erythrocytes competent for invasion and other cell types. Primary attachment of the polar merozoite appears to occur at any point on the surface of this parasite stage (Cowman 2006). The surface coat of merozoites is largely comprised of glycosylphosphatidylinositol(GPI)-anchored membrane proteins and their associated partners. Until this stage, there is no deformation of the erythrocyte membrane, only interactions between the proteins of the surface of the merozoite and the membrane of the erythrocyte. Thus, there is no modification of the erythrocyte and consequently no modification of the mass adhered to the PLL.

II) Secondary interactions. After the parasite reorientates, it must activate the invasion process, and this probably involves direct interaction of ligands at the apical end with erythrocyte receptors. Once apical interaction has occurred, the invading merozoite establishes a tight junction involving release of additional proteins from the micronemes and rhoptry organelles.

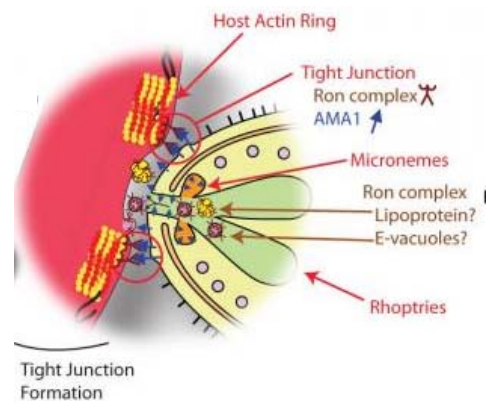


Figure 4-23. Apical interaction and tight junction of merozoite on erythrocyte

In this process of tight junction, the membrane of the erythrocyte remains stable and there are no significant changes to affect the mass deposited onto the quartz, thus the signal remains stable.

(III) The processes of invasion initiation, internalisation, and remodelling are highly associated with proteins which link the motors actine-myosine. This mechanism remains still unsolved, though it has been found that actin-myosin-based motility is important in merozoite locomotion during red-cell invasion and formation of the ring stage (Bannister 1995, Wasserman 2000).

At that moment, the membrane still remains stable and there are no changes in mass which can be associated to or translated in a signal with the biosensor system.

(IV) Ring stages. By definition, the ring stage commences shortly after invasion of the RBC by the merozoite, with the parasite flattening into a discoidal shape. The stage ends when the parasite adopts a more spheroidal shape and becomes a trophozoite at about 25 h into the cycle (*Bannister 2004*).

This was observed inside the system from the reinfection until the formation of the ring stage (24 hours) and controlled at the end through microscopic observation on the quartz to check the reinfection of the healthy erythrocytes.

Microscopic observations on the quartz 24 hours later evidently show that the healthy erythrocytes were reinfected. The presence of infected erythrocytes in ring stages is observed. The estimated percentage of parasitemia was ~1%. The infected erythrocytes show the presence of well-defined rings while the healthy erythrocytes maintain their morphological characteristics. These observations were also performed with TEM, watching in 3-D that, after 24 hours, the infected erythrocytes show a slight deformation in the membrane, which are different to the membrane of the non-infected erythrocytes. Figure 4-24 shows such observations.

The speed with which this complex process occurs requires optimal external conditions at all times such as temperature, pH of the medium, etc. as well as optimal internal conditions of the erythrocytes and merozoites so that they can adhere and control the traffic of proteins inside the erythrocyte.

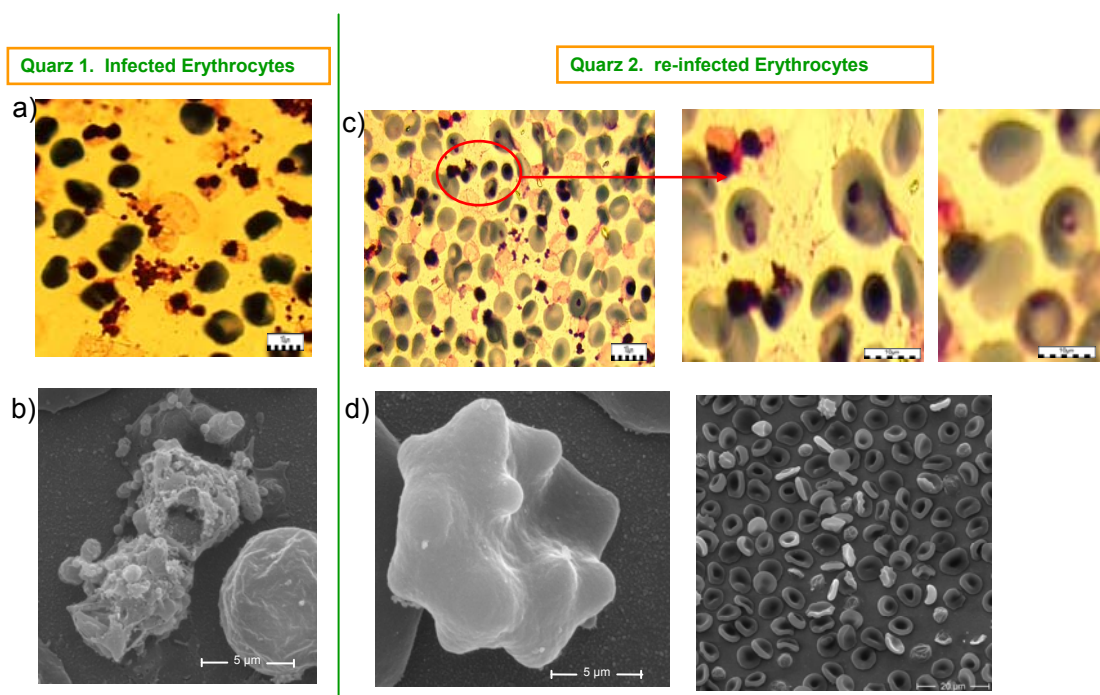


Figure 4-24. Re-infection of healthy erythrocytes inside the QCM system. The photographs show quartz 1 infected-erythrocyte and quartz 2 re-infected erythrocyte. a) and b) show schizont rupture and merozoite release ($\times 100$). c) and d) show formation of the ring stages 24 hours later. The presence of chromatin and well-defined rings is observed. b and d) TEM ($\times 30000$).

How merozoites selectively capture RBCs has been a persistent problem over the years, still not yet quite resolved. All species of Plasmodium are known to have restricted ranges of host species and some are also restricted within species to either reticulocytes or mature RBCs (Bannister 2009). *In vitro* studies of re-infection have shown a strong positive correlation between merozoite adhesion and species susceptibility to infection (Butcher 1973), pointing to initial contact being critical for selection. Another important aspect is the genetic variability of the RBC for the resistance to malaria, for example, blood groups in humans and protein adherence of proteins to the merozoite. It is also evident that the invading merozoite requires more than simply the red cell's membrane and glycocalyx for invasion to proceed: white ghosts are largely refractory to invasion, and a minimal content of red cell cytosol is required unless there is supplementation of the ghost contents with ATP.

4.5.1. RE-INFECTION CONTROL AND OPTIMISATION

The speed at which this complex process occurs requires optimal external conditions such as temperature, pH of the medium, etc., as well as optimal internal conditions of the erythrocytes and the merozoites at all times to be able to adhere and control the traffic of proteins inside the erythrocyte.

To control whether the re-infection process is carried out in an optimal manner inside the system, external controls were carried out. Graph 4-21 shows the experimental design. When the merozoites are released in accordance to the signal observed in the equipment, samples of merozoites+medium are collected in two different standard microtest tubes ~1mL, which are then to be analysed by FACS and microscopy. Healthy and fresh erythrocytes (for 1mL of sample collected 50 μ L erythrocytes) are put inside one microtest tube before the collection, while 1 mL of merozoites+medium is collected in the other microtest tube.

The objectives of these analyses are:

- I) Determine the efficiency of the re-infection method
- II) Determine the viability of the merozoites

4.5.1.1. Efficiency of the re-infection method

Once the re-infection has been observed inside the system and controlled through microscopy, an attempt to estimate the re-infection percentage of the system and the efficiency of the method is performed.

To achieve this, the samples collected were incubated for 24 hours at 31°C and analysed through FACS. Fluorochrom Acridine Orange (AO) was used to detect the erythrocyte content of parasitic DNA. This method allows for quantification of parasitemia and for quantification of parasites in different stages of differentiation according to DNA content.

According to the protocol described in the chapter about methods, the samples were stained with an AO stock stain (rendering a final AO concentration for 0.5 mg/mL) and incubated for 10 min at room temperature. As mentioned previously, samples were adequately diluted and then kept in the dark until acquisition. In flow cytometry,

logarithmic red fluorescence in the FL-1 channel using a 630 nm long pass filter were detected. Fluorescence of the non-infected population was adjusted to plot between 100 and 101 in both channels. Compensation was again set to 0 for all channels.

Results obtained in the re-infection experiment, displayed in figure 4-25, show a parasitemia percentage of ~1.2% for the sample incubated for 24 hours at 37° and collected directly in healthy erythrocytes of medium+erythrocytes released in the equipment (sample 1) compared to the parasitemia percentage of 0.1% in the sample treated in the same manner but not collected immediately in the healthy erythrocytes, but adding the latter one hour later. The correlation between cytometric and microscopic determination shows re-infection for sample 1, but not for sample 2. Ring stages are observed in the infected erythrocytes, with their ring perfectly defined. This result was reproducible in several experiments.

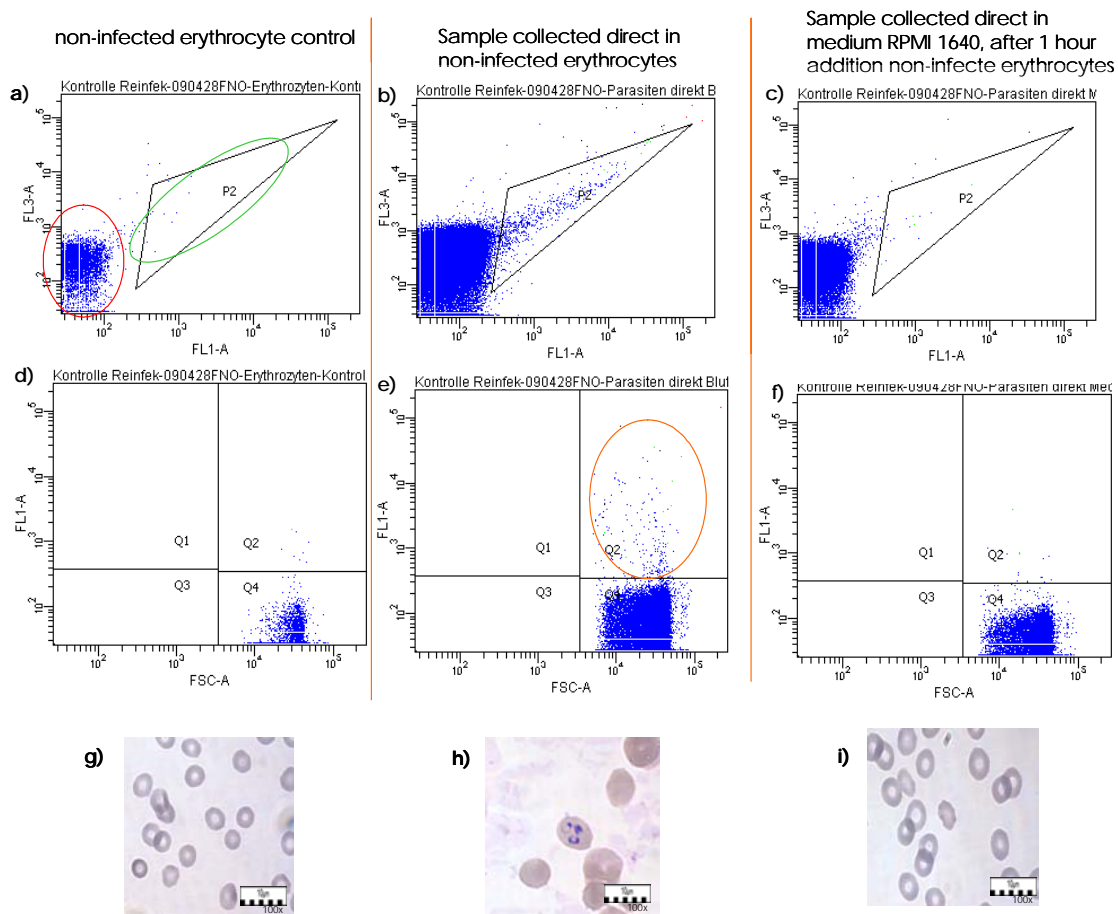


Figure 4-25. Validation by flow cytometry. Representative two-channel (FL-1/FL-3) dot plots of re-infection experiment examining parasitemia in samples with merozoites+medium direct from QCM in non-infected erythrocytes (sample 1) and merozoites+medium from QCM direct in medium RPMI 1640, addition of 50 μ L non-infected erythrocytes (sample 2) after 1 hour. The samples were incubated 24 hours at 37°C. Samples were stained with AO as described in Materials and Methods. Normal non-infected populations plot in the lower left corner (red circle), non-infected populations exhibiting nonspecific fluorescence stretch out diagonally from the lower left corner and plot between 10^2 and 10^5 on the AO red (FL-1). Infected RBC populations are gated and plot parallel above the non-infected population (green circle). a) sample acquisitions from negative controls (non infected erythrocytes) b) sample acquisitions from merozoite+medium from QCM collected directly in non-infected erythrocytes, c) sample acquisitions from merozoite+medium from QCM collected directly in medium, addition 50 μ L of non-infected erythrocyte after 1 hour. For each dot plot approximately 100000 events were acquired. Parasitemia (percent (Q2): (d) (0.1%) (18 events), (e) 570 (1.2%), (f) 0.1% 27 events. (g, h, i) Photographs with Giemsa stain (extern control samples from FACS) (g) non-infected red cell (negative control) (h) re-infected cell from merozoites obtained of the experiment with QCM. It shows ring stages and the correlation with analyses per FACS (i) 1 hour after the collection of the merozoites+medium and the addition of healthy erythrocyte there is not re-infection. Original magnification \times 1000.

An additional aspect intended for verification was whether this re-infection was the result of the detachment of some immobilised schizont on the PLL and whether they are

causing the re-infection of healthy erythrocytes on the second quartz, or if they really were the released merozoites. To do so, samples were taken immediately after the drop in the signal until before their release increase in the signal and analysed through cytometry to determine that the schizont remained immobilised all the time and that they were not causing the re-infection. These samples were treated in the same manner as sample 1 described above and collected on healthy erythrocytes (Figure 4-26).

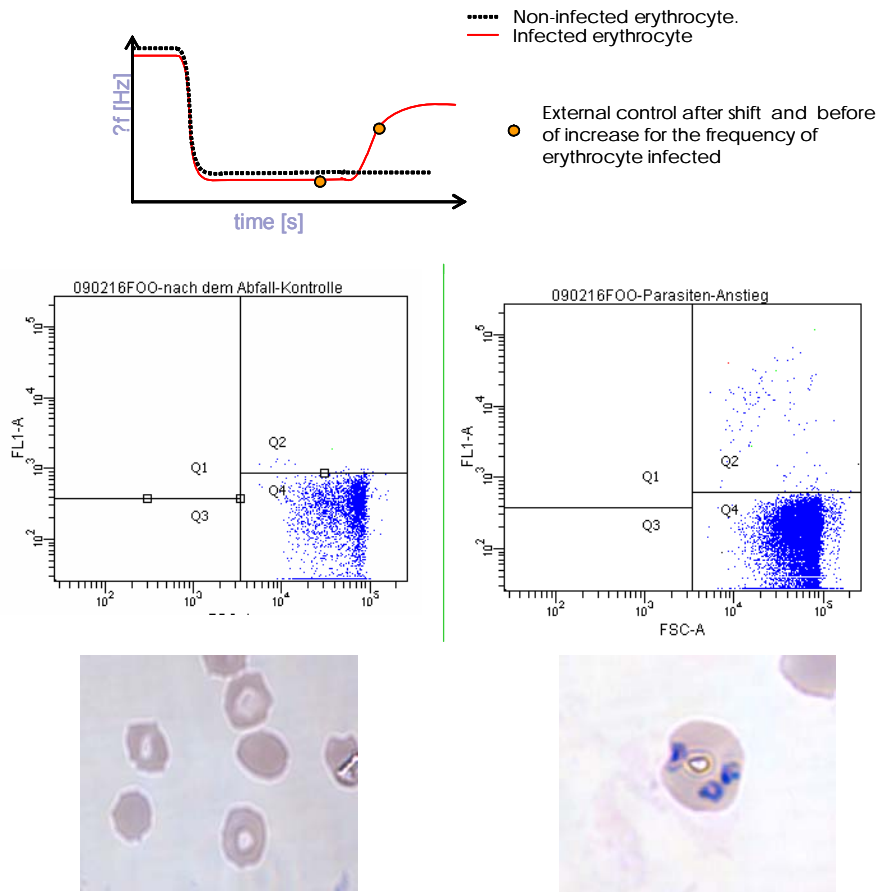


Figure 4-26. Re-infection control. The results of the flow cytometry for the sample taken after the immobilisation and for the sample during the signal increase are 0.1% and 1.2%, respectively. The microscopic correlation shows re-infection for the sample obtained when there is merozoite release but not for the sample taken before the increase in the signal.

4.5.1.2. Viability of the merozoites

The merozoite release, the re-infection on a second quartz within the system and the optimisation of the re-infection have been observed and validated so far. It also happens to be highly interesting that naturally-released merozoites can be isolated to carry out studies and for immunological applications through this method.

Studies utilizing several plasmodial species have demonstrated that erythrocytic merozoites serve to induce protective immunity and act a specific stage against which antimalarial antibody is directed. The isolation of erythrocytic merozoites has been achieved employing techniques based on chemical lysis (*Siddiqui 1979*), physical disruption (*Prior 1972*), natural release (*Dennis 1975, Mitchell 1977*) and free-flow electrophoresis (*Sterling 1984*).

As explained above, the molecular mechanism of merozoite invasion is complex, involving the interaction of a number of merozoite ligands and erythrocyte receptors, and is extremely sensitive to any changes in erythrocyte viability, morphology, and membrane physiology.

Since the invasion process is carried out rapidly (~1 min), the merozoites need all the optimal conditions and the life span from the moment they are released until the re-infection is no longer than 30 minutes, according to the literature (*Miller 1977*). Standardizing techniques of merozoite isolation, however, should make possible the isolation and characterization of antigen(s) from this life cycle stage responsible for inducing protection (*Sterling 1984*).

With this QCM-based isolation, the viability of the merozoites was questioned.

To answer this question and since merozoites can be isolated naturally through the procedure developed with QCM, samples are taken once they are released through the observation of the signal.

The merozoites (medium+merozoites) are collected in nine different microtubes (~200 μL) directly from the hoses in the equipment during the increase of the signal. They are then added at different time (5, 10, 20, 30, 60, 80, 120 and 160) aliquots of 10 μL of healthy and fresh erythrocytes. The first sample directly into blood was collected (time 0). These samples were incubated x 24 hours at 37°C and analysed through cytometry with parallel microscopic correlation. The hematocryte concentration is in proportion to the one of a culture of laboratory parasites (5% of hematocryte).

Graph 4-27 shows the process of addition of healthy erythrocytes at different times and the analyses performed through flow cytometry and parallel microscopic correlation. The parasitemia percentages for the experiments performed at times 0, 5, 10, 20 and 30

minutes are 0.7, 0.8, 1.0, 0.9 and 0.8 percent, respectively. After 30 minutes of the liberation of merozoites, no merozoite re-infection is observed and they are not significantly different from the control of non-infected erythrocytes ($\sim 0\%$ of parasitemia). The data were reproducible in all the experiments. Microscopic observations show a correlation with the results obtained: presence of ring stages 24 hours after having been incubated.

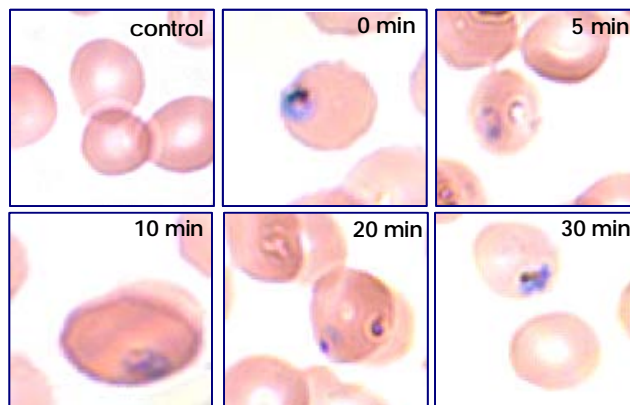
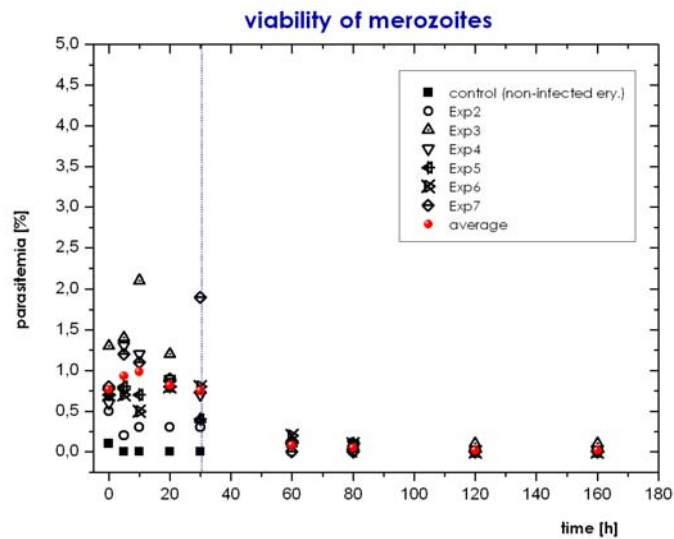
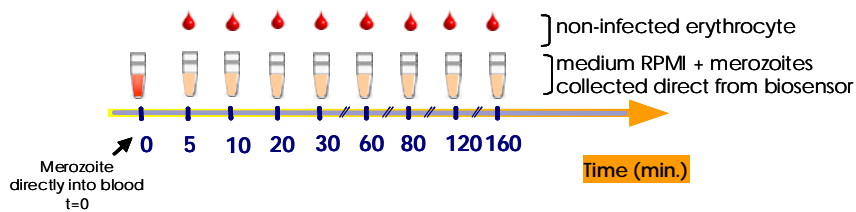


Figure 4-27. Merozoite viability. The graph shows the parasitemia percentage obtained when the healthy erythrocytes are injected on the medium+merozoite (collected from the quartz) at different times. The samples are analysed through FACS using acridine-orange as fluorochrome. Parasitemias of 0.7%, 0.8%, 1.0%, 0.9%, and 0.8% respectively are found for minutes 0, 5, 10, 20 and 30. After thirty minutes, no evidence of re-infection is shown. The microscopic correlation of the slides with Giemsa shows a relationship with the analyses through FACS: the presence of perfectly defined ring stages.

Studies suggest that there is a specific determinant (receptor) on the erythrocyte surface to which the merozoite attaches. As a corollary, the merozoite must have a ligand-like substance on its surface complementary to the receptor. The active group on the merozoite is functionally labile since merozoites will only attach to erythrocytes for approximately 10-15 min after release from an infected erythrocyte. These groups may be released from the surface or inactivated in some unknown way (*Miller 1977*).

4.6. STUDY OF THE MEROZOITE INHIBITION

A study of the merozoite inhibition was performed to test the applicability of the entire process described above.

The development of new strategies for the study of antimalarial agents is of vital importance for the treatment and control of the *P. falciparum* in endemic areas. The results with the QCM technique are not only an appropriate and important new tool to investigate parasite egress and re-invasion processes, but also might be crucial for the study of drugs or the immune system.

Tests of inhibitory activity of the merozoite release were carried out. In the first part, the study with the well-known antimalarial drug Artesunate and the natural-origin product, Chloro-tonyl is shown.

In the second part, an application using protease inhibitors (E64 and Leupeptin) is carried out to test whether merozoite inhibition is observed.

4.6.1. TESTS WITH ARTESUNATE

Artesunate is a semi-synthetic derivative of artemisinin. Artemisinin was first isolated from the herb *Artemisia annua* L., Sweet Wormwood, in 1972 (Klayman 1985). This compound, called qinghaosu (QHS, artemisinin), is a sesquiterpene lactone that bears a peroxide grouping and, unlike most other antimalarials, lacks a nitrogen-containing heterocyclic ring system. The compound has been used successfully in several thousand malaria patients in China, including those with both chloroquine-sensitive and chloroquine-resistant strains of *Plasmodium falciparum*. Derivatives of QHS, such as dihydroqinghaosu, artemether, and the water-soluble sodium artesunate, appear to be more potent than QHS itself. Sodium artesunate acts rapidly in restoring to consciousness comatose patients with cerebral malaria. Thus QHS and its derivatives offer promise as a totally new class of antimalarials.

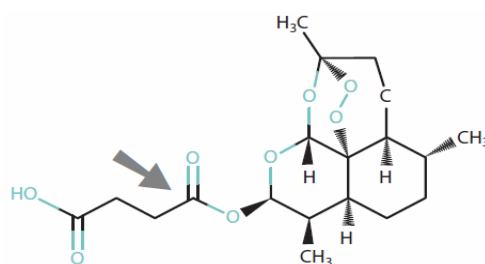


Figure 4-28. Chemical structure of Artesunate. ((3R,5aS,6R,8aS,9R,10S,12R,12aR)-Decahydro-3,6,9-trimethyl-3,12-epoxy-12H-pyrano[4,3-j]-1,2-benzodioxepin-10-ol, hemisuccinate MW: 384,4. Taken from (Center for Disease Control and Prevention 2007)

It is used for the treatment of both uncomplicated and severe malaria. It is formulated for oral, parenteral (intramuscular and intravenous) and rectal administration and used clinically worldwide. Because of rapid hydrolysis to dihydroartemisinin (also referred to as artemimol), artesunate is considered by many as a prodrug of the latter (Olliaro 2001).

Artemisinin are also termed endoperoxides for the presumptive pharmacophore: an endoperoxide bridge. The endoperoxide moiety is believed to interact with intraparasitic heme to form reactive C-centered radicals that disrupt parasite proteins (Meshnick 1994). A possible target appears to be the parasite-encoded sarco-endoplasmic reticulum Ca^{2+} -ATPase (PfATP6). The sarco-endoplasmic reticulum Ca^{2+} ATPase (SERCA) allows intracellular releasable Ca^{2+} stores by transporting cytosolic Ca^{2+} into the endoplasmic (ER) or sarcoplasmic reticulum (SR) (Eckstein-Ludwig 2003).

Artesunate is readily absorbed from the gastrointestinal tract. The oral bioavailability of artesunate is low due to the rapid and extensive conversion to Dihydroartemisin (DHA) (Batty 1998, Haynes 2001). DHA is further metabolized through glucuronidation (Nlett 2002) with a reported elimination half-life ranging from 0.4 to 12.5 hours (Bangchang 1994, Teja-Isavadbarm 1996).

Artesunate is administered concomitantly with other antimalarials to increase efficacy. Additionally, drug combinations can shorten duration of treatment, hence increasing compliance, and decrease the risk of resistant parasites arising through mutation during therapy (Kremsner 2004). However, their use in monotherapy is associated with high incidences of recrudescence infection, suggesting that combination with other antimalarials might be necessary for maximum efficacy. For example, the WHO developed

artesunate+amodiaquine for treatment of malaria in African children through a private–public partnership. Other treatments contain Artesunate+sulfadoxine-pyrimethamine or Artesunate+mefloquine.

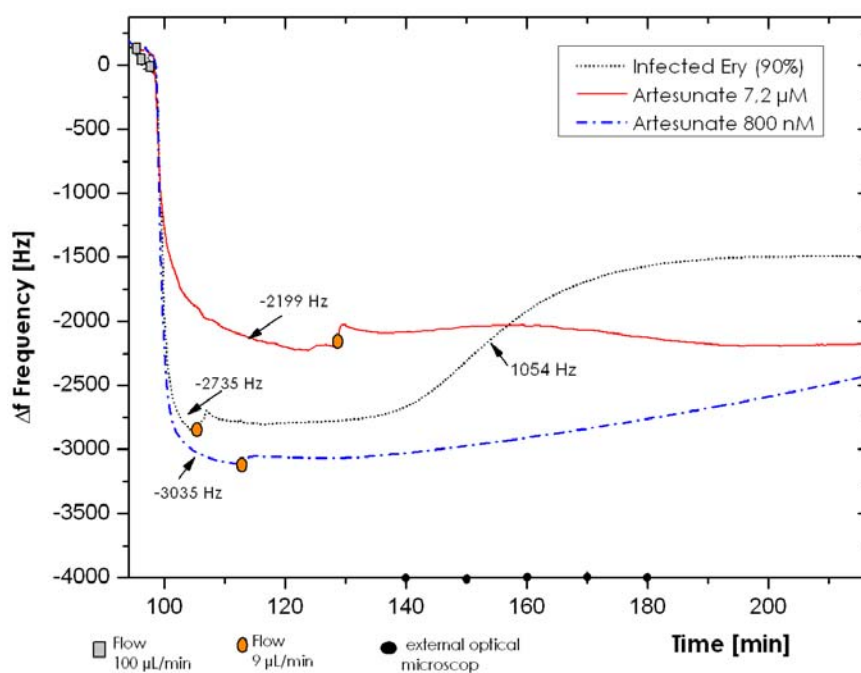
For the tests with this antimalarial inside the QCM system, different concentrations were used to evaluate the effect of inhibition of the merozoite release. It is found in reports that *in vitro* 50% inhibition (IC_{50}) of *Plasmodium falciparum* occurred in range at a concentration of 2 nM (0.8 μ g/L) to 4 nM (Carrara 2009, Rogers 2009). The sensitivity of inhibition also varies amongst different strains.

Strain 3D7 was used for this test (schizont stage) concentrated in the same manner as in the previous experiments. The concentrations used were 800 nM and 7200 nM in the RPMI 1640 medium, taking as a basis the fact that the parasitemia percentage on the quartz is 90%. A parallel control of infected erythrocytes without the solution of Artesunate was carried out (Quartz 2).

Microscopic observations were carried out on the quartz at the end of the experiment and parallel correlation through FACS, taking samples both from cell 1 as well as from cell 2 at the moment the signal increased.

Graph 4-29 shows merozoite release for the control (infected erythrocyte >90%) with an increase in the signal of 1054 Hz in 10 minutes, 20 minutes after the cells have been immobilised. For the concentration 7200 nM, no variation in the signal was shown. For the concentration of 800 nM, the curve showed a slow increase of approximately 492 Hz for ~1 hour. External control with an optical microscope showed a correlation with the increase in the signal and the merozoite release.

Inhibition of release with Artesunate



External control (optical microscopy) without Artesunate

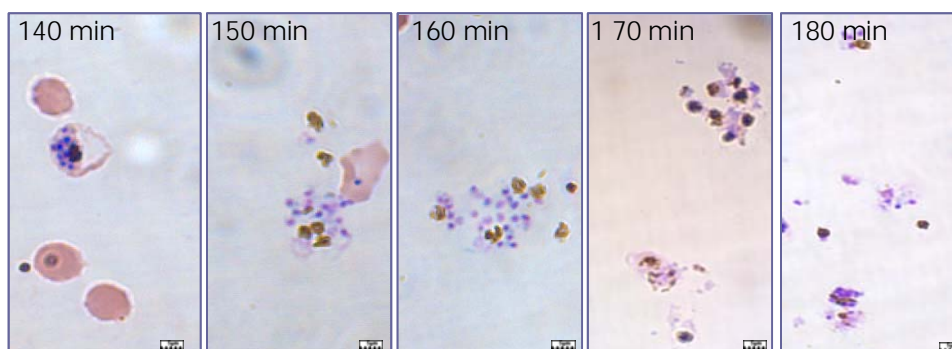


Figure 4-29. Inhibition with Artesunate of the merozoite release. The control (...) shows the normal merozoite release after 145 minutes with an increase of 1054 Hz in the signal. For the 800 nM concentration (---) a slight increase of 492 Hz occurs in a period of 1 hour. Artesunate in concentration 7.2 μM (—) shows as stable signal. External control of the infected erythrocytes over the Giemsa-stained slides during the experiment shows merozoite release after 145 minutes. Characteristics of merozoites are observed as well as the erythrocyte membrane.

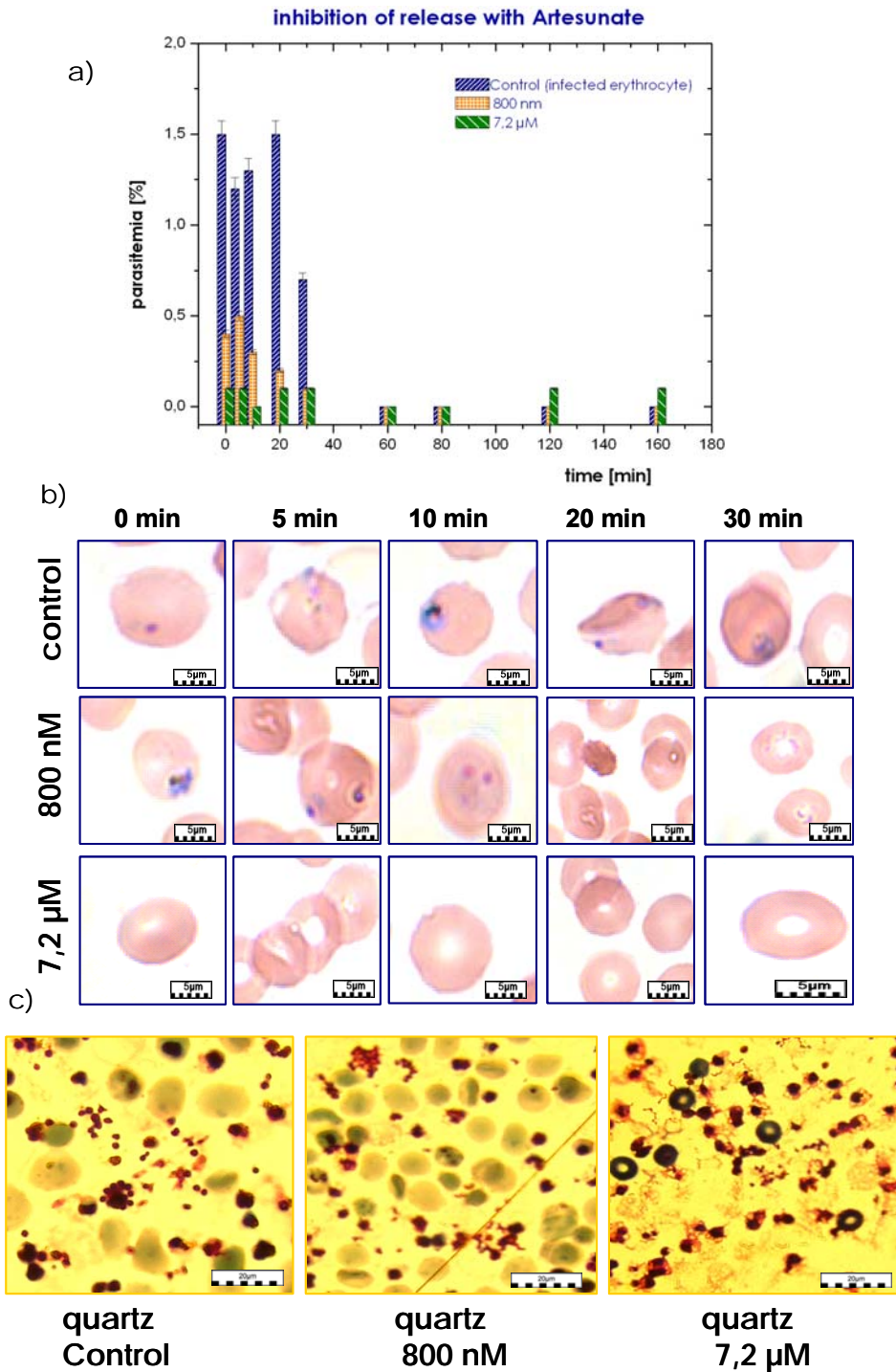


Figure 4-30. Validation of the Artesunate test. a) The graph shows the comparison of the parasitemia percentages obtained through the FACS. The samples were taken directly from QCM at the moment of the increase in the control signal and by injecting healthy erythrocytes at different times to allow re-infection. Acridine Orange was used as fluorochrome. b) The microscopic validation shows a relationship between the percentages obtained and the appearance of ring stages 24 hours later. For the control there is a re-infection time of 0-30 minutes while it is 0-10 minutes for the concentration of 800 nM. For a higher concentration of Artesunate 7,2 μM no re-infection is observed. c) The photos of the quartz for the three cases show a direct relationship with the analyses through FACS. In the higher concentration, the schizonts change their shape and characteristics (flat, oblate, small).

Graph 4-30 represents the validation performed through FACS and optical microscope over the slides of the samples used for the analysis through cytometry. Re-infection for the control and for the sample with an Artesunate concentration of 800 nM is observed. The re-infection percentage for the sample with Artesunate concentration of 800 nM is lower than the half (~0.4%) compared to the control (~1.2%) before those thirty minutes after liberation of merozoites. No re-infection is observed for the 7200 nM concentration. The slides show ring stages 24 hours after the incubation with addition of healthy erythrocytes at different times.

These results can be explained from different points of view: (I) The Artesunate has an inhibitory effect on the schizont stages for the merozoite release. This result is supported by reports found in the literature (*WHO 2006*). (II) Regarding the concentration used, this is much higher than the one used for IC₅₀ in *in vitro* studies, since the percentage of parasitemia used with the biosensor system is higher than 90%. This concentration (7.2 μM), 1000 times higher than the one used in *in vitro* studies, has a complete inhibitory effect on the release with this percentage of parasitemia used. (III) For the concentration of 800 nM, a slight increase (~492 Hz) occurs during a 1-hour-long period. Presumably the infected erythrocytes could have been affected by the Artesunate, causing a partial, not total, inhibition. Some infected cells continued their normal cycle (merozoite release) and these produced the re-infection over healthy erythrocytes, but others remained immobilised on the PLL. (IV) A re-infection is observed before the thirty minutes is observed for the control and the concentration of 800 nM, though the latter is lower in average (~0.4%) compared to the control (~1.2%). This result corroborates what has been observed in the viability of the merozoites (see number 4.5) before thirty minutes. (V) Microscopic observations of the quartz at the highest concentration of Artesunate (7200 nM) show the preservation of the schizont and the failure to release the merozoites, while for the other concentration (800 nM) a 20% percentage of merozoite release is observed. The schizonts present when used with the highest concentration of Artesunate change their shape, are smaller, oblate in shape and the erythrocyte membrane, the merozoites and the parasitic vacuole are not clearly identifiable. (VI) The control shows the normal development of the parasite and the egress of merozoites.

With this test of inhibition of the merozoite release, using these two concentrations of Artesunate is proven that the protocol designed for the erythrocytic study of the

Plasmodium falciparum, specifically in the last six hours is applicable to the study of drugs. However, it is worth noting several aspects: (I) The parasites concentrate the antimalarial by several hundred fold (Gu 1984) and it is important to know which is the exact concentration where this inhibition occurs. (II) Tests must be carried out to determine the exact moment of death of the parasite since only the inhibition of the release was determined. (III) If this derivate of artemisin shows structural similarities to thapsigargin, which is a highly specific inhibitor of sarco/endoplasmic reticulum Ca²⁺-ATPase (SERCA), it would be interesting to compare the activity of the Artesunate with this enzyme. (IV) Carry out a concentration curve vs. inhibition percentage to find out the minimal concentration of Artesunate for the inhibition of the release using this percentage of parasitemia and perform comparisons with other methods.

4.6.2. TESTS WITH CHLOROTONIL

Chlorotonil A (Figure 4-31) was isolated from myxobacterium *Sorangium cellulosum* by Höfle *et al.* at the HZI (Helmholtz Centre for Infection Research, Braunschweig, Germany) in 2004. Its structure was determined by NMR studies and X-ray analysis. The biological potential of Chlorotonil A is currently being evaluated. Its structural features, in conjunction with its potentially valuable biological activity in secondary metabolism, make it an attractive target for total synthesis (Rhan).

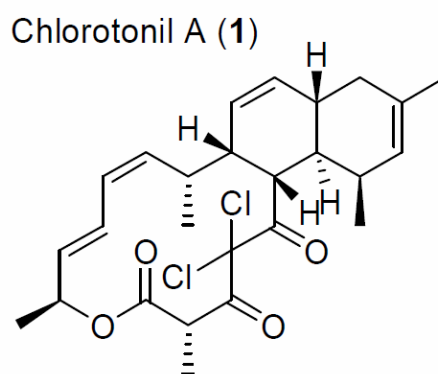


Figure 4-31. Chemical structure of Chlorotonil A. MW: 479,4 Taken from (Rahn 2007)

No published studies on the action of Chlorotonil as an antimalarial are found, but strains belonging to the genus *Sorangium cellulosum* have been found out to have structures exhibiting multiple biological activities that are useful as drugs or leads for further development. Examples include highly potent antibiotics such as the antifungal soraphens

and the antibacterial sorangicins and thuggacins as well as anticancer agents such as the epothilones (Gerbt 2008, Rabn 2007).

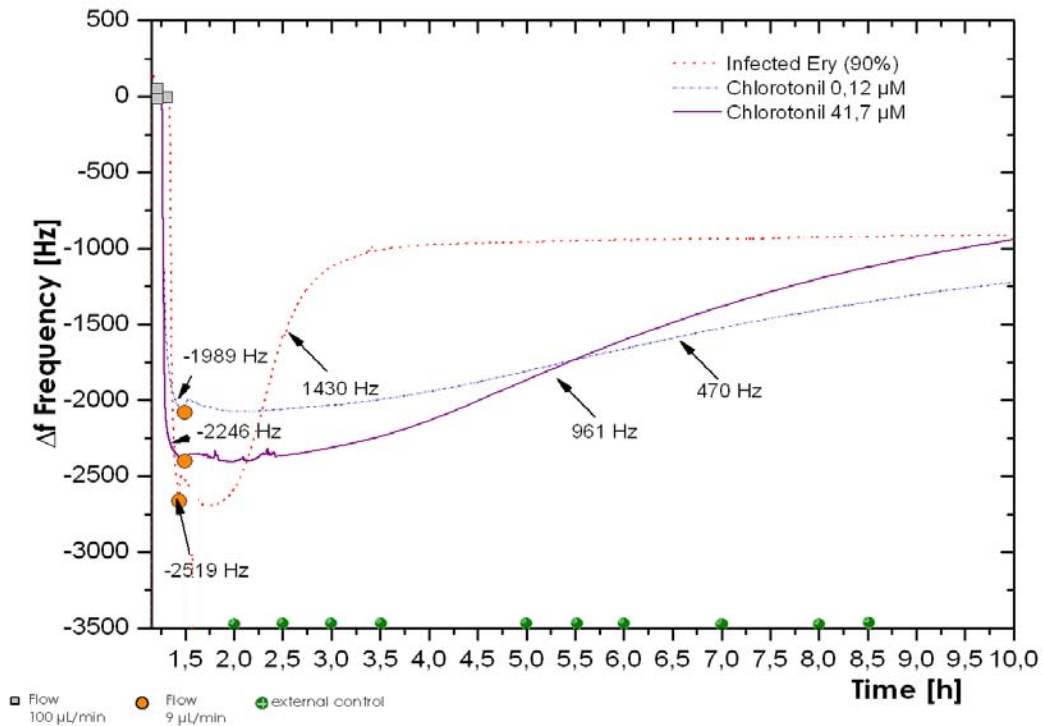
The objective of using this natural-origin substance is to evaluate the effect on the schizont stages used inside the QCM system, either acting as an inhibitor of the release or altering the normal development of the infected cells.

Two different concentrations of Chlorotonil were used, 0.12 μM and 41.7 μM . This substance was added to the medium RPMI 1640. The strain used was 3D7 in schizont stage with a parasitemia percentage of >90%.

External parallel controls were performed on the slides stained with Giemsa as well as analyses through FACS to evaluate the external re-infection on the healthy erythrocytes. In the same way, microscopic observations on the quartz were performed at the end of the experiment to determine the merozoite release or possible morphological changes of the infected cells.

Figure 4-32 shows the comparison of the two concentrations regarding the control of the infected erythrocytes without the addition of the Chlorotonil. The increase in the frequency for the control is 1430 Hz 2 hours after the beginning of the experiment, while for the infected erythrocytes exposed to concentrations of 0.12 μM and 41.7 μM no change in the signal in this period was observed. A change in the signal after five hours was observed with an increase of 961 Hz and 470 Hz for the concentrations of 41.7 μM and 0.12 μM respectively.

Inhibition of release with Chlorotonil



External control (optical microscopy)

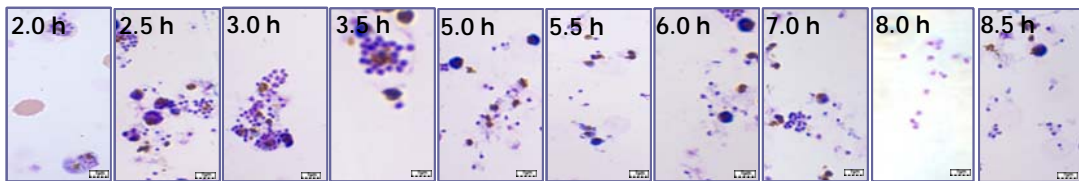


Figure 4-32 Inhibition test of Chlorotonil. The increase in the signal for the control (.....) shows an increase (1430 Hz) 2 hours after the beginning of the experiment, while for the 0.12 μM and 41.7 μM concentrations show variation in the signal of 470 Hz and 961 Hz, respectively, 3.0 hours after the beginning of the experiment with a variation in the duration of ~ 7.0 hours. The flow of RPMI + Chlorotonil (Quartz 1) and of RPMI – Chlorotonil (Quartz 2) was 9 $\mu\text{L}/\text{min}$ after the immobilisation of the cells (1.5 hours later). The external microscopic observations show a correlation with what was obtained in the graph, merozoite release after 2.0 hours, observing free merozoites (slides 2.5 hours) and haemozoin particles. For the next times (3.0-8.5 hours), more than 90% of the schizont had been lysed.

This interesting variation in the signal after five hours prompts two possible hypotheses: first, the evidence of merozoite release and second, the alteration in the change in mass, associated to a detachment of the cells on the PLL or the alteration of the infected cells.

The external control on the slides with Giemsa shows that the merozoite release occurred after two hours undergoing the change in the signal obtained for the control. In a 4-hour-long period, it is noticed that more than 90% of the infected erythrocytes have been lysed, displaying merozoite release.

The FACS analyses of the samples collected between 2 and 2.5 hours show (Figure 4-33) a percentage of ~1% of external re-infection on the healthy erythrocytes for the control, while there is no clear evidence of re-infection for the two concentrations of Chlorotoniil.

The microscopic control of the samples used for the analysis for FAC show a correlation of re-infection for the control, displaying well-defined ring stages. For the concentrations of 0.12 μM and 41.7 μM of Chlorotoniil there is a new aspect, not identified previously in the present paper: the presence of schizont but with different morphological characteristics. This characteristic was observed from time 0 (sample of the system directly on health erythrocytes) until 160 minutes (injection of healthy erythrocytes at different times).

The microscopic observation of the quartz showed the release of merozoites for the control, while there is a loss of cells in the quartz which had been exposed to the Chlorotoniil in the two concentrations. In the latter there are fragments of the erythrocyte, schizonts with different morphological shapes (small, shapeless, some outside the erythrocyte), and there is no presence of surrounding merozoites.

There are several relevant aspects here: (I) There is no evidence of re-infection with the use of Chlorotoniil. (II) The variation in the signal after five hours shows that there was involvement of the Chlorotoniil over the continuous development of the parasite. (III) No merozoite release, but detachment of the schizont+erythrocyte. (IV) Correlation between the microscopic observation of the slides both of the external control during the experiment and of the slides using the samples which had been analysed through FACS. (V) Direct relationship in the variation in the increase of the signal for the concentration

of 41.7 μM compared to the lower concentration of 0.12 μM . (VI) The parasitemia percentages for infected erythrocytes exposed to the Chlorotolil in the two concentrations do not exceed 0.3%. A low percentage of parasitemia compared to the one found in the control could more likely result in the detection of parasites in schizont stage than in a 'true' re-infection in accordance with the microscopic support.

How could these changes in the signal be associated for the two concentrations? Though there was no merozoite release and thus a re-infection of the healthy erythrocytes, the Chlorotolil causes an effect in the regular development of the parasite. In the previous experiment using the PLL, it was observed that it was stable and favours the normal development of the parasites; this new evidence shows the detachment of the cells through time. The cause of this phenomenon can be better explained through the involvement of Chlorotolil in the merozoite release and a change in the optimal conditions for the normal change of stage of the parasite. The schizonts observed in the samples used for the analysis through FACS after the incubation x 24 hours did not follow their normal development, so they did not re-infect the healthy erythrocytes.

Explaining what would be the mechanism of action on the parasite opens an important possibility for future experiments with Chlorotolil.

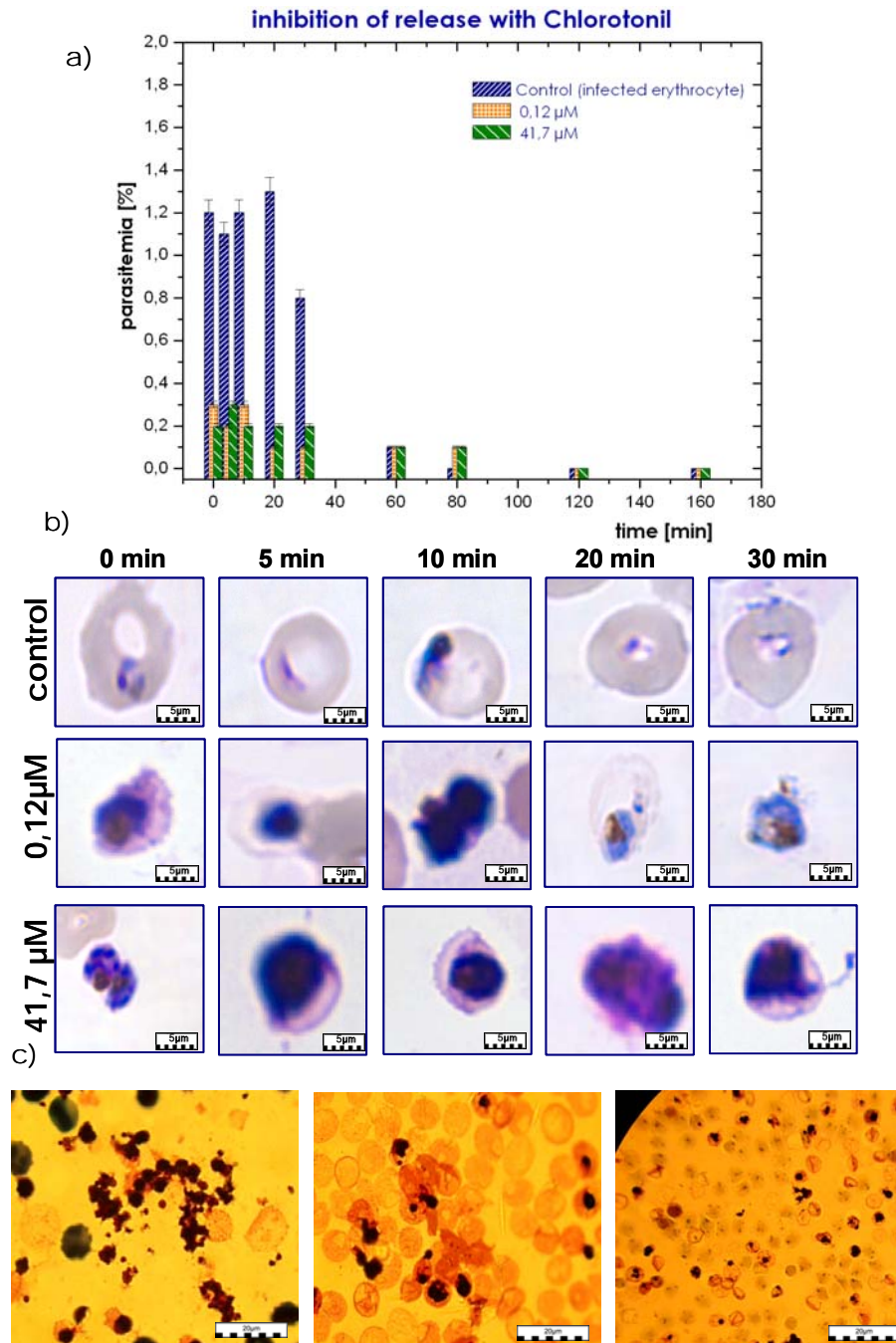


Figure 4-33. Validation of Chlorotonil test. a) The percentages of parasitemia obtained through FACS of the samples collected directly from the QCM during the increase of the signal in accordance with the control (erythrocytes not exposed to the Chlorotonil) and incubated \times 24 hours at 37°C. Acridine Orange was used as fluorochrome. b) External control of the samples used for the analysis through cytometry on slides stained with Giemsa. Re-infection is clearly observed through the appearance of ring stages on erythrocytes not exposed to chlorotonil, but there is an appearance of schizonts+erythrocytes with irregular morphological characteristics in the other two concentrations. c) Microscopic observations on the quartz after 24 hours clearly show release for the erythrocytes infected-chlorotonil (control), while the other two images of infected+chlorotonil erythrocytes show correlation with the observation of the slides and a decrease of the infected erythrocytes after 24 hours.

4.6.3. TESTS WITH PROTEASE INHIBITORS

The resistance of malaria parasites to antimalarials is a major contributor to the reemergence of the disease as a major public health problem and its spread in new locations and populations. Among potential targets for new modes of chemotherapy are malarial proteases, which appear to mediate processes within the erythrocytic malarial life cycle, including the rupture and invasion of infected erythrocytes and the degradation of hemoglobin by trophozoites. Cysteine and aspartic protease inhibitors are now under study as potential antimalarials. Lead compounds have blocked *in vitro* parasite development at nanomolar concentrations and cured malaria-infected mice (Rosenthal 1998, Sijwali 2003).

Inside the erythrocyte cycle, the *P. falciparum* have several sets of proteases, a number active in feeding on RBC hemoglobin and not relevant to merozoite release, but others present in schizonts and possible agents of merozoite release. These include two (or more) serine proteinases, plasmepsin II, and a cysteine proteinase. All of these are found in late schizonts, and except for the last, also have been localized by immunofluorescence antibody staining to the PVM. All can degrade red cell skeleton or membrane proteins, a requirement for red cell lysis. Proteases involved in merozoite release could be liberated by the schizont before the merozoites have formed, to be activated at the time of release, or could be secreted by the merozoites themselves. Such enzymes would have to cross the PVM to gain access to the RBC membrane, and as the PVM is apparently permeable to antibodies, it is likely to be leaky to enzymes. However, to identify which of these (or other) enzymes fits the case, specific inhibitors are needed to prevent lysis of the RBC membrane as well as the PVM (Bannister 2001).

Protease inhibitors may, of course, directly block proteases from lysing membranes, but they are also likely to interfere with the maturation of other molecules that would be the actual agents of lysis, as most merozoite (and many schizont) proteins are cleaved proteolytically before they can be active. Merozoites contain a number of proteases that may be involved in both escape and invasion. Electron microscopy also shows that mature merozoites inside schizonts secrete material that appears to disrupt the PVM and perhaps the RBC membrane, too, a process blocked by protease inhibitors. Significantly,

merozoite invasion into RBCs also is prevented by a number of protease inhibitors, suggesting that merozoite release and RBC invasion may be two sides of the same coin. There would be a significant advantage for the parasite if merozoites were involved in their own release, as they would by this time be mature enough to invade an RBC, thus minimizing exposure to the host defenses (*Bannister 2001*).

Haemoglobin (Hb) degradation is necessary for the growth of the parasite, apparently due to the production of free aminoacids for its own protein synthesis (*Rosenthal 1996*). Such degradation occurs mainly in trophozoites and early schizonts, in which the parasite is more active metabolically.

Two kinds of inhibitors proteases were used for the tests of inhibition in a possible merozoite release inside the QCM system: E64 (Sigma E3132) and Leupeptin (Roche 11 017 128 001).

4.6.3.1. Tests with E64

This kind of protease is an irreversible, potent and highly selective cysteine protease inhibitor, i.e. E-64 does not react with the functional thiol group of L-lactate dehydrogenase or creatine kinase, non-protease enzymes. E-64 does not inhibit serine proteases (except trypsin) like the cysteine protease inhibitors, leupeptin and antipain (*SigmaAldrich 1997*).

E-64 was reported from *Aspergillus japonicus*. In this case, *trans*- L-(SS)epoxysuccinic acid is the reactive group essential for inhibition. E-64 was first reported by Hanada *et al.* in 1978 (*Hanada 1978*) and it is the most well known of this class of natural compounds, the epoxysuccinyl peptides.

Cysteine proteases are so-named due to the function of a catalytic cysteine, which mediates protein hydrolysis via nucleophilic attack on the carbonyl carbon of a susceptible peptide bond. Cysteine proteases are sub-divided into clans (*Barrett 2001*). In the specific case of the *P. falciparum*, some main cysteine proteases have been characterised:

clan CA, includes four falcipains, three dipeptidyl peptidases, nine proteins related to the serine-rich antigen (SERA), and a calpain homolog

clan CD, which utilises a catalytic His-Cys dyad (in this order in the primary sequence) for activity.

clan CD proteases includes caspases in higher organisms, and sequence analyses suggest that members of the C13 and C14 families are present in plasmodia.

clan CE, which is characterised by catalytic residues in the order His, Glu (or Asp), Cys, is also represented in the *P. falciparum* genome.

E-64 is a very useful cysteine protease inhibitor for use in *in vivo* studies because it has a specific inhibition, it is permeable in cells and tissues, it has low toxicity, it is easily synthesized and it is stable (*Sigma-Aldrich 1997*)

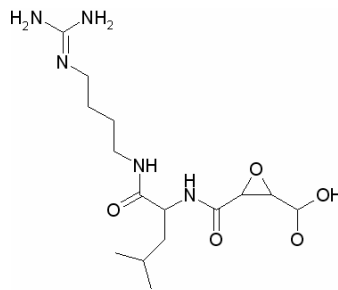


Figure 4-34 Chemical structure of the protease inhibitor E64. (2*S*,3*S*)-3-(*N*-((*S*)-1-[*N*-(4-guanidinobutyl)carbamoyl]3-methylbutyl)carbamoyl)oxirane-2-carboxylic acid (E-64) thiol protease inhibitors. MW: 357.4. Taken from (*Vickers 2009*)

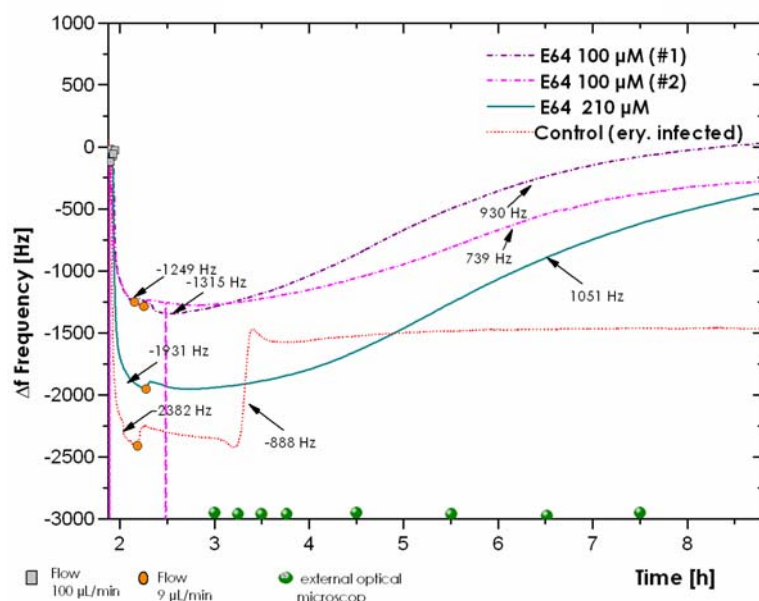
Cells infected with the strain 3D7 with a parasitemia higher than 90% were used in schizont stage, after having been microscopically controlled. The concentrations of E64 (Sigma) were 100 μ M and 210 μ M, many-fold more concentrated than with concentrations reported in the literature in a range between 10-50 μ M (*Sonni 2005*) due to a parasitemia percentage of 90% used with QCM. E64 was added to the medium RPMI 1640 which fed the cells immobilised on the quartz with a continuous flow of 9 μ L/min.

External controls were performed on the Giemsa-stained slides to the infected erythrocytes with no exposure to the enzyme during the entire experiment (before the immobilisation, during the merozoite release and during the injection of the medium+protease) through the observation of the signal obtained by the equipment.

Figure 4-35 shows the comparison of the signals obtained for the two concentrations of protease used (infected erythrocytes+E64) compared to the control (infected erythrocytes-E64). For the concentrations of 100 μ M (experiment #1 and experiment

#2), 210 μM of E64 and a drop in the frequency of -1315 Hz, -1249 Hz, -1931 Hz and -2382 Hz respectively in the control is obtained with a continuous flow of the medium of 100 $\mu\text{L}/\text{min}$. The merozoite release is clearly observed after 3.2 hours with an increase of 888 Hz in the frequency for the control while there is no variation in the signal for the infected erythrocytes with E64. A slow increase lasting approximately 4.0 hours is observed in the group of infected cells exposed to E64 with variation in the frequency of 930 Hz (E64 100 μM #1), 739 Hz (E 64 100 μM #2) and 1051 Hz (E64 210 μM) while the frequency measurement of the infected erythrocytes without E64 remains stable.

Inhibition of release with E64



External control (optical microscopy) without E64

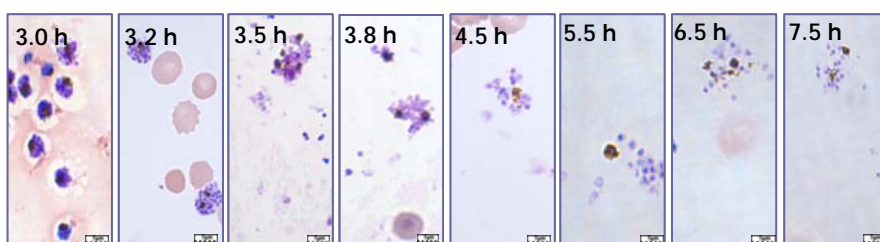


Figure 4-35 Inhibition of the merozoite release using protease inhibitors E64. Signals obtained through QCM for concentrations of 100 μM (exp #1 and exp #2), 210 μM and the control (infected erythrocyte without E64). An increase in the frequency for the control (.....) of 888 Hz is observed, while it is 930 Hz and 739 Hz for the concentrations of 100 μM exp #1 and 100 μM , respectively. The injection flow of medium+protease (quartz 1) and medium-protease (quartz 2) was 100 $\mu\text{L}/\text{min}$. External microscopic observations on the Giemsa-stained slides show merozoite release after 3.2 hours observing free merozoites and haemozoin particles. These pieces of evidence are correlated to what had been obtained in the graph. Data from three experiments.

The slow increase of the infected erythrocytes with exposure to the proteases is significantly similar between the different concentrations and reproducible for experiments where the same concentration was used (#1 and #2). In accordance to the external control, from 3.2 hours until 7.5 hours after the experiment, the infected erythrocytes were lysed as a result of the merozoite release. The explanation for this phenomenon in the increase may be given by the effect of the proteases on the schizont and the modification in the normal development of the cycle.

The samples analysed through FACS were collected at 3.25 hours while the increase in the signal is observed. The same as with the previous experiments with Artesunate and Chloroquinil, samples of the medium + proteases were taken and healthy erythrocytes incubated x 24 hours at 37°C were injected at different times to observe a possible re-infection. Graph 4-36 shows the validation of the test with protease inhibitors E64. In accordance to the protocol for analyses through FACS explained in the chapter of materials and methods, the samples were stained with Acridine Orange x 10 minutes and washed with PBS. External controls on the slides stained with Giemsa were carried out for every sample.

The results through FACS showed a parasitemia percentage of infected erythrocytes without E64 ~0.8% up to 30 minutes after of liberation of merozoites, while the erythrocytes infected with treatment with protease show parasitemia percentages of ~0.2% and 0.04% for concentrations of 100 µM and 210 µM, respectively. Thirty minutes after of liberation of merozoite (signal increase) no reinfection is obtained for any of the samples.

The controls of the samples analysed through FACS on the Giemsa-stained slides show an interesting aspect on the morphology of the schizont and the erythrocytes (representative observations at two times, 0 and 10 minutes, are presented). Re-infection is clearly observed for the control, displaying the typical rings, while there are remains of haemozoin and erythrocyte membrane for the erythrocytes with different concentrations of E64, but there is no presence of ring stages, mainly on the slides. This was consistent for the two concentrations. The appearance of these clusters of merozoites was smaller in size than the schizont observed before the experiment. Some of these parasites were

possibly stained with the fluorochrome and were being detected by the equipment, which is why parasitemia percentages are obtained for infected erythrocytes treated with E64.

The question now is: how did these parasites escape the immobilised membrane on the erythrocyte? In the normal development of release, the merozoites are released through the rupture of the erythrocyte membrane and display re-infection on the healthy erythrocytes again. With this test, observations like the ones carried out by Salmon et al. and Wickham (*Salmon 2001, Wickham 2003*), amongst others are supported; these observations state that the merozoite release is performed in two steps: the rupture of the PVM and then the rupture of the erythrocyte membrane. What is the first step of the merozoite release? This question has been controversial until now, since experiments carried out by Salmon et al. proposed an initial breakdown of RBCM, followed by the rupture of the PVM and release of invasive merozoites, whereas the latter report (*Wickham 2003*) suggested primary rupture of the PVM resulting in free-floating merozoites within RBC, followed by the secondary rupture of RBCM. Yet another group reported that an aperture is made through the PVM as well as the red cell membrane to allow merozoite exit, and concluded that the release process involves a simultaneous breakdown of the two membranes encapsulating the intracellular parasite (*Winograd E. 1999*).

Slow release of the schizont evident through a much bigger increase of the signal (~5 hours) compared to the increase in the control (~0.5 h), suggests an effect of the protease inhibitors E64 on the development of the parasite possibly to destabilize the erythrocyte membrane skeleton, thus producing a loss of cells on the quartz and affecting the signal.

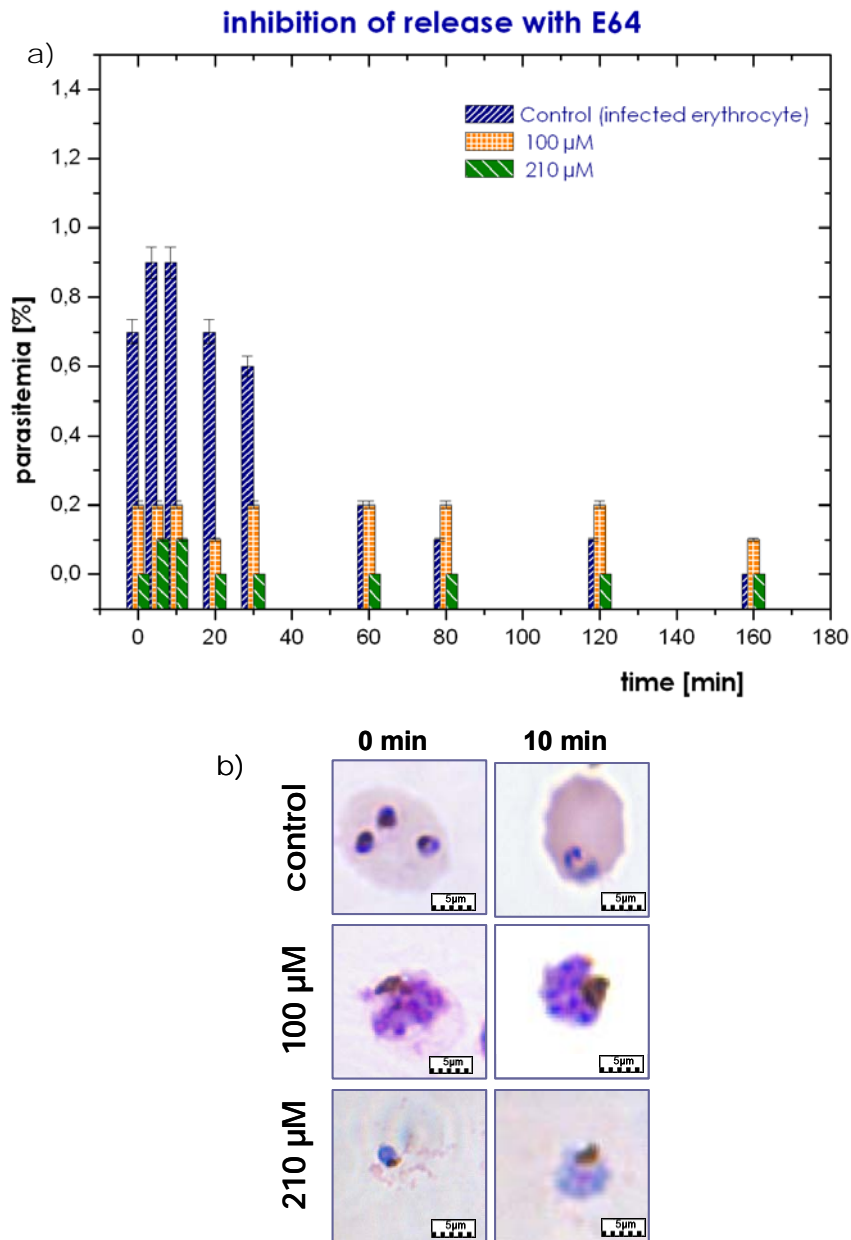


Figure 4-36 Validation of the test with protease E64. a) Results obtained through FACS of the samples collected during the increase of the signal in accordance with the control (erythrocytes infected without E64) and with the injection of healthy erythrocytes at different times. Acridine Orange was used as fluorochrome in accordance with the protocol described in the chapter of materials and methods. b) Observation over Giemsa-stained slides of the samples used for the cytometry analyses. The appearance of ring stages 24 hours later is observed, while morphological changes over the schizont and the erythrocyte membrane are observed for the different protease concentrations 100 μ M and 210 μ M. Data of two experiments.

4.6.3.2. Tests with Leupeptin

Leupeptin (antibiotic) represents a number of peptidyl aldehydes isolated from *Streptomyces* species, which is believed to inhibit the enzyme by forming a tetrahedral hemithioacetate between its aldehyde and the thiolate of the enzyme active site. However, these are not selective inhibitors. It is a reversible inhibitor of serine and cysteine proteases, e.g. plasmin, trypsin, papain, cathepsin B, thrombin, calcium-dependent protease calpain. The half maximal inhibitory concentration (IC_{50}) depends on the protease and ranges from 0.5 to 10 $\mu\text{g}/\text{ml}$ (Jayashankar 2007).

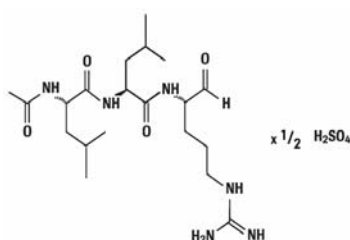


Figure 4-37 Chemical structure of the protease inhibitor Leupeptin. MW: 475,6. The strong inhibitory effect is explained by formation of a covalent hemiacetal adduct between the aldehyde group in the inhibitor and the serine hydroxyl function in the active site of the protease. Taken from (Roche 2007)

Just like with the test with E 64, the samples of the strain 3D7 were treated in the same manner for the exposure of infected erythrocytes with Leupeptin but in different concentrations: 21 μM and 210 μM as well as infected erythrocytes without exposure to the protease. In reports found on the studies of the parasite, the concentration of Leupeptin used is in a concentration range of 10 μM – 180 μM (Sonni 2005).

The infected erythrocytes exposed to Leupeptin display different signals compared to E-64. Figure 4-38 show a drop in the signal of -2300 Hz, -1585 Hz and -2720 Hz for the control (infected erythrocyte without Leupeptin), Leupeptin 210 μM and Leupeptin 21 μM , respectively. After the immobilisation of the cells on the quartz, increases in the signal at a flow of 9 $\mu\text{L}/\text{min}$ of medium + Leupeptin are observed in the different concentrations 1.5 hours after having started the experiment while the erythrocytes infected without Leupeptin remain stable until 2.2 hours, when a quick increase of 950 Hz with (~20 min.) was observed.

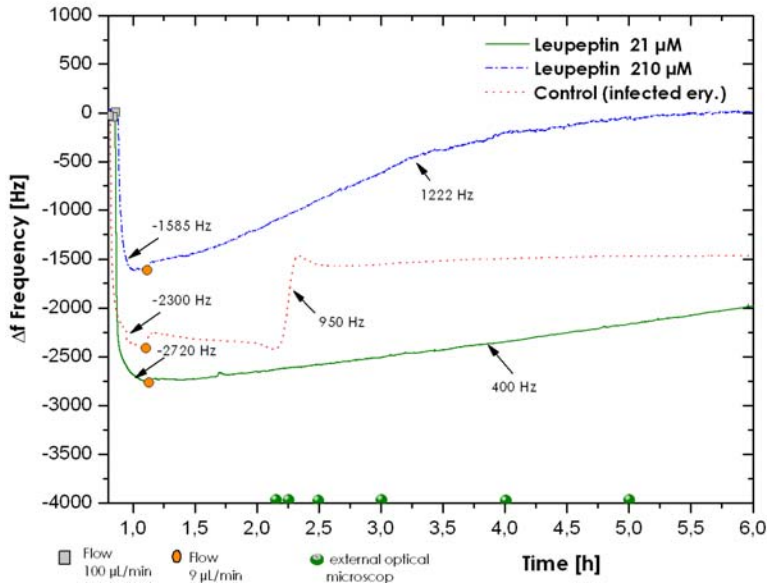
Amongst the increases in the signal, the value is significantly lower than $\sim 10\%$ (400 Hz in ~ 5 hours) compared to Leupeptin $200 \mu\text{M}$ $\sim 90\%$ (1222 Hz in ~ 5 hours). The external results of microscopy over Giemsa-stained slides of the sample used for the test with QCM with the absence of Leupeptin, presents and corroborates what had been observed in the control signal: merozoite release after 2.25 hours.

Samples are taken according to the increase in the signal given by the control to validate the test with Leupeptin, along with the injection, at different times, of healthy erythrocytes incubated x 24 hours at 37°C and analysed through FACS with the use of Acridine Orange as a Fluorochrome. Figure 4-39 shows parasitemia percentages of $\sim 1.0\%$ before thirty minutes for the control and of 0.3% and 0.1% for the concentrations of Leupeptin $21 \mu\text{M}$ and $210 \mu\text{M}$, respectively. Once again, after 30 minutes the release of merozoite, no reinfection is observed.

External observation over the Giemsa-stained slides with the samples used for the analysis through FACS show re-infection for the control contained mostly early rings in contrast to the different concentrations of Leupeptin. They display a lower percentage (0.01%) for the concentration $21 \mu\text{M}$, where clearly defined clusters of merozoites are found, than the ones obtained for $210 \mu\text{M}$ (0.05%) estimated through the count of parasites on the slide. Parasite death is observed for the concentration of $210 \mu\text{M}$ since both the erythrocyte membrane and the schizont are small, wrinkled, without the morphologically defined shape, with an estimation of 5% over the slides.

Two interesting aspects are given in this test: the influence of the protease on the schizont and the effect over the signal obtained by the biosensor.

Inhibition of release with Leupeptin



External control (optical microscopy) without Leupeptin

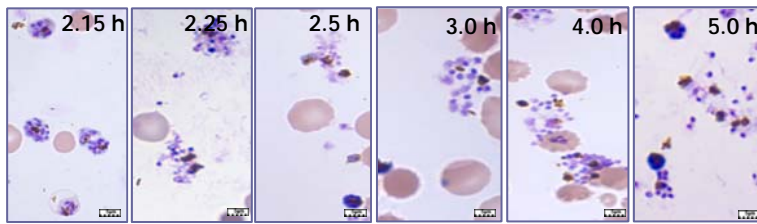


Figure 4-38 Inhibition of merozoite release using protease inhibitors Leupeptin. The results obtained through QCM show an increase of 950 Hz at 2.25 hours for the control (-----). Increase in the signal of 400 Hz ~ 5 hours and of 1222 Hz ~ 5 hours for the two concentrations of Leupeptin of 21 μM (—) and 210 μM (-.-.-.-). The continuous flow of medium + Leupeptin (quartz 1) and medium - Leupeptin (quartz 2) after the immobilisation of the cells was of 9 μL/min. The external control on the Giemsa-stained slides of the sample used for QCM shows direct correspondence with what had been obtained in the signal: merozoite release after 2.25 hours. Data from two experiments.

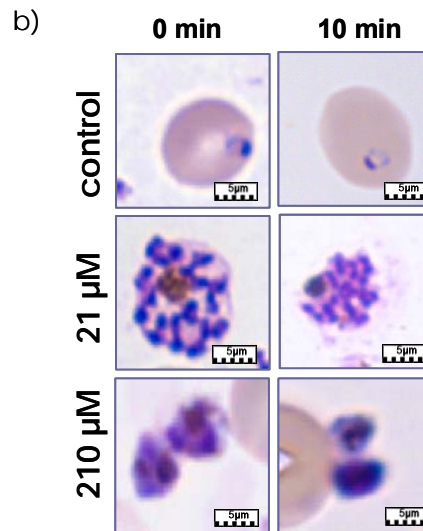
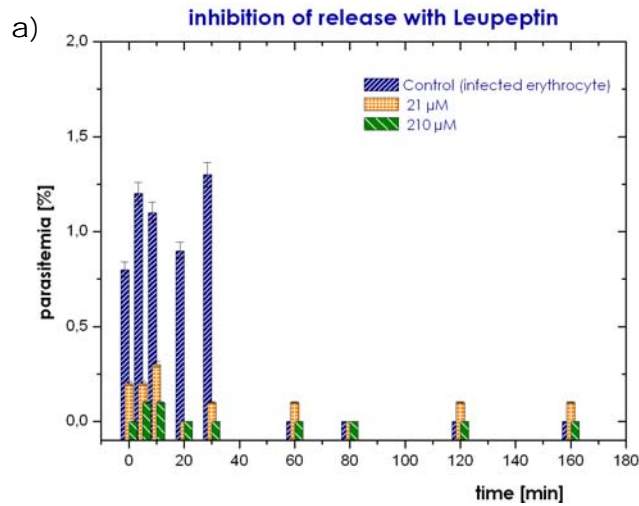


Figure 4-39. Validation test with Leupeptin. a) Parasitemia percentage obtained through cytometry with the samples collected during the increase in the signal in accordance with the control (infected erythrocytes without protease) with injection of healthy erythrocytes at different times. Acridine orange was used as fluorochrome in accordance with the protocol set in the chapter of materials and methods. b) Microscopic observations over Giemsa-stained slides of the samples analysed through cytometry. Re-infection is observed through the appearance of ring stages for the control, while morphological changes in the structure of the parasite are found for the different concentrations of Leupeptin.

The microscopic observations carried out at the end of the experiment (after 24 hours) with continuous flow of the medium with Leupeptin for quartz 1 and the medium without Leupeptin for quartz 2 are presented in figure 4-40.

Observations for protease inhibitor E64: In the photographs of the Giemsa-stained slides, merozoite build-up (100 μ M and 210 μ M) associated with the particles of haemozoin is observed for the cells treated with this protease. Correspondingly, the photograph on the quartz for the control shows the normal merozoite release, whereas there is a cluster of merozoites for the two concentrations of E64. The appearance of these clusters of merozoites in the samples collected show that there was a disruption in the erythrocyte membrane. This phenomenon is proven through the signal obtained (slow increase in the frequency) translated into the detachment of these clusters of merozoites, and, through observations on the quartz, since it is shown that only a total of 30% of the cells remained immobilised while the rest were transported through the flow of the medium+protease of the quartz (note the empty spaces on the quartz).

Observations for protease inhibitor Leupeptin: In the case of the schizont treated with this protease, the photographs on the slides show a cluster of merozoites covered by a thin membrane for the lowest concentration (21 μ M), while they show apparently dead parasites for the highest concentration (210 μ M). This could be explained through a cytotoxic and non-inhibitory effect of the highest concentration, making the parasites build up this protease. This relationship can also be seen in the significantly higher increase in the signal of 1222 Hz (90% compared to the drop) compared to the lower concentration, where the signal was stable. The appearance of clusters of merozoites adhered onto the quartz for the lowest concentration of Leupeptin is also observed on the photographs over the quartz. The detachment of more than 90% of the immobilised cells over the PLL and irregular shapes of the schizonts (small, wrinkled, poorly defined) are observed for the highest concentration.

Treatment of schizont-infected RBCs with leupeptin and E64 for 24 hours resulted in the accumulation of clusters of merozoites held together with a residual body presumably containing haemozoin particles. These microscopic observations showed that individual merozoites were in close proximity to PVM, and that the entire cluster of merozoites was devoid of the host RBC suggesting that Leupeptin and E64 inhibited PVM lysis but had no effect on host cell membrane. These data are supported in other studies reported (*Salmon 2001, Sonni 2005, Wickham 2003*).

How can this behaviour of proteases on the parasite be analysed?

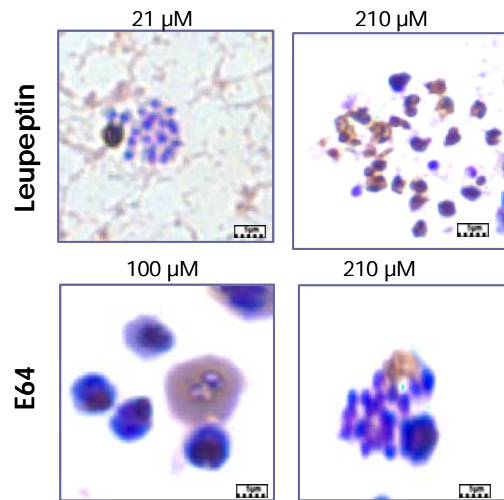
The stage-specific expression of a cysteine protease (35,000–40,000 *Mr*) and a serine protease (75,000 *Mr*) found in mature schizonts and merozoites, respectively, implicates them in the process of rupture or invasion. Studies carried out by Winograd et al., through a microscopic video about schizonts, showed that the merozoite release is done through an opening in the host erythrocyte, and the release of merozoites was not mediated by an explosive event (*Winograd E. 1999*).

It is important to observe that the effect of the proteases acts independently. The release process given in the two steps (rupture of the PVM and rupture of the erythrocyte membrane) can be selectively inhibited. This statement is supported by works reported in the literature. The photographs with Leupeptin show the vacuolar lysis while with E64, the erythrocyte membrane ruptures. This fact is the result of E64 having the inhibitory effect of cysteine proteases that does not inhibit serine proteases. It is likely that the protease(s) involved in parasitophorus vacuole lysis is a cysteine protease. Leupeptin can have inhibiting trypsin-like serine proteases.

The results with QCM reported in this paper show a direct relationship between the changes in the development of the parasite through variation in the signal using these two kinds of protease inhibitors. These data show that the breakdown of PVM occurs extraerythrocytically and a parasite-derived cysteine protease(s) is likely to be responsible for this process. There are reports showing that the *P. falciparum* contains relatively few cysteine proteases. The best-characterized cysteine proteases are the four falcipains (FP-1, -2, -2V, and -3) that are expressed during the intraerythrocytic stage of the parasite (*Sijwali 2003*).

The validation between the data obtained through the variation in the frequency, the data analysed through cytometry and microscopic controls make it possible to perform an in-depth study of the effect of proteases on the merozoite release through QCM. Though the merozoite release process and the reinvasion conform a very quick event, completed in seconds –which limits accessibility of the different experimental approaches to visualise each step clearly, using the QCM allows the obtainment of new perspectives for the study of the immune response against the parasite and the possibility of studying new targets of drugs for this moment of cycle of the *P. falciparum*

External control of infected erythrocytes with protease inhibitor
(sample used to QCM) at 24 hours



Quartz with immobilised erythrocyte at 24 hours

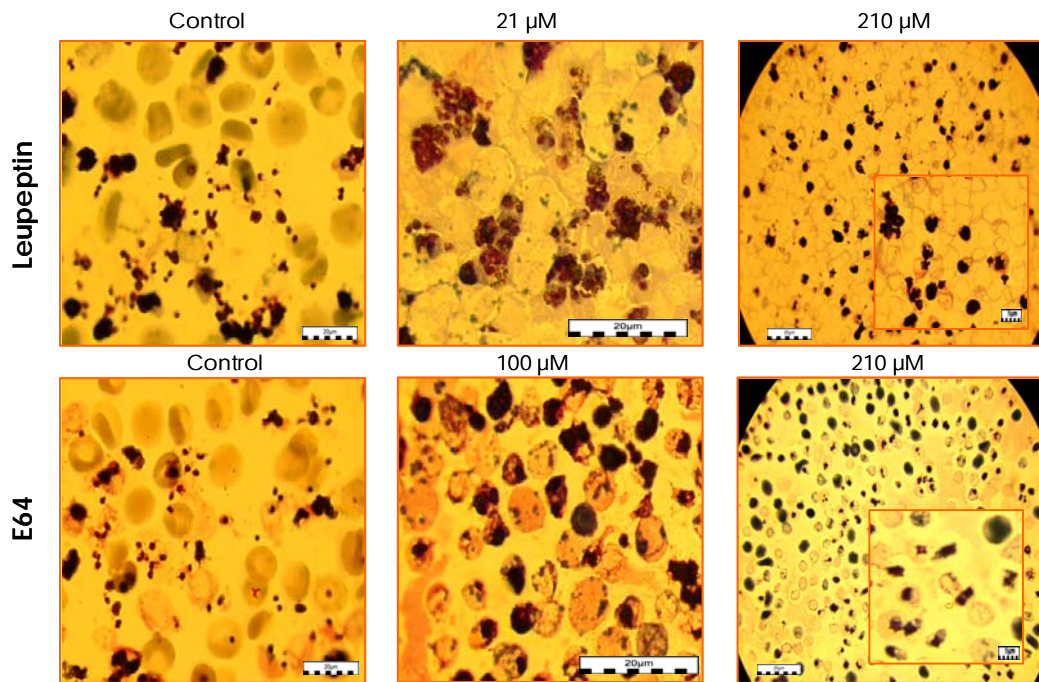


Figure 4-40 Comparison external sample used for the tests with QCM and the quartz pieces at the end of the experiment 24 hours later.

.An important issue, for example, is the evaluation of the reversible inhibitory effect of proteases. It has been reported that upon removal of E64, the parasites are capable of release from PEMS and can establish normal infections. Likewise, the purification of PVM-enclosed merozoite structures (PEMS) can be used as a biochemical tool for study of both the PVM and merozoites.

5. SUMMARY

The main results of the doctoral research paper as well as an outlook of its possible application and research options using QCM in the field of malaria are presented below.

The following objectives could be achieved in the present doctoral paper:

- (I) Development of a real-time technique for the detection of the merozoite release
- (II) Reinfection by the released merozoites on a second quartz containing erythrocytes inside the biosensor system.
- (III) Test of the effects of antimalarial compounds in the biosensor system

For the development of this technique, the biological conditions of immobilisation for both the infected and the non-infected erythrocytes had to be established first. The immobilising agent used was Poly-L-Lysine (70-150 KDa) 0.5 mg/mL in distilled water. The changes in frequency associated with the immobilisation or adsorption of the cells on the quartz surface were >1500 Hz. This polycationic agent readily interacts with the negative charges of the erythrocyte membrane, resulting in a strong bonding, stable for long periods. In this work, the observation of a QCM signal over a 48-hours period is presented for the first time. The response obtained was stable and maintaining the cells' vitality. This biological layer was characterised by the observation through optical microscopy and through TEM.

Once the biological conditions for immobilisation had been established, the conditions for the cultures of parasites were established. This was possible thanks to the cooperation of the Institute for Tropical Medicine of the University of Tübingen, performing the protocols for the parasite culture, growth, parasite synchronization and control. Since the study of the erythrocyte cycle focused mainly on the last six hours of the cycle, parasites in schizont stage were used (strain 3D7 and D10) before the merozoite release.

For the observation of the infected erythrocytes and non-infected erythrocytes, and to evaluate the merozoite release in real-time, the influence of the concentration of parasitemia was first investigated in the frequency measurement and secondly, the conditions of the infected erythrocytes in the system were established so as to allow the normal development of the cycle.

Regarding the concentration of parasitemia and taking into account that for a proper growth of a culture of parasites, they cannot exceed a percentage higher than 2%, to obtain far higher percentages of parasitemia, the MAC separation technique was used, taking advantage of the characteristic of the malaria parasites to degrade haemoglobin (an Fe(II) diamagnetic complex) into haemozoin (an Fe(III) paramagnetic complex), making the magnetic purification of parasitized red blood cells containing haemozoin possible through a column containing micro beads. At parasitemia concentrations lower than 90%, no significant change in the signal was observed. The comparative graph of the concentrations for the parasitemia shows that for 90% of parasitemia, when there is merozoite release, there is an increase in the frequency of ~50% compared to the drop caused by coupling of the RBC. These data were reproducible in all the experiments, this observation thus being the central axis of the research.

In this context, the following things needed to be established:

- (I) Conditions for the management of the purified parasites through the MACS technique so that they can be used by the biosensor system.
- (II) Effect of conditions such as nutrients, gas atmosphere, parasite synchronization, so that not only the vitality of the infected erythrocytes was unaffected but no interference with the obtained signal occurred.

In this way, the infected erythrocytes were adapted to the biosensor system with degasified medium RPMI 1640 and gas atmosphere free of carbonate content to avoid bubble production, stable temperature of the system, sterility of the materials and reactants, preparation of the PLL film, maximum 2 hours before the experiment.

To provide a stronger basis for the observations of the signal of the infected erythrocytes and, at the same time, to compare it with non-infected erythrocytes, the results were validated through external controls on Giemsa-stained slides and observed through optical microscopy, as well as TEM photographs directly on the quartz at the end of the of the experiment. The microscopic results reported a direct relationship between the increase in the signal and the merozoite release since on Giemsa-stained slides, taken during the entire moment of change of the signal, the schizonts were lysed, allowing the observation of the structures of the apicomplex (merozoite), fragments of the erythrocyte

membrane and haemozoin. More than 90% of the parasites were released at the end of the experiment. In the results by TEM, which provided a still much clearer picture due to its 3D structure, the merozoite release and the structures of the host (erythrocyte) were clearly confirmed. The quartzes were affixed with PFI 4% and Glutaraldehyde 2.5% for this microscopic technique and washed with PBS to preserve the hydration of the cells.

Regarding the second objective of the research project, a reinfection protocol by the released merozoites entering non-infected erythrocytes on a second quartz inside the biosensor system was developed and optimised through the combination of two measuring chambers. It was possible to perform the reinfection on the non-infected erythrocytes and to analyse the behaviour through the signal obtained by keeping the same biological conditions. There was no significant change of the QCM signal upon reinfection on the second quartz since the mass deposited (merozoite invasion) on the healthy erythrocytes was too small. The schizonts have approximately ~15-30 merozoites when they are released; due to the rupture of the erythrocyte membrane, they provide a significant change in mass which is translated to an increase in the signal. On the other hand, when a single merozoite manages to invade an RBC, this does not affect the size of the erythrocyte or the structure of the erythrocyte membrane. However, the microscopic observations (optical and TEM) and the validation of the experiment through FACS shows the reinfection satisfactorily. The reinfected erythrocytes were observed to continue their development cycle 24 hours after the experiment, finding ring stages and a reinfection percentage of ~1% inside the biosensor system. The reinfection process occurs rapidly (~60 seconds) and it is a complex system, which depends upon the biological, physical, chemical and molecular interactions between the parasite and the host cell. This makes the study of this process so fascinating and obtaining in vitro results through this technique opens the possibility to study more about the basic concepts of the biology of the parasite.

The analyses through cytometry using Acridine Orange 0.5 mg/mL as fluorochrome and allowing the detection of the parasites yield parasitaemia results of ~1%. The microscopic observations performed on the sample used for cytometry corroborate the results, both in the microscopic observation of the quartz as well as the results through FACS. After a 24-hour-long incubation at 37°C, the parasites were found in ring stage with their corresponding morphological characteristics.

Another aspect which has been object of several studies is the viability of the merozoites. Through this technique, it is observed that the merozoites have a very short life span and that the interaction between the parasite and the RBC must be really fast for the invasion to be effective. The merozoites show reinfection after the first thirty minutes after having been released. Data obtained through cytometry showed reproducibility in all the experiments supported by microscopic observations of Giemsa-stained slides of the samples obtained used for FACS. Bibliographic reports found support for these results obtained by the biosensor.

Experiments with Artesunate (antimalarial drug) and Chloroquine by this newly developed technique showed an inhibitory activity for Artesunate. The signal obtained along with the microscopic correlation of Giemsa-stained slides of the sample used for the experiments show an inhibition of the release for the highest concentration of (7.2 μM), while there was a partial inhibition for the lowest concentration (800 nM). Validation through cytometry shows higher reinfection when the lowest concentration is used ($\sim 0.4\%$) than when the highest concentration is used, in which this effect is not present. The control shows normal development of the parasite and reinfection $\sim 1.2\%$ through microscopic control, observing the ring stages of the parasite after 24 hours of incubation at 37°C .

Chloroquine, a substance of natural origin with unpublished reports of antimalarial activity was also tested in our system. With both concentrations tested (0.12 μM and 41.7 μM) there was an increase in the frequency signal. This was, however, due to effects on the vitality of the infected cells resulting in partial desorption of the bound cells. The microscopic observations and the results through cytometry show no ring stages after 24 hours of incubation at 37°C , but rather morphological changes of the infected erythrocytes (small, wrinkled, irregular), which suggests an effect of this substance on the normal development of the parasite, but not on the inhibition of the merozoites. It is necessary to carry out more experiments on this new substance to attempt to explain the mechanism of action on the infected erythrocytes.

Finally, the applications of this technique for the inhibition of the merozoite release using protease inhibitors (E64 and Leupeptin) show that the stages of merozoite release involve several events and that the proteases are associated with the release of the parasite. Results

through cytometry and optical microscopy show that though there was an increase in the signal, no reinfection was observed, but there was release of clusters of merozoites which were bordered by a thin membrane, presumably PVM. In contrast, a rupture of the PVM is observed with Leupeptin, but not of the erythrocyte membrane, consequently there is no variation in the signal in a concentration of 21 μ M. Both experiments were compared with infected erythrocytes with no exposure to the proteases showing a normal reinfection \sim 1% and reproduction of the experiments.

According to the results presented and the applications with this technique, two important aspects are concluded: (I) The possibility of detecting and observing in real-time and in a parallel manner the merozoite release in contrast to the non-infected erythrocytes. (II) A groundbreaking technique which allows carrying out the “in vitro” reinfection process opens the possibility to understand and clarify the processes involved in the invasion of the parasite. What has been stated above implies the optimisation of the biological conditions for the study of these two fundamental processes (release and reinfection) with the possibility to know new basic aspects of the biology of the parasite. This technique allows the isolation of the parasite for the study with drugs or target for a vaccine with proteins expressed by the merozoite; it allows the study of the activity of new drugs to evaluate the inhibitory effect of the parasite release, minimising times which are otherwise longer through other techniques.

6. BIBLIOGRAPHY

- Abdalla S, G. P. Malaria: A Hematological Perspective. 2004.
- Aikawa M, L.H. M, J.G. J, Rabbege J. Erythrocyte entry by malaria parasites. A moving junction between erythrocyte and parasite. . *Journal Cell of Biology*. 1978;77(72-82).
- Aizawa H, Kurosawa S, Tanaka M, Wakida S, Talib ZA, et al. Conventional diagnosis of treponema pallidum in serum using latex piezoelectric immunoassay. *Materials Science and Engineering C*. 2001;17:127-32.
- Amano Y, Cheng Q. Detection of influenza virus: traditional approaches and development of biosensors. *Analytical Bioanalytical Chemistry*. 2005;381(1):156-64.
- Aultman KS, Gottlieb M, Giovanni MY, Fauci AS. Anopheles gambiae Genome: Completing the Malaria Triad. *Science*. 2002;298:13.
- Bangchang KN, Karbwang J, Thomas CG, Thanavibula A, Sukontason K, et al. Pharmacokinetics of artemether after oral administration to healthy Thai males and patients with acute, uncomplicated falciparum malaria. *British journal of clinical pharmacology*. 1994;37(3):249-53.
- Bannister L. Looking for the exit: How do malaria parasites escape from red blood cells? *PNAS*. 2001;98(2):383-4.
- Bannister L, Mitchell G. The fine structure of secretion by Plasmodium knowlesi merozoites during red cell invasion. *J Protozool*. 1989;36:362-7.
- Bannister L, Mitchell G, Butcher GA, Dennis ED, Cohen S. Structure and development of the surface coat of erythrocyte merozoites of Plasmodium knowlesi. . *Cell Tissue Res*. 1986a;245:281-90.
- Bannister LH, Dluzewski AR. The ultrastructure of red cell invasion in malaria infections: a review. *Blood Cells*. 1990;16(2-3):257-92; discussion 93-7.
- Bannister LH, Hopkins J, Margos G, Dluzewski A, Mitchell G. Three-Dimensional Ultrastructure of the Ring Stage of Plasmodium falciparum: Evidence for Export Pathways. *Microsc Microanal*. 2004;10:551-62.
- Bannister LH, Hopkins JM, Fowler RE, Krishna S, Mitchell GH. A brief illustrated guide to the ultrastructure of Plasmodium falciparum asexual blood stages. *Parasitol Today*. 2000 Oct;16(10):427-33.

-
- Bannister LH, Mitchell GH. The malaria merozoite, forty years on. *Parasitology*. 2009;136:1435-44.
- Bannister LH, Mitchell GH. The role of the cytoskeleton in Plasmodium falciparum merozoite biology: an electron-microscopic view. *Ann Trop Med Parasitol*. 1995;89(2):105-11.
- Bannister LH, Mitchell GH, Butcher GA, Dennis ED. Lamellar membranes associated with rhoptries in erythrocytic merozoites of Plasmodium knowlesi: a clue to the mechanism of invasion. *Parasitology*. 1986b Apr;92 (Pt 2):291-303.
- Barrett AJ, Rawlings ND. Evolutionary lines of cysteine peptidases. . *Biol Chem*. 2001;382:727-33.
- Bass C, Foster M. The Cultivation of Malarial Plasmodia (Plasmodium Vivax and Plasmodium Falciparum) in vitro. *J Exp Med*. 1912;16(4):567-79.
- Batty KT. A pharmacokinetic and pharmacodynamic study of intravenous vs oral artesunate in uncomplicated falciparum malaria. *Clinical of Pharmacology*. 1998;45(2):123-9.
- Baum J, Richard D, Healer J, Rug M, Krnajski Z, et al. A conserved molecular motor drives cell invasion and gliding motility across malaria life cycle stages and other apicomplexan parasites. *J Biol Chem*. 2006 Feb 24;281(8):5197-208.
- Bergeret A. Tecnologías de miniaturización de biosensores. Screen printed biosensors. *Monografía vinculada a la conferencia del Ing Quim Juan Bussi sobre "Biosensores para determinaciones analíticas" del 20 de abril de 2004*. 2004:1-3.
- Bickerstaff G. Immobilisation of Enzymes and Proteins on Red Blood Cells. *Immobilisation of Enzymes and Cells*. 1997(Cap 18):143.
- Bloand P. Drug resistance in malaria. *World Health Organisation*. 2001.
- Blum LJ, Coulet PR. Biosensor principles and applications. New York: Marcel Dekker, Inc.; 1991.
- Born GV, Palinski W. Unusually high concentrations of sialic acids on the surface of vascular endothelia. *British journal of experimental pathology*. 1985;66(5):543-9.
- Bouyer G, Egée S, Thomas S. Three types of spontaneously active anionic channels in malaria-infected human red blood cells. *Blood Cells, Molecules, and Diseases*. 2006;36:248-54.
- Boxer DH, Jenkins RE, Tanner JA. The Organization of the Major Protein of the Human Erythrocyte Membrane. *Biochemical Journal*. 1974;137:531-4.

-
- Bozdech Z, Llinás M, Pulliam BL, Wong E, Zhu J, et al. The Transcriptome of the Intraerythrocytic Developmental Cycle of *Plasmodium falciparum*. *PLoS Biology*. 2003;1(1):85-100.
- Bruce-Chwatt LJ, Black RH, Clyde DF, Canfield C, Peters W. Chemotherapy of malaria. *World Health Organisation*. 1986.
- Budiansky S. Creatures of Our Own Making. *Science*. 2002;298:82-6.
- Butcher GA, Mitchell GH, Cohen S. Mechanism of host specificity in malarial infection. *Nature*. 1973;244:40-2.
- Camus D, Hadley T. A *Plasmodium falciparum* Antigen That Binds to Host Erythrocytes and Merozoites. *Science*. 1985;230:553-6.
- Carrara V, Zwang J, Ashley E, Price R, Stepniewska K, et al. Changes in the Treatment Responses to Artesunate-Mefloquine on the Northwestern Border of Thailand during 13 Years of Continuous Deployment. *PLoS One*. 2009;4(2):1-11.
- Center for Disease Control and Prevention. Artesunate now available to treat severe malaria in US. http://www.cdc.gov/malaria/features/artesunate_now_available.htm. 2007.
- Chirea M, García V, Manzanares J, Pereira C, Gulaboski R, et al. Electrochemical Characterization of Polyelectrolyte/Gold Nanoparticle Multilayers Self-Assembled on Gold Electrodes. *J Phys Chem B*. 2005;109:21808-17.
- Claußen J. Entwicklung biologischer Schichten für die Blutanalytik mit Schwingquarzsensoren. 2006.
- Clavijo C, Mora C, Winograd E. Identification of Novel Membrane Structures in *Plasmodium falciparum* Infected Erythrocytes. *Mem Inst Oswaldo Cruz*. 1998;93(1):115-20.
- Cook GMW, Heard DH, Seaman GVF. Sialic acid and the electrokinetic charge of the human erythrocyte. *Nature*. 1961;191:44-7.
- Cooper MA, Singleton VT. A survey of the 2001 to 2005 quartz crystal microbalance biosensor literature: applications of acoustic physics to the analysis of biomolecular interactions. *Journal of Molecular Recognition*. 2007;20:154-84.
- Cooper MA, Whalen C. Profiling molecular interactions using label-free acoustic screening *Drug Discovery Today: Technologies*. 2005;2(3):241-5.
- Cowman A, Baldi D, Healer J, Mills K, O'Donnell R, et al. Functional analysis of proteins involved in *Plasmodium falciparum* merozoite invasion of red blood cells. *FEBS Letters*. 2000;476:84-8.

-
- Cowman A, Crabb B. Invasion of Red Blood Cells by Malaria Parasites. *Cell*. 2006;124:755-66.
- Deans J. A., Knight A. M., Jean W. C., Waters A. P., S. C, et al. Vaccination trials in rhesus monkeys with a minor, invariant, Plasmodium knowlesi 66 kD merozoite antigen. *Parasite Immunology*. 1988;10:535-52.
- Dennis ED, Mitchell G, Butcher GA, Cohen S. In vitro isolation of Plasmodium knowlesi merozoites using polycarbonate sieves
475. *Parasitology*. 1975;71:475.
- Diederich A. BG, Winterhalter M. Influence of Polylysine on the Rupture of Negatively Charged Membranes. *Langmuir* 1998. 1998;14:4597-605.
- Dowse T.J., Koussis K., Blackman M.J., D. S-F. Roles of proteases during invasion and egress by Plasmodium and Toxoplasma. *Sub-Cellular Biochemistry*. 2008;47:121-39.
- Dvorak JA, Miller LH, Whitehouse WC, Shiroishi T. Invasion of Erythrocytes by Malaria Merozoites. *Science*. 1975;187:748-50.
- Eckstein-Ludwig U, Webb RJ, van Goethem IDA, East JM, Lee AG, et al. Artemisinins target the SERCA of Plasmodium falciparum. *Nature*. 2003;424(6951):957-61.
- Elsom J, Lethem MI, Rees GD, Hunter C. Novel quartz crystal microbalance based biosensor for detection of oral epithelial cell-microparticle interaction in real-time. *Biosensors and Bioelectronics* 23 (2008) 1259-1265. 2008 23:1259-65.
- Eylar EH, Madoff MA, Brody OV, Oncley J. The contribution of sialic acid to the surface charge of the erythrocyte. *The Journal of Biological Chemistry*. 1964;237:1992-2000.
- FDA FaDA-. BacT/Alert Bottles.
<http://www.fda.gov/downloads/BiologicsBloodVaccines/BloodBloodProducts/ApprovedProducts/SubstantiallyEquivalent510kDeviceInformation/UCM070896.pdf>. 2002.
- Field SJ, J.C. P, Clough B, A. D, Wilson M, et al. Actin in the merozoite of the malaria parasite, Plasmodium falciparum. . *Cell Motil Cytoskel*. 1993;25:43-8.
- Frey B, Corn R. Covalent Attachment and Derivatization of Poly(L-lysine) Monolayers on Gold Surfaces As Characterized by Polarization-Modulation FT-IR Spectroscopy. *Analytical Chemistry*. 1996;68:3187-93.
- Furtado LM, Thompson M. Hybridization of complementary strand and single-base mutated oligonucleotides detected with an on-line acoustic wave sensor. *The Analyst*. 1998;123(10):1937-45.

-
- García L, Bullock-lacullo S, Fritsche T, Grady K, Healy G, et al. Laboratory Diagnosis of Blood-borne Parasitic Diseases; Approved Guideline. **NCCLS**. 2000.
- Gehring F. Schwingquarzensensorik in Flüssigkeiten. Entwicklung eines Blutanalysegerätes. **Dissertation, Technische Universität Kaiserslautern**. 2005.
- Gerdon AE, Wright DW, Cliffel DE. Quartz crystal microbalance detection of glutathione-protected nanoclusters using antibody recognition. **Analytical Chemistry**. 2005;77(1):304-10.
- Gerht K, Steinmetz H, Höfle G, Jansen R. Chlorotonil A, a Macrolide with a Unique gem-Dichloro-1,3-dione Functionality from *Sorangium cellulosum*, So ce1525. **Angewandte Chemie**. 2008;47:600-2.
- Ghafouri S, Thompson M. Electrode modification and the response of the acoustic shear wave device operating in liquids. **The Analyst**. 2001;126 (12):2159-69.
- Ghislaine DC, Cofea J, Jiangb L, Hartlc D, Tracya E, et al. Glycophorin B is the erythrocyte receptor of *Plasmodium falciparum* erythrocyte-binding ligand, EBL-1. **PNAS**. 2009;106(13):5348-52.
- Gilson P, Crabb B. Morphology and kinetics of the three distinct phases of red blood cell invasion by *Plasmodium falciparum* merozoites. **International Journal for Parasitology**. 2009;39:91-6.
- Ginsburg H, Stein WD. The New Permeability Pathways Induced by the Malaria Parasite in the Membrane of the Infected Erythrocyte: Comparison of Results Using Different Experimental Techniques. **J Membrane Biol**. 2004;197:113-22.
- Glassford A. Response of a Quartz Crystal Microbalance to a liquid Deposit. **Journal of Vacuum Science and Technology**. 1978;15(6):1836-43.
- Glushakova S, Yin D, Gartner N, Zimmerberg J. Quantification of malaria parasite release from infected erythrocytes: inhibition by protein-free media. **Malaria Journal**. 2007;6(61):1-5.
- Glushakova S, Yin D, Zimmerberg J. Membrane Transformation during Malaria Parasite Release from Human Red Blood Cells. **Current Biology**. 2005;15:1645-50.
- Go M, Liu M, Wilairat P, Rosenthal P, Saliba K, et al. Antiplasmodial Chalcones Inhibit Sorbitol-Induced Hemolysis of *Plasmodium falciparum*-Infected Erythrocytes. **Antimicrobial Agents and Chemotherapy**. 2004;48(9):3241-5.
- Göpel W, P. H. Interface analysis in biosensor design. **Biosensors & Bioelectronics**. 1995;10:853-83.
- Greenwood B, Mutabingwa T. Malaria 2002. **Nature**. 2002;415:670-3.

-
- Gu HM, warhurst DC, Peters W. Uptake of [3H] dihydroartemisinin by erythrocytes infected with Plasmodium falciparum in vitro. *Transactions of the Royal Society of Tropical Medicine and Hygiene*. 1984;78:265-70.
- Guenberg J, Allred D, Shermann I. Scanning Electron Microscope-Analysis of the Protrusions (Knobs) Present on the Surface Plasmodium falciparum-infected Erythrocytes. *The Journal of Cell Biology*. 1983;97:795-802.
- Guilbault GG, Jordan JM. Analytical Uses of Piezoelectric Crystals: A Review. *CRC Crit Rev Anal Chem*. 1988;19(1):1-28.
- Guto P, Kumar C, Rusling F. Thermostable Peroxidase-Polylysine Films for Biocatalysis at 90 °C. *J Phys Chem B*. 2007;111:9125-31.
- Hadley T, Aikawa M, Miller LH. Plasmodium knowlesi: studies on invasion of rhesus erythrocytes by merozoites in the presence of protease inhibitors. *Exp Parasitol*. 1983 Jun;55(3):306-11.
- Halamek J, Makowe A, Knosche K, Skladal P, Scheller FW. Piezoelectric affinity sensors for cocaine and cholinesterase inhibitors. . *Talanta*. 2005;65(2):337-42.
- Halit M. peaking of Fixation: Part 1. *Miscap Magazine*. 2000.
- Hanada K, Tamai M, Yamagishi M, Ohmura S, Sawada J, et al. Isolation and characterization of E-64, a new thiol protease inhibitor. . *Agricultural and Biological Chemistry*. 1978;42:523-8.
- Haynes RK. Artemisinin and derivatives: the future for malaria treatment? *Current Opinion in Infectious Disease*. 2001;14(6):719-126.
- Heitmann V, Reiß B, Wegener J. The Quartz Crystal Microbalance in Cell Biology: Basics and Applications. *Springer Ser Chem Sens Biosens*. 2007;5:303-38.
- Hook F, Kasemo B, Nylander T, Fant C, Sott K, et al. Variations in coupled water, viscoelastic properties, and film thickness of a Mefp-1 protein film during adsorption and cross-linking: A quartz crystal microbalance with dissipation monitoring, ellipsometry, and surface plasmon resonance study. *Analytical Chemistry*. 2001;73:5796-804.
- Höök f, Rodahl M, Brzezinski P, Kasemo B. Energy Dissipation Kinetics for Protein and Antibody-Antigen Adsorption under Shear Oscillation on a Quartz Crystal Microbalance. *Langmuir*. 1998;14:729-34.
- Hook R, Brzezinski P, Kasemo B. Energy dissipation kinetics for protein and antibody-antigen adsorption under shear oscillation on a quartz crystal microbalance. *Langmuir*. 1998;14:729-34.

-
- Hyde J. Drug-resistant malaria - an insight. *FEBS J.* 2007;274:4688-98.
- ICH W. Immunocytochemistry Methods, Techniques and Protocols. 2007;
http://www.ihcworld.com/protocols/general_ICC/fixation.htm.
- Ikeda T. Fundamentals of Piezoelectricity. *Oxford University Press.* 1996.
- Ilett KF, Ethell BT, Maggs JL, Davis TM, Batty KT, et al. Glucuronidation of dihydroartemisinin in vivo and by human liver microsomes and expressed UDP-glucuronosyltransferases. *Drug Metabolism and Disposition.* 2002;30(9):1005-12.
- Janshoff A, Steinem C. Quartz Crystal Microbalance for Bioanalytical Applications. *Sensors Update.* 2001;9(1):313-54.
- Janshoff A, Steinem C, Sieber M, Baya A, Schmidt MA, et al. Quartz crystal microbalance investigation of the interaction of bacterial toxins with ganglioside containing solid supported membrane. *Eur Biophys J (1997) 26: 261-270.* 1997;26:261-70.
- Jayashankar L, Awasthi S, Ganguri M, Sundar S. Cathepsin B: Novel cysteine proteases of the papain family. *Latest Reviews.* 2007.
- Johnson M, Bergstrand N, Edwards K, Stalgren J. Adsorption of a PEO- PPO- PEO-triblock co-polymer on small unilamellar vesicles: Equilibrium and kinetic properties and correlation with membrane permeability. *Langmuir.* 2001;17:3902-11.
- Johnston M, Tiller P. Piezoelectric Ceramics: Science Meets Pottery. *Electronic Design.* 2008 Febrero 14.
- Kanazawa K, Gordon J. K. Keiji Kanazawa and Joseph Gordon II, "Frequency of a Quartz Microbalance in Contact with Liquid", Anal Chem. 57(1985) 1770. *Analytical Chemistry.* 1985;57:1770-1.
- Kaspar M, Stadler H, Weiß T, Ziegler C. Thickness shear mode resonators ("mass-sensitive devices") in bioanalysis. *Fresenius J Anal Chem.* 2000;366:602-10.
- Kats L, Cooke B, R. C, Black C. Protein Trafficking to Apical Organelles of Malaria Parasites – Building an Invasion Machine. *Traffic.* 2008;9:176-86.
- Kenneth M. The Quartz Crystal Microbalance and the Electrochemical QCM: Applications to Studies of Thin Polymer Films, Electron Transfer Systems, Biological Macromolecules, Biosensors, and Cells. *Piezoelectric Sensors.* 2007;5(Part C):371-424.

-
- Kenneth M. Quartz Crystal Microbalance: A Useful Tool for Studying Thin Polymer Films and Complex Biomolecular Systems at the Solution–Surface Interface. *Biomacromolecules*. 2003;4(5):1099-120.
- Keusgen M. Biosensors: new approaches in drug discovery. *Naturwissenschaften*. 2002 Oct;89(10):433-44.
- Kistler. Piezoelectric effect. [http://www.kistler.com/it it-
it/Technology/Piezoelectric/The-Piezoelectric-Effect.html](http://www.kistler.com/it_it-
it/Technology/Piezoelectric/The-Piezoelectric-Effect.html). 2008.
- Klayman DL. Qinghaosu (artemisinin): an antimalarial drug from China. *Science*. 1985;228:1049-55.
- Kremsner P, Krishna S. Antimalarial combinations. *Lancet* 2004. 2004;364:285-94.
- Kumar A. Biosensors Based on Piezoelectric Crystal Detectors: Theory and Application. *JOM~e - The Minerals, Metals & Materials Society*. [Journal]. 2000 October 2000;52.
- Kumaratilake L, Ferrante A. Opsonization and Phagocytosis of Plasmodium falciparum Merozoites Measured by Flow Cytometry. *Clinical and Diagnostic Laboratory Immunology*. 2000:9-13.
- Kutnera D, Barucha H, Ginsburg H, Cabantchik ZI. Alterations in membrane permeability of malaria-infected human erythrocytes are related to the growth stage of the parasite, open. *Biochimica et Biophysica Acta (BBA) - Biomembranes*. 1982;687(1):113-7.
- Kyes S, Horrocks P, Newbold C. Antigenic Variation at the Infected Red Cell Surface in Malaria. *Annu Rev Microbiol*. 2001;55:673-707.
- Lambros C, Vanderberg P. Synchronization of Plasmodium falciparum Erythrocytic Stages in Culture. *The Journal of Parasitology*. 1979;65(3):418-20.
- Lekana JB, Sterkers Y, Lépolard C, Traoré B, Costa F, et al. Adhesion of normal and Plasmodium falciparum ring-infected erythrocytes to endothelial cells and the placenta involves the rhoptry-derived ring surface protein-2. *Red Cells*. 2002;101(12):5025-32.
- Lew V. Malaria: Endless Fascination with Merozoite Release. *Current Biology Vol 15 No 18*. 2005;15(18):R760-R1.
- Ljungström I. PH, Schlichtherle M, Scherf A, Wahlgren M. Methods in Malaria Research. 2004.
- Llinas M. Basic Culture Maintenance. <http://www.molbio1.princeton.edu/labs/llinas/protocols.html>. 2008.

-
- Long Y, Liu Y, Lei L, Nie LH, Yao SZ. Constructions and application of phenytoin anion-selective electrode based on bulk acoustic wave (BAW) sensing technique. *The Analyst*. 2001;126:1090-4.
- Lord MS, Modin C, Foss M, Duch M, Simmons A, et al. Monitoring cell adhesion on tantalum and oxidised polystyrene using a quartz crystal microbalance with dissipation. *Biomaterials*. 2006;26:4529-37.
- Lyon J., J. H. Plasmodium Falciparum Antigens synthesized by Schizont and stabilized at the Merozoite surface when Schizont mature in the presence of Protease Inhibitors. *The Journal of Immunology*. 1986;136(6):2245-51.
- Marshall V, Silva A, Foley M, S. C, Wang L, et al. A Second Merozoite Surface Protein (MSP-4) of Plasmodium falciparum That Contains an Epidermal Growth Factor-Like Domain. *Infection and Immunity*. 1997:4460-7.
- Martin S, Granstaff VE, Frye GC. Characterization of a Quartz Crystal Microbalance with Simultaneous Mass and Liquid Loading. *Analytical Chemistry*. 1991;63:2272-81.
- Matteelli A. , F. C. Life Cycle of Malaria.
<http://www.waifoit/english/resources/online/books/other/malaria/2-Lifecycle%20of%20malarial%20parasitepdf>
- Matuschewski K, Mueller AK. Vaccines against malaria - an update. *FEBS J*. 2007 Sep;274(18):4680-7.
- Mazia D. SG, and W Sale. Adhesion of cells to surface coated with Polylysine. *Journal of Cell Biology*. 1975:198-200.
- MedPedia. Clinical:Malaria. <http://wikimedpediacom/Clinical:Malaria>. 2007.
- Meshnick SR. The mode of action of antimalarial endoperoxides. *Society Tropical Medicine and Hygiene*. 1994;88(Suppl 1):31-2.
- Michalzik M, Wendler J, Rabe J, Buttgenbach S, Bilitewski UB. Development and application of a miniaturised quartz crystal microbalance (QCM) as immunosensor for bone morphogenetic protein-2. . *Sensors and Actuators B: Chemical*. 2005;105(2):508-15.
- Miečinskas P, Leinartas K, Uksienė V, Juzeliūnas E. QCM study of microbiological activity during long-term exposure to atmosphere—aluminium colonisation by Aspergillus Niger. *Journal of Solid State Electrochemistry*. 2007;11:909-13.
- Miller LH. Hypothesis on the mechanism of erythrocyte invasion by malaria merozoites. *Bulletin of the World Health Organization*. 1977;55(2-3):157-62.

-
- Miller LH, Aikawa M, Johnson JG, Shiroishi T. Interaction between cytochalasin B-treated malarial parasites and erythrocytes. Attachment and junction formation. . *Journal of Experimental Medicine*. 1979;149:172-84.
- Miller LH, Baruch D, Marsh K, Doumbo O. The pathogenic basis of malaria. *Nature*. 2002;415:673-9.
- Miller LH, Mason SJ, Dvorak JA, McGinniss MH, Rothman IK. Erythrocyte receptors for (Plasmodium knowlesi) malaria: Duffy blood group determinants. *Science*. 1975;189:561-3.
- Miltenyibiotec.
http://www.miltenyibiotec.com/en/NN_29_MACS_Cell_Separation_Columns.aspx. 2009.
- Mitchell G, L. B. Malaria parasite invasion: interactions with the red cell membrane. *Critical Reviewy in Oncologie/Hematology*. 1988;8(4):225-310.
- Mitchell GH, Butcher GA, Richards WHS, Cohen S. Merozoite Vaccination of Douroucouli Monkeys against Falciparum Malaria. *The Lancet*. 1977;309(8026):1335-8.
- Murphy SC, Fernandez-Pol S, Chung PH, Prasanna Murthy SN, Milne SB, et al. Cytoplasmic remodeling of erythrocyte raft lipids during infection by the human malaria parasite Plasmodium falciparum. *Blood*. 2007 Sep 15;110(6):2132-9.
- Nagao E, Osamu K, A. DJ. Plasmodium falciparum-Infected Erythrocytes: Qualitative and Quantitative Analyses of Parasite-Induced Knobs by Atomic Force Microscopy. *Journal of Structural Biology*. 2000;130:34-44.
- Nomura T, Okuhara M. Frequency-shifts of piezoelectric quartz crystals immersed in organic liquids. *Analytica Chimica Acta*. 1982;142:281-4.
- Olliaro P, Nair N, Sathasivam K, Mansor S, Navaratnam V. Pharmacokinetics of artesunate after single oral administration to rats. *BMC Pharmacology*. 2001;1:1-4.
- Pasvol G. How many pathways for invasion of the red blood cell by the malaria parasite? *TRENDS in Parasitology*. 2003;19(10):430-2.
- Pavey K. Quartz crystal analytical sensors: the future of label-free, real-time diagnostics? *Expert Review of Molecular Diagnostic*. 2002;2(2):173-86.
- Pinder J.C., Fowler RE, Dluzewski A., Bannister L.H., Lavin F.M., et al. Actomyosin motor in the merozoite of the malaria parasite, Plasmodium falciparum: implications for red cell invasion. *Journal of Cell Science*. 1998;111:1831-9.

-
- Pohanka M, Skladal P. Piezoelectric immunosensor for Francisella tularensis detection using immunoglobulin M in a limiting dilution. . *Analytical Letters*. 2005;38(3):411-22.
- Preiser P, Kaviratne M, Khan S, Bannister LH, Jarra W. The apical organelles of malaria merozoites: host cell selection, invasion, host immunity and immune evasion. *Microbes and Infection*. 2000;2:1461-77.
- Prior R, Kreier J. Plasmodium berghei freed from host erythrocytes by a continuous-flow ultrasonic systemstar, open *Experimental Parasitology*. 1972;32(2):239-43.
- Qiagen. Erythrocyte Invasion by Plasmodium falciparum.
<https://www1qiagencom/GeneGlobe/pathwayView.aspx?pathwayID=164>. 2003a.
- Qiagen. Structure of Plasmodium Falciparum.
<https://www1qiagencom/GeneGlobe/PathwayView.aspx?pathwayID=423>. 2003b.
- Rahn N. Die Totalsynthese von Chlorotonil A. *Gottfried Wilhelm Leibniz Universität Hannover*. 2007.
- Ramya TN, Surolia N, Surolia A. Survival strategies of the malarial parasite *Plasmodium falciparum*. *Science*. 2002;83(7):818-25.
- Rayner JC. Erythrocyte exit: Out, damned merozoite! Out I say! *TRENDS in Parasitology*. 2006;22(5):189-92.
- Reipa V, Almeida J, Cole KD. Long-term monitoring of biofilm growth and disinfection using a quartz crystal microbalance and reflectance measurements. *Journal of Microbiological Methods*. 2006;66:449-59.
- Rengifo A., T. F. Disminución del número de neuronas que expresan GABA en la corteza cerebral de ratones infectados con rabia. *Biomédica*. 2007;27(4).
- Rhan N, Kalesse M, Leibniz Universität Hannover IfOC, Schneiderberg 1B, D-30167 Hannover. The Total Synthesis of Chlorotonil A via Intramolecular Diels-Alder Reaction. <http://wwwchemical-genomicsde/docs/Rahnpdf>
- Ribaut C, Berry A, Chevalley S, Reybier K, Morlais I, et al. Concentration and purification by magnetic separation of the erythrocytic stages of all human Plasmodium species. *Malaria Journal*. 2008;7:1-5.
- Ribaut C, RK, Torbiero B, Launay J, Valentin A, Reynes O, Fabre P-L, Nepveu F. Strategy of red blood cells immobilisation onto a gold electrode: Characterization by electrochemical impedance spectroscopy and quartz crystal microbalance. *ITBM-RBM*. 2008;29:141-8.

Roche. Leupeptine. 2007.

Rogers ME, Williams DT, Niththyananthan R, Rampling MW, Heslop KE, et al. Decrease in erythrocyte glycoprotein sialic acid content is associated with increased erythrocyte aggregation in human diabetes. *Clinical Sciences*. 1992;82(3):309-13.

Rogers W, Sem R, Tero T, Chim P, Lim P, et al. Failure of artesunate-mefloquine combination therapy for uncomplicated Plasmodium falciparum malaria in southern Cambodia. *Malaria Journal*. 2009;8(10):1-9.

Rosenthal P. Cysteine proteases of malaria parasites. . *International Journal of Parasitology*. 2004;34:1484-9.

Rosenthal P. Proteases of Malaria Parasites: New Targets for Chemotherapy. *Emerging Infectious Diseases*. 1998; 4(1):49-57.

Rosenthal P, Meshnick SR. Hemoglobin catabolism and iron utilization by malaria parasites *Molecular and Biochemical Parasitology*. 1996;83(2):131-9.

Sachs J, Malaney P. The Economic and Social burden of Malaria. *Nature*. 2002;415:680-5.

Salmon B, Oksman A, Goldberg D. Malaria parasite exit from the host erythrocyte: A two-step process requiring extraerythrocytic proteolysis. *PNAS*. 2001;98(1):271-6.

Sam-Yellowe TY, Shio H, Perkins ME. Secretion of Plasmodium falciparum rhoptry protein into the plasma membrane of host erythrocytes. *Journal Cell of Biology*. 1988;106:1507-13.

Sauerbrey G. Verwendung von Schwingquarzen zur Wägung dünner Schichten und zur Mikrowägung. *Zeitschrift für Physik*. 1959;154(2):206-22.

Scheufele B. Sensorik und Aktorik mit piezoelektrischen Schwingquarzen. Nachweis von blutgruppenspezifischen Antikörpern in humanem Vollblut. 2009.

Seaman GVF, Uhlenbruck G. The surface structure of erythrocytes from some animal sources. . *Archives of biochemistry and biophysics*. 1963;100:493-502.

Segrest JP, Kahane I, Jackson RL, Marchesi VT. Major glycoprotein of the human erythrocyte membrane: evidence for an amphipathic molecular structure. *Archives of biochemistry and biophysics*. 1973;155:167-83.

Shen Z, Stryker GA, Mernaugh RL, Yu L, Yan HP, et al. Single-chain fragment variable antibody piezoimmunosensors. *Analytical Chemistry*. 2005;77(3):797-805.

Sherman IW, Eda S, Winograd E. Erythrocyte aging and malaria. *Cellular and Molecular Biology*. 2004;50(2):159-69.

Siddiqui WA, Taylor D, Kan SC, Kramer K, Richmond-Crum SM, et al. Siddiqui, W. A. et al. Bull. Wld Hlth Org. 57, Suppl. 1, 199–203 (1979). *Bulletin of the World Health Organisation*. 1979;57(Supplement 1):199-203.

SigmaAldrich. E64 - Product Information.

http://www.sigmaaldrich.com/etc/medialib/docs/Sigma/Product_Information_Sheet/e3132pisPar0001Filetmp/e3132pispdf. 1997.

Sijwali P, Rosenthal P. Gene disruption confirms a critical role for the cysteine protease falcipain-2 in hemoglobin hydrolysis by Plasmodium falciparum. *PNAS*. 2003;1010(13):4384–9

Sonni S, Dhawan S, Rosen K, Chafel M, Chishti A, et al. Characterization of events preceding the release of malaria parasite from the host red blood cell. *Blood Cells, Molecules, and Diseases*. 2005;35:201-11.

Stanford Research System. QCM100- Quartz Crystal Microbalance Theory and Calibration. *www.thinkSRSc.com*. 2006;408.

Sterling C. In vitro Isolation of Plasmodium chabaudi Merozoites by Continuous Flow Ultrasound, Cell Sieving, Concanavalin A-Affinity Chromatography and Poly-L-Lysine Coated Bead Support Columns. *The Journal of Parasitology*. 1984;70(6):945-54.

Su XL, Li YB. A QCM immunosensor for Salmonella detection with simultaneous measurements of resonant frequency and motional resistance. *Biosensors & Bioelectronics*. 2005;21(6):840-8.

Sun-Young A, Mi-Young S, Young-A K, Ji-Ae Y, Dong-Hwan K, et al. Magnetic separation: a highly effective method for synchronization of cultured erythrocytic Plasmodium falciparum. *Parasitol Res*. 2008;102:1195-200.

Tan YG, J. L, Peng H, Nie LH, Yao SZ. A study of a new TSM bio-mimetic sensor using a molecularly imprinted polymer coating and its application for the determination of nicotine in human serum and urine. *Bioelectrochemistry*. 2001a;53:141-8.

Tan YG, Nie LH, Yao SZ. A piezoelectric biomimetic sensor for aminopyrine with a molecularly imprinted polymer coating. *Analyst The Analyst*. 2001b;126(5):664-8.

Teja-Isavadharm P, Noste F, Kyle DE, Luxemburger C, Kuile F, et al. Teja-Isavadharm, P., et al., Comparative bioavailability of oral, rectal, and intramuscular artemether in healthy subjects: use of simultaneous measurement by high performance liquid chromatography and bioassay. *British journal of clinical pharmacology*. 1996;42(5):599-604.

Thera MA, Doumbo OK, Coulibaly D, Diallo DA, Kone AK, et al. Safety and immunogenicity of an AMA-1 malaria vaccine in Malian adults: results of a phase 1 randomized controlled trial. *PLoS One*. 2008;3(1):e1465.

-
- Torii M, Aikawa M. Ultrastructure of Asexual Stages. *American Society of Microbiology*. 1998:123-34.
- Touré YT, Oduola A. Disease Watch - Focus - Malaria. *Nature*. 2004;2:276-7.
- Trager W. On the release of merozoites. *TRENDS in Parasitology*. 2002;18(2):60-1.
- Trager W, Jensen JB. Human malaria parasites in continuous culture. 1976. *J Parasitol*. 2005 Jun;91(3):484-6.
- Trigg P. Recent advances in malaria parasite cultivation and their application to studies on host-parasite relationships: a review. *Bulletin of the World Health Organization*. 1985;63(2):387-98.
- Uhlemann A, Staalsoe T, Klinkerta M, Hviidb L. Analysis of Plasmodium falciparum-infected red blood cells. *MACS&more*. 2000;4(2):7-8.
- Vickers T. E64. <http://commons.wikimedia.org/wiki/File:E-64.png>. 2009.
- Wahlgren M, Perlmann P. Malaria Molecular and Clinical Aspects. 1999.
- Ward G., Miller LH, Dvorak JA. The origin of parasitophorous vacuole membrane lipids in malaria-infected *Journal of Cell Science*. 1993;106:237-48.
- Wasserman M, Forero C. Isolation and Identification of Actin-binding Proteins in Plasmodium falciparum by Affinity Chromatography. *Mem Inst Oswaldo Cruz*. 2000;95(3):329-37.
- Wernsdorfer W, Hay S, Shanks D. Learning from History. *The Global Health Group*. 2009:95-107.
- WHO. Guidelines for the treatment of malaria/World Health Organization. 2006.
- WHO. Malaria risk areas 2008.
<http://gamapserverwho.int/mapLibrary/app/searchResults.aspx>. 2009.
- Wickham M, Culveno J, Cowman A. Selective Inhibition of a Two-step Egress of Malaria Parasites from the Host Erythrocyte. *The Journal of Biological Chemistry*. 2003;278(39):37658-63.
- Winograd E., Clavijo C., Bustamante L., M. J. Release of merozoites from Plasmodium falciparum-infected erythrocytes could be mediated by a non-explosive event. *Parasitol Res*. 1999;85:621-4.
- Winzeler EA. Malaria research in the post-genomic era. *Nature*. 2007;455:751-6.

Wiser M. Malaria. <http://www.tulane.edu/~wiser/protozoology/notes/malaria.html>. 2008.

Wiser M. Plasmodium Species Infecting Humans. http://www.tulane.edu/~wiser/protozoology/notes/pl_sp.html. 2009.

Wongsrichanalai C, Pickard A, Wernsdorfer W, Meshnick SR. Epidemiology of drug-resistant malaria. *The Lancet Infectious Diseases*. 2002;2:209-18.

Wu ZY, Shen GL, Wang SP, Yu RQ. Quartz-crystal microbalance immunosensor for Schistosoma-japonicum- infected rabbit serum. . *Analytical Science*. 2003;19(3):437-40.

APPENDIX 1. Relationship Between Added Mass and Frequency Shift

Equation Sauerbrey

$$\Delta f = \frac{-2\Delta m f_0^2}{A\sqrt{\rho_q \mu_q}} = -\frac{2f_0^2}{A\sqrt{\rho_q \mu_q}} \Delta m, \quad \text{Equation (1)}$$

Where:

f_0 – [Resonant frequency](#) (Hz), Δf – Frequency change (Hz), Δm – Mass change (g), A – [Piezoelectrically](#) active crystal area (Area between electrodes, cm²), ρ_q – [Density](#) of quartz ($\rho_q = 2.648 \text{ g/cm}^3$), μ_q – [Shear modulus](#) of quartz for AT-cut crystal ($\mu_q = 2.947 \times 10^{11} \text{ g/cm.s}^2$), v_q – Transverse wave velocity in quartz (m/s)

Summarising, the equation is:

$$\Delta f = -Cf \cdot \Delta m, \quad \text{Equation (2)}$$

Where, Cf - the sensitivity factor for the crystal used (i.e. 56.6 Hz $\mu\text{g}^{-1} \text{ cm}^2$ for a 5MHz AT-cut quartz crystal at room temperature.)

Equation Kanazawa

$$\Delta f = -f_u^{3/2} \cdot [(Q_L \eta_L) / (\Pi \cdot Q_q \mu_q)]^{1/2} \quad \text{Equation (3)}$$

where,

f_u - frequency of oscillation of unloaded crystal, Q_q - density of quartz – 2.648 g . cm-3, μ_q - shear modulus of quartz- 2.947.1011 g.cm-1.s-2, Q_L - density of the liquid in contact with the electrode, and η_L - viscosity of the liquid in contact with the electrode

Modelo Butterworth-Van Dyke

$$\Delta R = [n \cdot \omega_s \cdot Lu / \Pi] \cdot [(2 \cdot \omega_s \cdot Q_L \eta_L) / (Q_q \mu_q)]^{1/2} \quad \text{Equation (4)}$$

Where,

ΔR - change in series resonance resistance, in Ω , n - number of sides in contact with liquid, ω_s - angular frequency at series resonance(= 2. Π . f_s , where f_s is the oscillation frequency in solution in Hz), and Lu - Inductance for the unperturbed (i.e. dry) resonator, usually in mH.

APPENDIX 2. Properties of Some Important Merozoite Proteins in *P. falciparum*

Name	Accession Number	KO	Features/Structure
GPI-Anchored (Known or Putative) Surface Proteins			
MSP-1	PFI1475w	N	Putative band 3 ligand; processing and removal of bulky complex essential for invasion; C-terminal double EGF domains functionally redundant across divergent molecules/compact side-by-side arrangement of EGFs
MSP-2	PFB0300c	N ^a	Highly polymorphic; two major alleles functionally identical; potential species-specific function
MSP-4	PFB0310c	N ^a	C-terminal single EGF domain
MSP-5	PFB0305c	Y ^a	Not required for invasion; homolog of MSP-4
MSP-10	MAL6P1.221	N ^a	Surface and apical appearance; C-terminal double EGF module
Pf12	PFF0615c	ND	Member of 6-cys family; surface-only/6-cys domains modeled as similar to <i>T. gondii</i> surface protein SAG1
Pf38	PFE0395c	ND	Member of 6-cys family; surface and apical appearance
Pf92	PF13_0338	N ^a	Cysteine-rich surface protein
Pf113	PF14_0201	N ^a	Putative surface protein
Microneme Proteins			
AMA-1	PF11_0344	N	Partial complementation between <i>P. falciparum</i> and rodent species; antibodies and peptides block invasion/merozoite reorientation/PAN domains, polymorphisms surround conserved hydrophobic pocket
EBA-140/BAEBL	MAL13P1.60	Y	Binds glycophorin C (Gerbich antigen)
EBA-175	PF07_0128	Y	Binds to glycophorin A; disruption in <i>P. falciparum</i> (W2mef) leads pathway switch to Rh4-dependent invasion/"handshake" association between region II dimers creates grooves for GlyA glycan binding
EBA-181/JESEBL	PFA0125c	Y	Binds trypsin-resistant receptor W on RBCs
EBL1	PFD1145c	ND	No known function
MTRAP	PF10_0181	N	Motor-associated protein
ASP	PFD0295c	ND	Contains "sushi" domain, hence the name apical sushi protein, ASP; putative micronemal GPI-anchored protein
SUB2	PF11_0381	N ^a	Subtilisin-like serine protease; MSP-1/AMA-1-processing "shedase"
Peripheral Surface Proteins			
ABRA	PFL1385c	Y ^b	No known function but putative protease; probably nonessential as not trafficked correctly in MSP-3 knockout
S-antigen	PF10_0343	N ^a	Chr10 locus; no known function
GLURP	PF10_0344	ND	Chr10 locus; no known function
MSP3	PF10_0345	Y	Chr10 locus; abundant but weakly associated with surface/elongated tetrameric molecule; helical heptad repeats predicted to form coiled coil
MSP6	PF10_0346	Y ^a	Chr10 locus "MSP3-like" protein; weakly associated with MSP1
H101	PF10_0347	Y	Chr10 locus "MSP3-like" protein; no known function
H103	PF10_0351	Y	Chr10 locus "MSP3-like" protein; no known function
MSP7	PF13_0197	Y ^a	MSP-1 binding protein; strongly associated; disruption in <i>P. berghei</i> suggests role in normocyte (not reticulocyte) invasion
MSP7-like	MAL13P1.174	ND	Putative MSP1 binding protein
MSP7-like	PF13_0196	ND	Putative MSP1 binding protein, associated with detergent-resistant membranes

Continuation table: Properties of Some Important Merozoite Proteins in *P. falciparum*

Name	Accession Number	KO	Features/Structure
Pf41	PFD0240c	ND	Member of 6-cys family; apical end of merozoites
SERA3	PFB0350c	Y	Cysteine protease domain with active-site serine
SERA4	PFB0345c	Y ^a	Cysteine protease domain with active-site serine; schizont expression
SERA5	PFB0340c	N	Cysteine protease domain with active-site serine; strong schizont expression
SERA6	PFB0335c	N	Cysteine protease domain with active-site cysteine; schizont expression
Rhoptry Proteins			
RAMA	MAL7P1.208	N ^a	GPI anchored, possibly associating with rhoptry complexes
RAP1	PF14_0102	Y	Low-molecular-weight rhoptry complex, nonessential, truncation disrupts trafficking of RAP2 and 3
RAP2	PFE0080c	Y ^b	Low-molecular-weight rhoptry complex; nonessential
RAP3	PFE0075c	Y ^b	Low-molecular-weight rhoptry complex; nonessential
RhopH1(2)	PFB0935w	ND	High-molecular-weight rhoptry complex; CLAG2
RhopH1(3.1)	PFC0110w	ND	High-molecular-weight rhoptry complex; CLAG3.1
RhopH1(3.2)	PFC0120w	ND	High-molecular-weight rhoptry complex; CLAG3.2
RhopH1(9)	PFI1730w	Y	High-molecular-weight rhoptry complex; CLAG9
RhopH2	PFI1445w	ND	High-molecular-weight rhoptry complex
RhopH3	PFI0265c	N ^a	High-molecular-weight rhoptry complex
Rhoptry Neck Proteins			
Rh1	PFD0110w	Y	Binds red blood cells via receptor Y
Rh2a	PF13_0198	Y	No demonstrated function
Rh2b	MAL13P1.176	Y	Involved in invasion pathway through receptor Z
Rh3	PFL2520w	Y	Probable transcribed pseudogene
Rh4	PFD1150c	Y	Differential expression allows invasion-pathway switching
Rh5	PFD1145c	N	No known function

Proteins are grouped according to their localization.

APPENDIX 3. Clinical correlation of parasitemia

Parasitemia	Parasites/ μ l	Clinical Correlation
0.0001-0.0004%	5-20	Number of organisms that are required for a positive thick film (sensitivity) NOTE (TBF): Examination of 100 TBF fields (0.25 μ l) may miss infections up to 20% (sensitivity of 80-90%); at least 300 TBF fields should be examined before reporting a negative result. NOTE (THBF): Examination of 100 THBF fields (0.005 μ l); at least 300 THBF should be examined before reporting a negative result; BOTH TBF and THBF should be examined for every specimen submitted for a suspect malaria case. ONE SET (TBF + THBF) OF NEGATIVE BLOOD FILMS DOES NOT RULE OUT A MALARIA INFECTION.
0.002%	100	Patients may be symptomatic below this level
0.2%	10,000	Level above which immune patients will exhibit symptoms
2%	100,000	Maximum parasitemia of <i>P. vivax</i> and <i>P. ovale</i> (infect young RBCs only)
2-5%	100,000-250,000	Hyperparasitemia, severe malaria ^b , increased

APPENDIX 4. Reagents and Equipments

Reagents

Cleaning of Quartz	Aceton (HPLC)	Sigma Aldrich GmbH, 27,072-5
	"Piranha" (3:1) H ₂ SO ₄ (98%):H ₂ O ₂	Labor preparation
	N ₂ (5.0)	Firma Mast-Tübingen
	distilled water	
Coating PLL	Poly-l-lysine Hydrobromide (70-150 Kda) 0,5 mg/mL in water	Fluka Chemie GmbH, 81339
Quartz Regeneration	NaOH 0,1M	Merck GmbH, Darmstad/C754962
Malaria culture	RPMI 1640-complett	
	500mL RPMI 1640	R0883, Sigma
	500 µL Gentamicin 50 mg/mL	Gibco, Cat No.15750-037
	5 mL L-Glutamine 200 mM	G7512, Sigma
	12 mL HEPES 1M	H0997, Sigma
	50 mL Albumax II 10X	Labor preparation
	Albumax II 10X	
	5,2 g RPMI pulver (+ L-glutamine, - NaHCO ₃)	51800-035, Gibco
	500 µL, Gentamicin 50 mg/mL	Gibco, Cat No.15750-037
	2,98 g HEPES ≥99,5%	H9377, Sigma
	1,67 g NaHCO ₃	Merck GmbH, Darmstad
	1,0 g Glucose	6780.1, Roth
	0,1 g Hypoxanthine	H-9377, Sigma
	25 g Albumax II	Gibco, Cat No.11021-037
Fixation infected erythrocyte (slides)	Giemsa stain modified, 12% in Phosphat Puffer	GS1L, Sigma
	Methanol ACS reagent ≥99,8%	179337, Sigma
	Phosphat puffer 1X	Labor preparation
Synchronisation of parasites	Sorbitol 5% sterile in water	
	Sorbitol ≥99,0%	24850, Sigma
Experiment of infected erythrocyte with QCM	RPMI 1640-withouth NaHCO ₃ complett*	Labor preparation
	RPMI 1640-complett (-NaHCO ₃)	R7388, Sigma
Fixation infected and non-infecte erythrocytes on quartz	Paraformaldehyde 4% in PBS	
	Glutaraldehyde 2,5% in PBS	
	Glutaraldehyde 25%, Grade I	G5882, Sigma
	PBS Tablets	
	PBS Tablets	Gibco, Cat 18912-014
Gas atmosphere	Malaria culture	
	CO ₂ (4.5) 5%, O ₂ (4.5) 5%, N ₂ (5.0) 90%	Firma Mast-Tübingen
	Experiment with QCM	
	O ₂ (4.5) 5%, residual N ₂ (5.0)	Firma Mast-Tübingen
Flow Cytometric	Acridine Orange (AO) 1 µL/mL PBS	Labor preparation
Disinfection QCM	Sodium Hypochlorite solution 4% in water	23.950-5, Sigma
Disinfection malaria labor	Perform ®	UKT, Tübingen
	Descosept AF ®	UKT, Tübingen

Equipments

Laminar flow	Thermo scientific, NSF 49
Icubation	Incub Safe
Microscop	Zeiss Axioskop 2
	Leica
FACS	FACS Canto II
Accujet-Pro	Brand
Analytical balance	ABJ Max. 220 g
Agitator	CAT VM4